MAGSAT Anomalies and Crustal Structure of the Churchill-Superior Boundary Zone

by

I.A. Noble

A thesis
presented to the University of Manitoba
in partial fulfillment of the
requirements for the degree of
Master of Science
in
Geophysics

Winnipeg, Manitoba, 1983

MAGSAT Anomalies and Crustal Structure of the Churchill-Superior Boundary Zone

BY

I.A. NOBLE

A thesis submitted to the Faculty of Graduate Studies of the University of Manitoba in partial fulfillment of the requirements of the degree of

MASTER OF SCIENCE

I hereby declare that I am the sole author of this thesis.

I authorize the University of Manitoba to lend this thesis to other institutions or individuals for the purpose of scholarly research.

I.A. Noble

I further authorize the University of Manitoba to reproduce this thesis by photocopying or by other means, in total or in part, at the request of other institutions or individuals for the purpose of scholarly research.

I.A. Noble

ABSTRACT

MAGSAT, a satellite designed specifically to survey crustal magnetic fields, was in orbit from October 30, 1979 to June 11, 1980. During its more than 3400 orbits, it crossed the boundary separating the Churchill and Superior provinces of the Canadian Shield at an altitude of approximately 400 kilometres several hundred times. The Churchill and Superior provinces are sufficiently different in structure and geophysical characteristics to produce a measurable signature in the satellite magnetic data. The signature was extracted from the data using data processing techniques not generally applied to satellite measurements. This observed signature was modelled using an equivalent point source technique employing spherical prisms. The modelled signature resulting from a simple step-like thickening of a lower crustal magnetic layer agrees quite well with the observed signature.

A large positive magnetic anomaly over the Ungava peninsula was investigated and modelled. The source of the Ungava anomaly appears to be unrelated to the Churchill-Superior boundary, but may be related to tectonic effects of the formation of the Richmond Gulf aulocagen structure.

ACKNOWEDGMENTS

The author wishes to express his thanks and appreciation to Dr. D.H. Hall for suggesting this thesis topic, and for his advice and supervision of this work.

Sincere appreciation is also extended to the Faculty of Graduate Studies Graduate Fellowship Committee, the Department of Earth Sciences G.M. Brownell Prize selection committee, and the Canadian Society of Exploration Geophysicists Scholarship Trust Fund (Grant Geophysical Limited) for their generous financial support.

Special thanks to D.J. for many hours spent in proof-reading and drafting.

CONTENTS

<u>Appendix</u> <u>page</u>

LIST OF FIGURES

LIST OF TABLES

Chapter I

INTRODUCTION

Satellite measurements of the geomagnetic field began with the launch of Sputnik 3 in May 1958. To date, only the Polar Orbiting Geophysical Observatory and MAGSAT satellites have provided an accurate global survey of the Earth's field. Until 1975, when the first crustal magnetic anomaly maps were constructed from POGO data, it was not thought possible to detect the extremely small variations in satellite-observed fields due to the crust. MAGSAT was designed specifically to survey the crust-related fields and to enhance the data quality of these fields. The overall reliability in isolating the crustal fields has been confirmed by several studies involving comparisons of upward continued aeromagnetic data to satellite derived anomaly maps.

Modelling and interpretation of satellite anomaly maps is in its infancy. Frey (1982a, 1982b) has shown that there is a definite tendency for satellite-observed anomalies to be associated with large features such as shields, platforms, subduction zones, basins, rifts, and age province boundaries. One such feature, the Churchill-Superior province boundary zone, has been the object of a great deal of study over the past 15 years. Much work has been done in the effort to obtain an accurate description of the location, extent, and crustal structure of the boundary, using aeromagnetic, gravity, and seismic data. The disinctive change in crustal structure at the boundary proposed by several authors is sufficient to produce an observable signature in satellite data. Such a signature is not readily observable in MAGSAT or POGO anomaly maps.

This study was undertaken in an effort to identify the field variations in MAGSAT data due to the crustal structure of the Churchill-Superior boundary zone. Techniques in data processing common to other fields, but not generally employed in satellite magnetometry, were utilized in isolating the Churchill-Superior boundary signature. Individual satellite profiles were analyzed much the same as seismic traces, and the boundary signature was separated from effects due to current systems and to unrelated crustal fields. The crustal model developed to explain the signature is in good agreement with several of the seismic and magnetic models of the boundary zone.

Chapter II

SATELLITE MAGNETOMETRY

Satellite magnetometry is a very recent aspect of geomagnetism, the oldest branch of geophysics. The magnetic data collected by satellites has been utilized in the production of spherical harmonic field models, studying the structure of the crust, and various modelling studies including the fluid dynamics of the outer core and current systems in near-Earth space. The interpretation of the various measurements possible using satellites is not yet well developed, but satellites have proven to be a valuable source of information in geomagnetic studies.

2.1 THE GEOMAGNETIC FIELD

As a first approximation, the geomagnetic field may be considered as resulting from a dipole located near the Earth's centre with its poles near Thule, Greenland and Vostok, Antarctica. The field is a vector quantity and has generally been described with two angular measures (inclination below horizontal, and declination from geographic north) and field strength or magnitude. In satellite magnetometry, it is often more convenient to describe the vector in terms of its components, usually north, east, and vertical (positive down). The magnitude of the field is usually referred to as the scalar field.

The geomagnetic field is not static, but undergoes various changes in time. The variations experienced by the field can be distinctly grouped according to the time span of the variation. Reversals in polarity, secular variations, diurnal variations, as well as irregular changes of much smaller time scales, are directly linked to the contributing sources of the field. In terms of satellite magnetometry, the geomagnetic field may be considered to have three principal sources of differing relative magnitudes. At least 96% of the magnitude measured by satellites is due to the main field generated in the core of the Earth. Up to 4% is contributed by various current systems in near-Earth space, and less than 0.04% is due to magnetization of the crust.

2.1.1 Spherical Harmonic Field Models

In order to better understand the geomagnetic field, it is generally described with a mathematical model. It is convenient to describe the field as resulting from a series of multipoles with the dipole portion dominant. The spherical harmonic series used in this description is not necessarily physically meaningful, but is a convenient representation. This function depends on the colatitude ϕ, longitude λ, radial distance from the Earth's centre ρ, and time t. The geomagnetic field is then derived from a series representation of the magnetic scalar potential;

$$A = \frac{a}{\mu_0} \sum_{n=1}^{\infty} \left\{\frac{a}{\rho}\right\}^{n+1} \sum_{m=0}^{n} \{(g_n^m) \cos m\lambda + (h_n^m) \sin m\lambda\} P_n^m(\emptyset)$$

where A = magnetic scalar potential

a = mean radius of the Earth

μ_0 = permeability of free space

m = order of the spherical harmonic

n = degree of the spherical harmonic

$P_n^m(\emptyset)$ = Schmidt quasi-normalized spherical functions.

The spherical harmonic field model, then, is a set of Gauss coefficients g_n^m, h_n^m as well as, in some models, the time derivatives of the Gauss coefficients. The coefficients are determined by measuring the field on a global scale to get an accurate representation of the behavior of $A(\rho, \emptyset, \lambda)$. A least-squares fit procedure is then used to determine the coefficients required to accurately model the observed fields. The field measurements must be carried out over as short a time span as possible in order to avoid inaccuracies arising in the secular changes. In this respect, satellites are ideally suited since global coverage is obtained in a very few days. The time derivatives of the coefficients are determined by examining the field models required at different times, generally a few years apart.

The dipole portion of the field is given by g_1^0, g_1^1, and h_1^1. For the MGS481#2 model (Appendix C);

g_1^0 = -29987 nT along the geocentric rotation axis

g_1^1 = - 1957 nT through Greenwich meridian and equator

h_1^1 = + 5605 nT normal to g_1^0 and g_1^1 .

The remaining terms describe the so-called non-dipole portion of the field. In theory, the summations are carried to infinity to perfectly predict the field at any location for a specific time, known as the epoch for the model. In practice, however, the series is terminated at a degree and order chosen to accurately model the main field only. Langel and Estes (1982) examined the power spectra of field models given by;

$$R_n = (n+1) \sum_{m=0}^{n} \{ (g_n^m)^2 + (h_n^m)^2 \} \quad .$$

They found a distinct change of slope in the power spectrum at n=14. This was interpreted as signifying that degrees up to 13 describe core- generated fields, while degrees 15 and up describe crustal fields. Since the crustal fields are generally studied as anomaly fields or residuals, most models are terminated at degree and order 13 to avoid modelling the crust.

2.1.2 The Main Field

The main field is the largest contributor to satellite observed magnetic fields. The magnitude of the main field at satellite altitudes is typically from 30,000 to 60,000 nanotesla. The most notable feature of the main field is its secular variations. These variations are slow, amounting to changes of up to 1% per year. The periodic reversals in polarity occur on a much longer time span, and are preserved in the magnetic "striping" of oceanic crust adjacent to speading ridges. Nagata (1965) identified five features of the secular variation:

1. A decrease in the moment of the dipole portion of the field by 0.05% per year.
2. A westward precessional rotation of the dipole axis of 0.05 degrees of longitude per year.
3. A rotation of the dipole axis toward the geographic axis of 0.02 degrees of latitude per year.
4. A westward drift of the non-dipole field of 0.2 degrees of longitude per year.
5. Growth and decay of features of the non-dipole field with average changes of about 10 nanotesla per year.

The rates of change observed preclude the possibility that they are related to plate tectonics or mantle convection. This, combined with spherical harmonic analysis, has determined the source of the main field to be the outer core of the Earth (Stacey; pp218).

Seismic evidence indicates the outer core of the Earth behaves like a liquid. Geochemical and density considerations are consistent with an outer core composed mainly of iron, a good magnetic and electric conductor. Most theories of the origin of the main field draw upon these two observations to explain the magnetic field generation in terms of a magnetohydrodynamic or kinematic dynamo.

These theories are based on Larmor's suggestion that suitable internal motion in a large conducting fluid could cause it to act as a self- exciting dynamo, and were investigated originally by Elsasser (1946a and 1946b), and by Bullard and Gellman (1954).

The theoretical studies of magnetohydrodynamic dynamos and kinematic dynamos are based on the highly non-linear equations of hydromagnetics, thermodynamics, and electrodynamics. Most of the recent progress has been in the study of kinematic dynamos. Kinematic dynamo theories differ from magnetohydrodynamic dynamo theories in their approach to the problem. In the case of kinematic theories, fluid motions within the core are postulated, and non-decaying solutions are then sought for the resulting electrodynamic equations. Magnetohydrodynamic dynamo theories, on the other hand, seek to derive the necessary fluid motions to explain the observed fields. Regardless of the approach, the main field is proposed to be due to electric currents in the outer core.

The mathematics involved in magnetohydrodynamic and kinematic dynamo theories is fairly elaborate, but the physical principles are fairly straightforward. Assuming the outer core to be a conducting fluid, magnetic field lines will be "frozen" in the conducting fluid if the fluid motion exceeds the rate at which the field is able to diffuse out of the conductor. These field lines will then be dragged around with the fluid as it circulates. If the fluid circulation is such that the moving field lines generate electric currents that reinforce the field lines, the system becomes self-exciting. The particular circulation pattern that produces this phenomenon is the subject of much debate, but it is generally believed to incorporate some form of convection cell. The convection cells are probably produced by the action of gravity on density inhomogeneities, and the source of power required to maintain the convection is betlieved to be gravitational potential energy which is released by the redistribution of mass as the inner core grows in size (Franck; 1982). The fact that the rotational and magnetic poles nearly coincide has prompted Hide (1982) to suggest that fluid motions associated with dynamos are strongly influenced by Coriolis forces due to a general rotation.

2.1.3 Magnetospheric and Ionospheric Current Systems

In addition to the secular variations in the main field, the geomagnetic field undergoes systematic diurnal variations and irregular variations on a time scale of seconds to days. These additional variations are manifest as changes in the vector field by as much as 2000 nanotesla at satellite altitudes. The magnetic field is termed magnetically quiet if the variations are regular, and magnetically disturbed if the variations are irregular. A magnetic substorm is said to occur if the irregular changes are of high amplitude and confined to high latitudes. Magnetic storms occur when the high amplitude irregular variations are observed world-wide.

Diurnal and irregular variations are due to several complicated electric current systems in space surrounding the Earth. The similarity of the main field to that of a dipole is severely distorted in space by the solar wind, a stream of ionized particles flowing out from the sun in all directions. The solar wind, comprised mainly of protons and electrons, confines the geomagnetic field to a cavity called the magnetosphere within a bag-like boundary known as the magnetopause. Figure 2.1 illustrates the pre-1960's and present day views of the geomagnetic field. The magnetosphere is compressed on the magnetic noon (sunward) side, and is combed out into a comet-like tail on the midnight side. The solar wind is a neutral, highly conductive ionized gas called a plasma. By Lenz's law, interplanetary and solar magnetic field lines are "frozen" into the plasma and carried along with it. Similarly, magnetic fields external to the plasma are frozen out. The magnetosphere is therefore warped upon "contact" with the solar plasma since the geomagnetic field lines are forbidden entry. The solar plasma compresses the Earth's field ahead of it until the Earth's magnetic field density is equal to the plasma energy density. This occurs at approximately ten Earth radii and, at that point, the plasma breaks up and most of it slips around the Earth, giving rise to the magnetophere's tail.

Some of the charged particles comprising the plasma are trapped in the geomagnetic field by processes not yet fully understood. The motions of these charged particles under the influence of the geo-

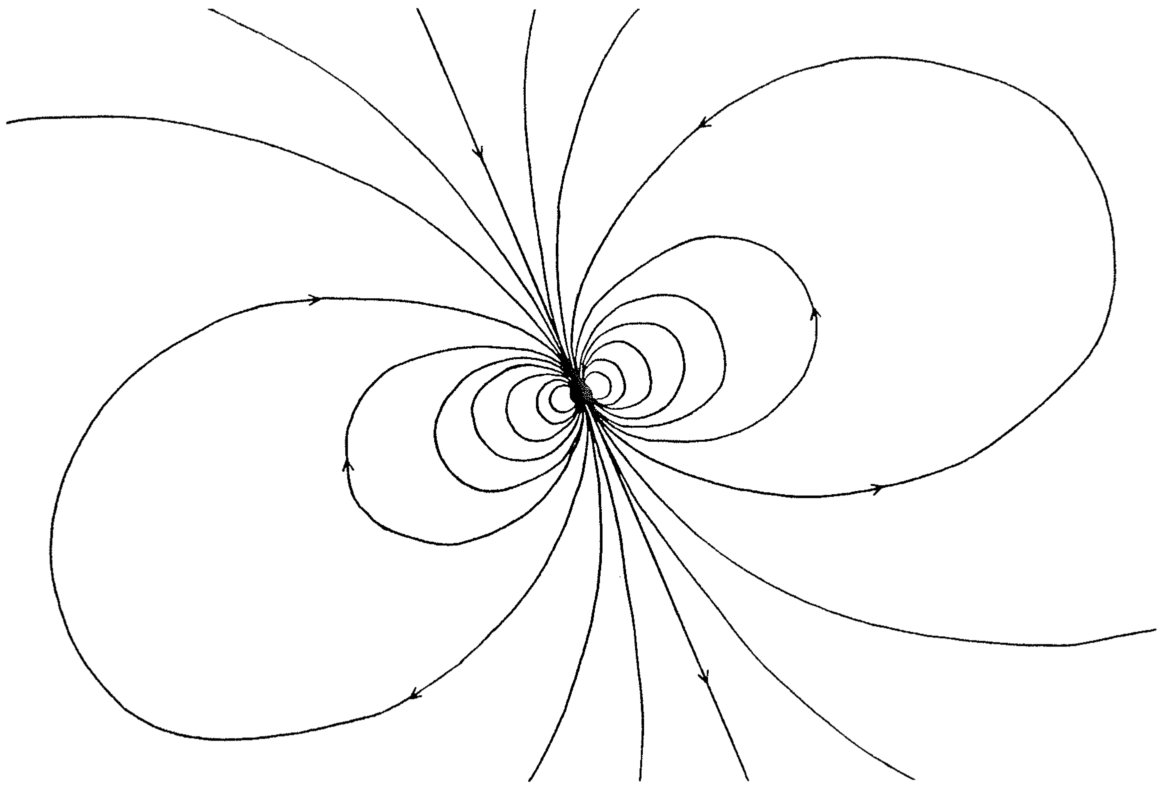

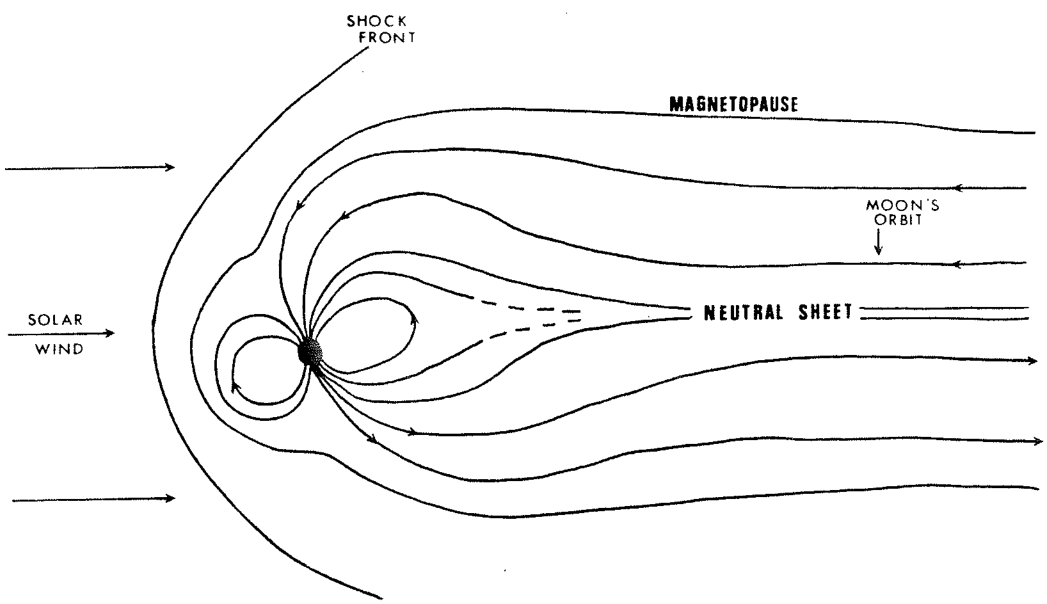

Figure 2.1: Effect of the solar wind on the dipole field. The upper diagram illustrates the classical view of the geomagnetic field in the absence of a solar wind, while the lower diagram illustrates the comet-like appearance of the field due to the solar wind.

magnetic field and their own kinetic energy constitute currents within the magnetosphere and on the magnetopause. As illustrated in Figure 2.2, the current systems and the magnetosphere are rather complicated. As well as within the magnetosphere and on the magnetopause, currents flow across the tail in the neutral sheet separating incoming from outgoing field lines. Some of the trapped particles drift in a westerly direction, giving rise to the westard flowing equatorial electrojet, or ring current.

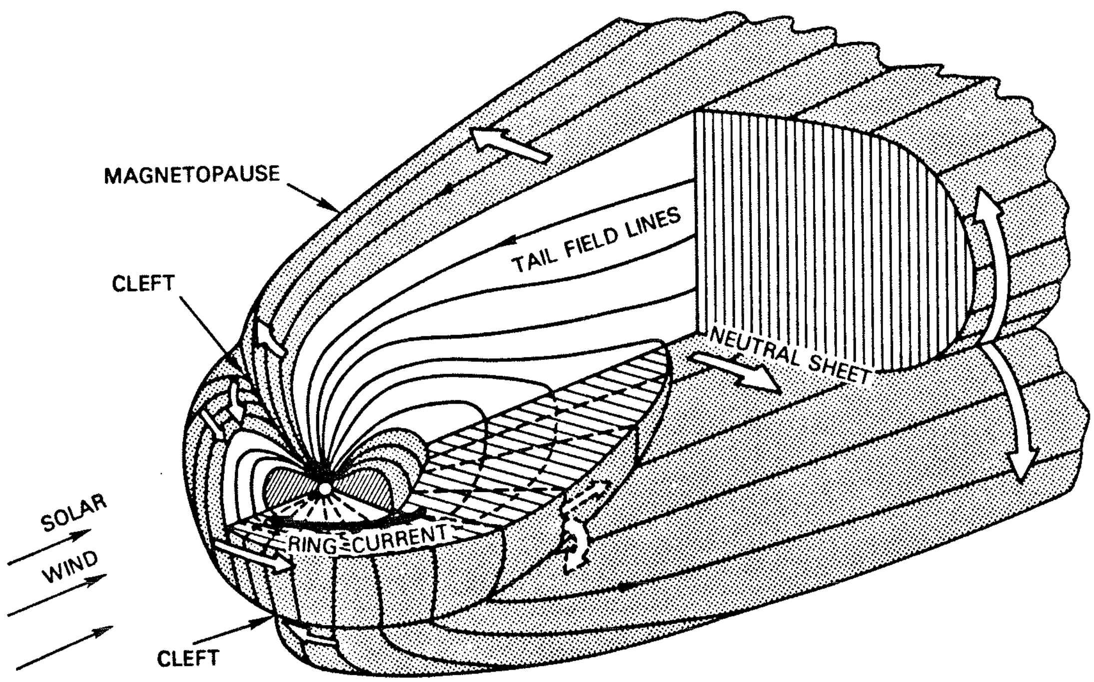

Figure 2.2: Artist's conception of the magnetosphere. Some of the magnetospheric current systems are illustrated with broad arrows. The ring current is illustrated with the heavy black arrow. (from Langel; 1980)

Most of the magnetospheric currents are fairly distant from Earth and cause little variation in fields at MAGSAT altitudes. The ring current, however, can produce substantial fields at MAGSAT altitudes, particularly during disturbed times.

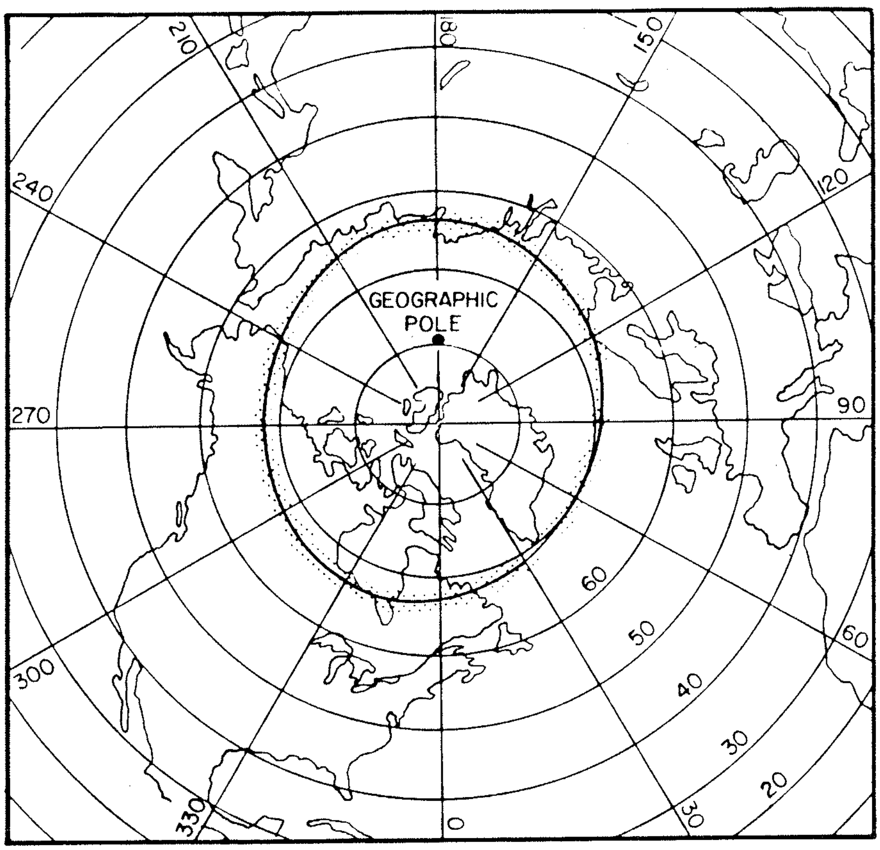

Figure 2.3: Auroral zone in the northern hemisphere. Locus of maximum auroral activity around the North geomagnetic pole is illustrated as the black line. Ionospheric currents are active 240 nights per year in the auroral zone. Note co-ordinates are geomagnetic. (from Garland; 1979)

The ring current and auroral currents (where trapped particles are injected into the Earth's ionosphere) are the most important for the present discussion. Figure 2.3 illustrates the locus of maximum auroral activity related to the ionospheric current systems. Hughes and Rostoker (1977) analyzed ground-based magnetometer array data and determined that the average current configuration for northern latitudes involved three main current systems:

1. A downward field-aligned current in the noon and pre-noon which diverges to ionospheric Hall currents in the following proportions;
   - 35% eastward electrojet toward dusk
   - 60% westward electrojet toward dawn
   - 5% equatorward which closes through the mid-latitude ionosphere and re-enters the auroral zone through poleward flows in the pre-dusk
2. A westward electrojet across the midnight meridian which gradually bleeds up the field lines in the pre-midnight poleward of the east electrojet.
3. An eastward electojet which gradually bleeds up the field lines and dies out approximately at midnight.

The electrojets have associated with them Birkeland current sheets illustrated in Figure 2.4. These are cone-shaped sheets of field aligned currents which are particularly troublesome in the separation of current and crustal magnetic anomalies. Since the Birkeland currents are nearly vertical, they have their greatest influence on the horizontal components of the geomagnetic field, par-

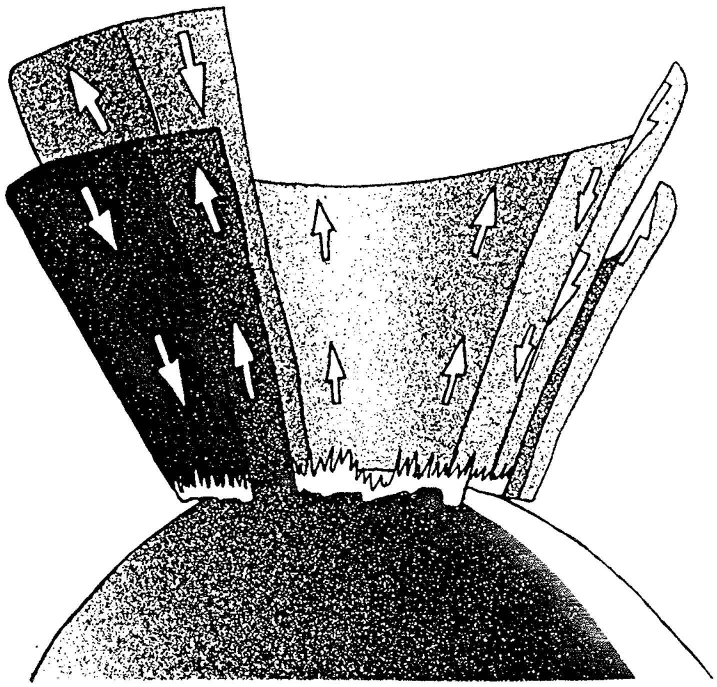

Figure 2.4: Artist's conception of Birkeland current sheets. The injection of charged particles into the ionosphere gives rise to the aurora illustrated at the base of the conical current sheets. Note the reversal in current direction near noon and midnight. (after Potemra; 1980)

ticularly the east component. Figure 2.5 illustrates the effect of Birkeland currents on the vector components of the satellite observed field.

Klumpar and Greer (1982) have modelled currents in northern latitudes and have compared the resulting magnetic profiles with those observed in MAGSAT data. Figures 2.6 and 2.7 summarize their model and its performance. Note the differing scales on the plots, and the reversal in polarity as the anomaly profiles cross from dusk to

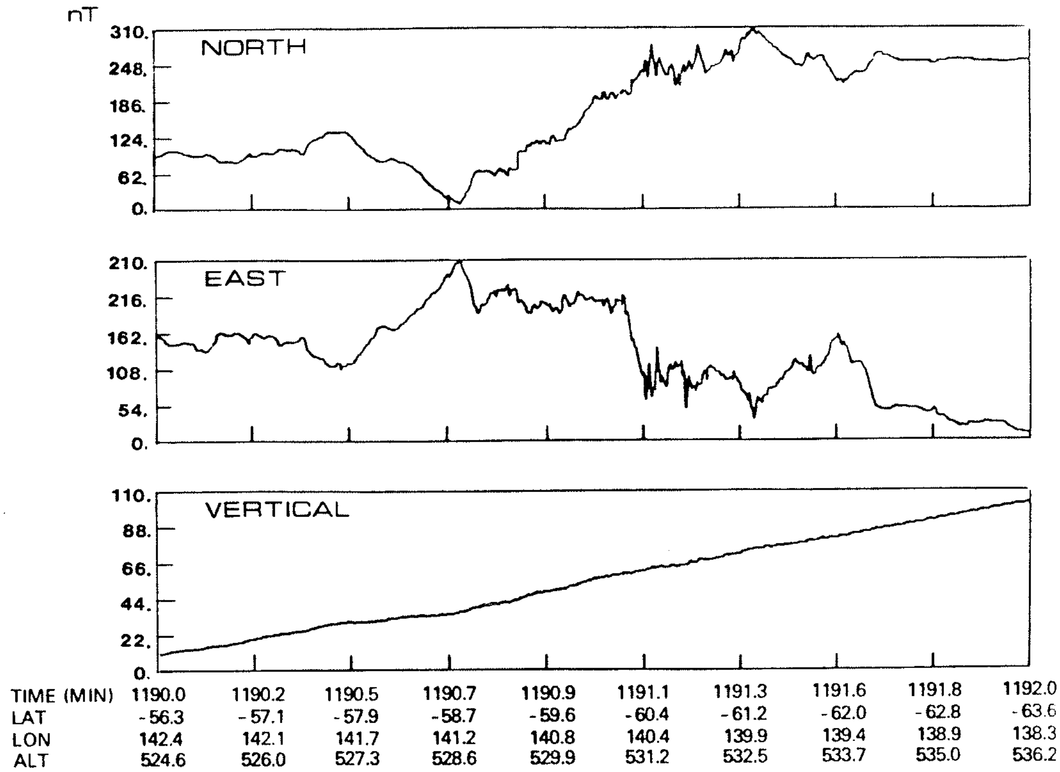

Figure 2.5: Field variations due to field-aligned currents in the southern high latitudes. The scales, in nanotesla, are relative. (from Langel; 1980)

dawn sectors. Hughes and Rostoker (1979) used ground-based observations to model the current systems of the northern latitudes. Their model incorporated a more complex current system involving the magnetophere and ionosphere and three-dimensional current loops. Figure 2.8 illustrates the current systems used to generate the modelled profiles, which are compared with observed profiles in Figure 2.9.

The equatorial ring current in the magnetosphere influences fields in northern latitudes, but is not an important contributor

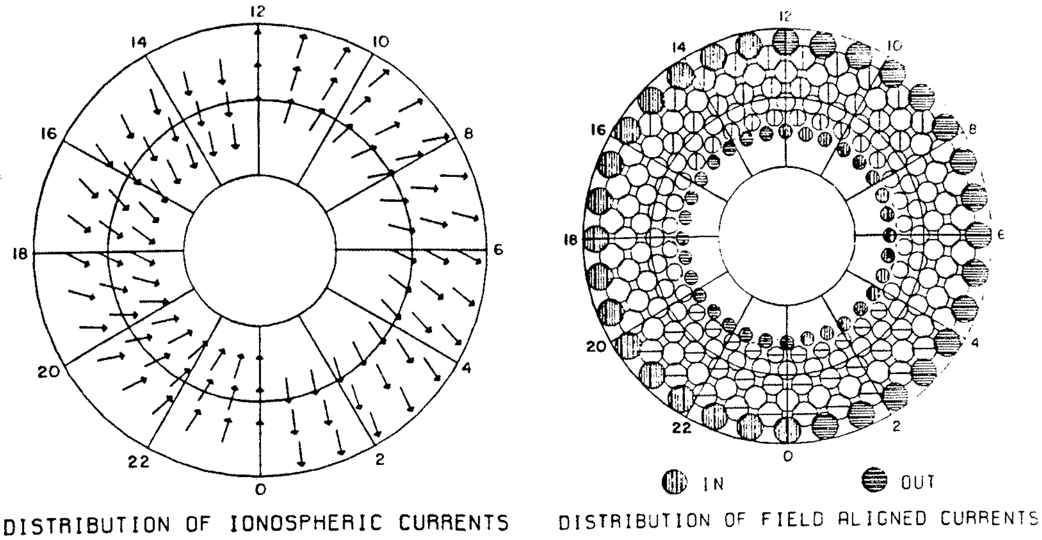

Figure 2.6: Ionsopheric and Magnetospheric current models. Current distributions used to generate the latitude profiles of Figure 2.7. (from Klumpar and Greer; 1982)

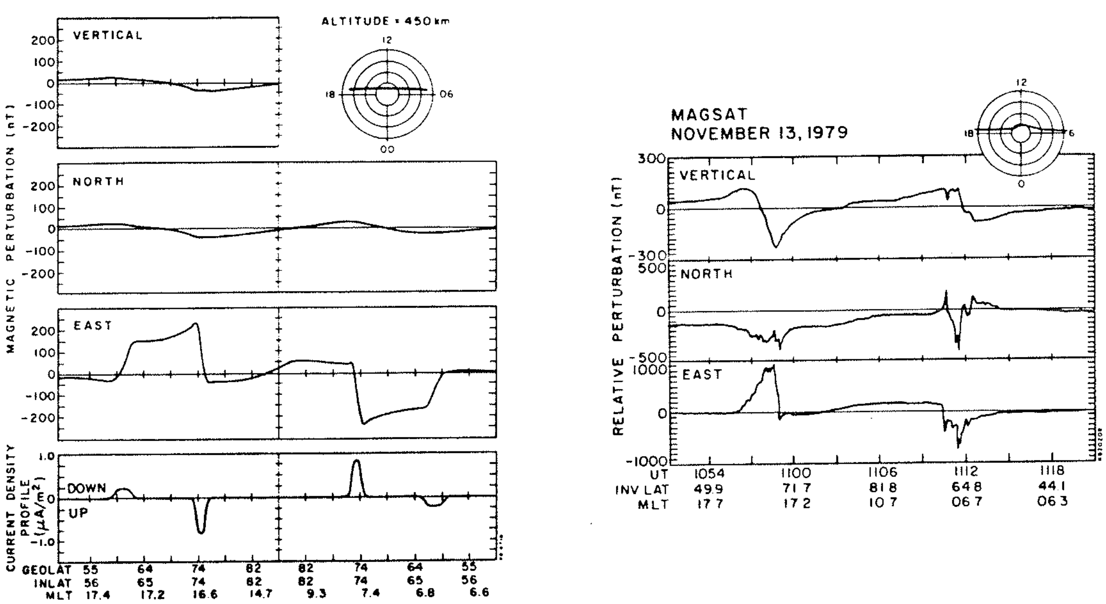

Figure 2.7: Modelled current signatures. Computed and satellite-observed latitude profiles due to current systems of Figure 2.6. (from Klumpar and Greer; 1982)

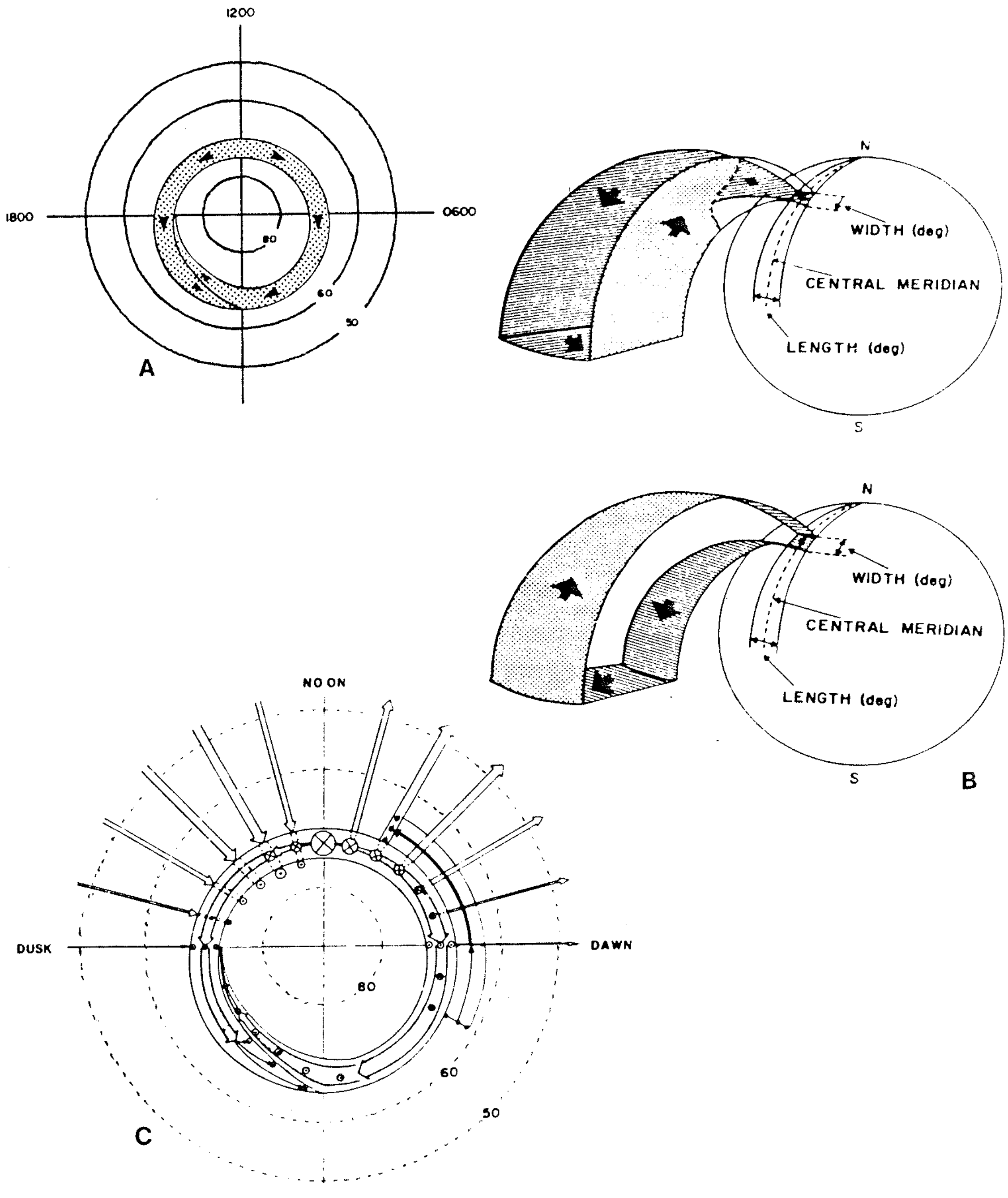

Figure 2.8: Three dimensional current model. Schematic diagram of current systems employed in modelling the fields of Figure 2.9. A) Auroral oval contour used in the electrojet model. B) Model three dimensional current loops. C) Schematic of electrojet components of the complete current system; net downward field-aligned currents indicated by ⊗ , upward by ⊙ . The width of the current arrows is an indication of the ionospheric current strength. Note geomagnetic co-ordinates are used. (from Hughes and Rostoker, 1979)

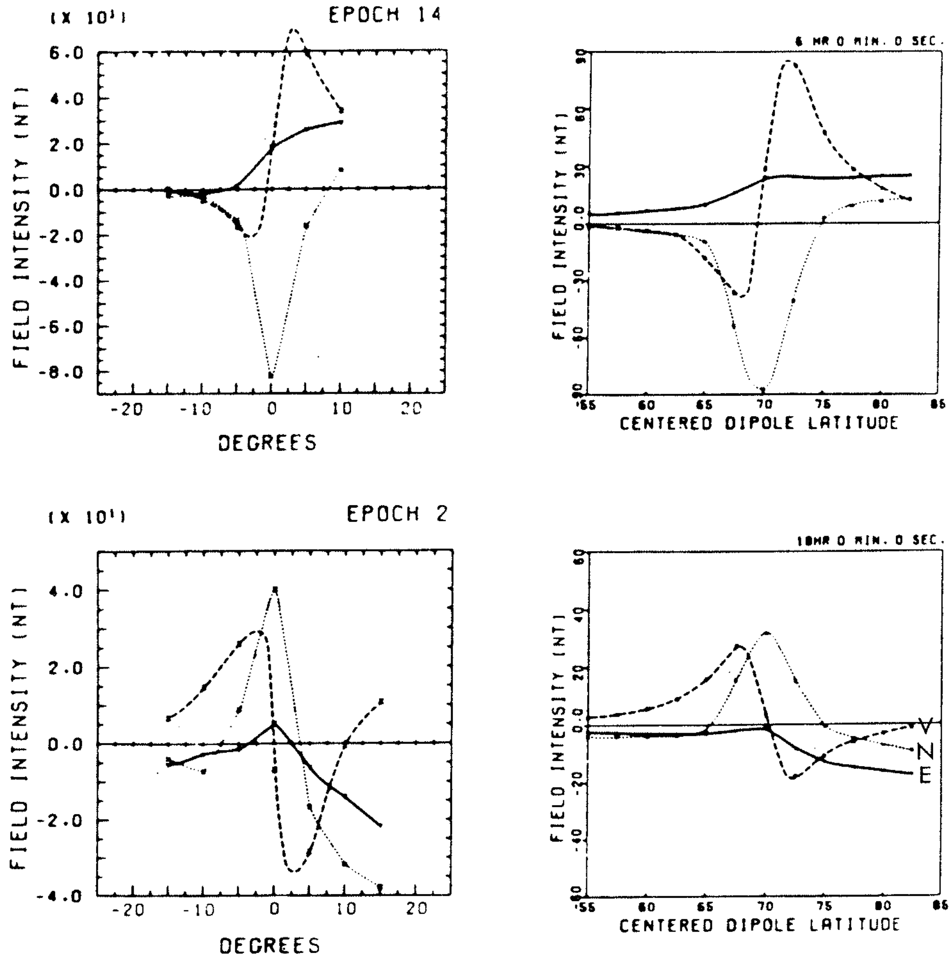

Figure 2.9: Latitude profiles of current fields. Comparison of fields generated by the current systems of Figure 2.8 with those observed by ground stations. Calculated profiles are on the right. Only dawn and dusk profiles are illustrated. Note the polarity reversal in dawn and dusk profiles. (from Hughes and Rostoker; 1979)

during magnetically quiet times. The ionospheric currents, on the other hand, are most important to high latitude studies, and are present in some degree at almost all times. Zanetti and Potemra (1982) studied the Birkeland current signatures in MAGSAT and TRIAD satellite data and concluded that the Birkeland current system is a permanent feature of the magnetospheric and ionospheric current systems. As well, they noted that the Birkeland system is well correlated with the global magnetic activity Kp index. The fact that the ionospheric current systems produce anomalies with wavelengths comparable to those of lithospheric origin makes them particularly difficult to identify and separate.

2.1.4 Crustal Magnetization

Having magnitudes of from 0 to 30 nanotesla, the fields due to variations in geophysical properties of the crust are by far the smallest effect observed by satellites. Since the fields are directly related to the crust, time variations are on a geological time scale, varying with continental drift and tectonic events.

Most rocks contain a small percentage of iron oxides and iron sulfides which have ferrimagnetic properties. These minerals have small positive magnetic susceptibilities that increase with temperature until their Curie temperature is reached, at which point the ferrimagnetic mineral loses its ability to retain magnetism and becomes paramagnetic. The Curie temperature for magnetite, the most important of the magnetic minerals, is approximately 575 degrees Celsius. The magnetic minerals occur as small grains dispersed throughout the paramagnetic or diamagnetic host matrix of silicate minerals. Most minerals are paramagnetic, having very small positive susceptibilities. The few diamagnetic minerals, having very small temperature-insensitive negative susceptibilities, have a very weak effect.

Of the magnetic minerals, the cubic iron oxides are strongly magnetic. These include the Magnetite (Fe_3O_4) - Titanomagnetite (Fe_2TiO_4) solid solution minerals, as well as Maghemite (γ- Fe_2O_3). The rhombohedral iron sulfides are a much weaker family of magnetic minerals, but are still important sources of crustal anomalies. These include the Hematite (α- Fe_2O_3) - Ilmenite ($FeTiO_3$) solid solution minerals as well as Pyrrhotite (FeS_x, $1<x<2.14$). In addition to the remanent magnetization of the above minerals, induced magnetization plays an important role in crustal anomalies. In paramagnetic and diamagnetic substances, the susceptibility is independent of the magnetizing force, and the induced magnetization is linearly proportional to the magnetizing force. Thus, an otherwise uniform magnetic field is increased by the presence of a paramagnetic substance, and decreased by the presence of a diamagnetic substance. In the case of ferromagnetic, antiferromagnetic, and ferrimagnetic substances, the susceptibility depends on the magnetizing force, but in the study of the geomagnetic field, the susceptibility is assumed to be constant over the small range of geomagnetic magnetizing forces. Ferrimagnetic minerals, then, are treated as paramagnetic with much larger susceptibilities.

Since the magnetic minerals lose their ferrimagnetism at temperatures in excess of their Curie temperature, it is important to determine the "depth to Curie point". For the Canadian Shield, Hall (1977b) derived a simplified theoretical temperature-depth relation valid in the upper 150 km of crust;

$$T = 103 + 10.6 \; z$$

where T is in degrees Celsius and z is in kilometres. Coles (1973) determined Curie temperatures for several rock samples collected from the Superior Province of the Canadian Shield. He found that the Curie temperature was approximately 575 degrees Celsius, consistent with magnetite contributing the magnetic component. This was also supported by polished surface mineralogy. Solving the above equation for T=575 yields a Curie depth of approximately 45 kilometres in the Canadian Shield. This depth, of course, varies according to the regional heat flow, and is much shallower over most of the world.

The particular location within the crust of the magnetization observed by satellites has come under considerable attention recently. From a study of the long wavelength component of aeromagnetic data, Hall (1974) concluded the magnetization of the lower crust was considerably higher than magnetizations observed in surface rocks. Several studies before and since have supported this contention, including Pakiser and Zietz (1965), Zeitz et al (1966), Shuey et al (1973), and Krutikhovskaya and Pashkevich (1977). The composition of the lower crust, then, is of high importance in satellite magnetometry, since the fields observed at satellite altitudes are influenced by the entire crust, not simply the upper portion. Wasilewski and Fountain (1982) studied the Ivrea zone of northern Italy, presumed to be a representative cross-section of the deep continental crust. They observed a "deep crustal" layer of mafic-ultramafic granulite facies rocks with high magnetization, and concluded that this layer would form an appropriate source for long wavelength anomalies. From a study of crustal xenoliths, Waselewski and Mayhew (1982) found that metabasic xenoliths in granulite facies were generally highly magnetic, but mantle xenoliths were essentially nonmagnetic. Thus the Mohorovicic discontinuity may be a magnetic lower boundary in regions of low heat flow where the Curie depth is below Moho.

In addition to the evidence indicating higher magnetization at depth due to petrologic variations, the effect of temperature must be considered. The Hopkinson effect results in the susceptibility increasing substantially with temperatures approaching the Curie point. Dunlop (1974) indicates a factor of two enhancement in susceptibility of deeply buried crustal rocks. Thus, the effective magnetization of the lower crust will generally be greater than 5 amperes per metre, much higher than magnetizations measured near the surface. In surface surveys, the close proximity of the upper crustal layer effectively "drowns out" the long wavelength contribution of the lower crust, and the data must be filtered in order to observe the lower crustal contribution. At satellite altitudes of 300 to 800 kilometres, the deeper crustal component dominates, due to its greater magnetization.

2.2 THE MAGSAT MISSION

Many satellites have measured the Earth's magnetic field, but most of them have been at altitudes or in orbital planes unsuited to the global study of the very small component contributed by the crust. Satellites giving global coverage in a short time period are required for adequate field modelling. Previous to MAGSAT, only the polar Orbiting Geophysical Observatory (POGO) series 2, 4, and 6 provided such data. The POGO's spanned 1965 to 1971, and measured the scalar field over an altitude range of 400 to 1500 kilometres. Their orbital plane was very nearly polar, providing global coverage. The Soviet KOSMOS-49 was in orbit for eleven days, and covered the region between 50 degrees south latitude and 50 degrees north latitude. KOSMOS-49 also measured the scalar field, but at an average altitude of only 375 kilometres.

Regan et al (1975) illustrated that the crustal component could be extracted from the satellite data obtained by the POGO series. On the basis of their results, MAGSAT was designed for crustal studies. The primary objectives of the MAGSAT mission were to obtain global data for improved field modelling, and to map variations in strength and vector characteristics of crustal magnetization. Initial plans were to launch MAGSAT during the quiet part of the 11 year solar cycle but, due to various delays, it was launched on October 30, 1979 and remained in orbit until June 11, 1980. Unfortunately for crustal studies, this was very near the peak of the 11 year cycle, one of the most active of many recent cycles. However, this allowed much data on the magnetospheric and ionospheric current systems to be obtained.

MAGSAT was launched into a dawn-dusk orbital plane having an inclination of 97.76 degrees from the Earth's equator, with a 561 kilometre apogee and a 352 kilometre perigee. Inclining the MAGSAT orbit 7 degrees from the Earth's rotational axis caused the orbital plane to precess approximately 1 degree per day due to the Earth's equatorial bulge. This precession was just the correct amount to turn the orbital plane toward the Sun as the Earth orbited the Sun (see Figure 2.10). MAGSAT, then, remained in the dawn-dusk sector thoughout its lifetime. This was advantageous since the ionospheric and magnetospheric current systems are quietest in the dawn-dusk sectors, and MAGSAT would be sunlit almost constantly, enabling it to derive its power from solar cells. As well, the nearly polar orbit enabled MAGSAT to obtain global coverage in a very short time span (see Figure 2.11). MAGSAT made approximately 15 orbits per day while the Earth rotated beneath it, giving rise to the spiral-like ground track.

MAGSAT carried both vector and scalar magnetometers. These were located at the end of an extendable boom in order to avoid ambient

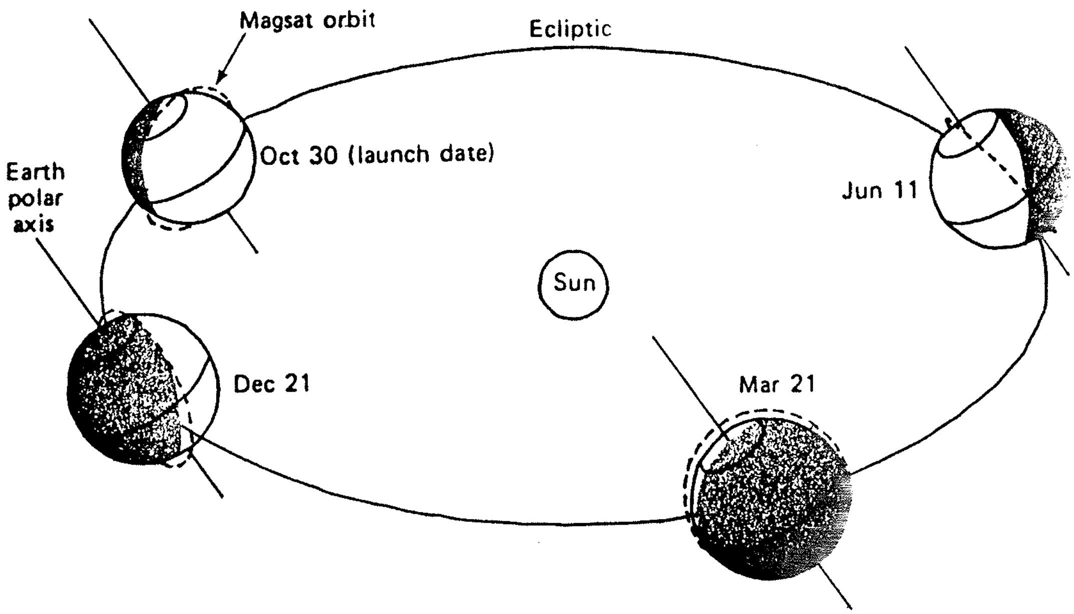

Figure 2.10: Precession of the MAGSAT orbital plane with time. MAGSAT orbital plane is inclined 7° toward the Sun from the Earth's north rotational axis. (after Potemra, Mobley, and Eckard; 1980)

fields due to the satellite (see Figure 2.12). A Cesium vapor optical-pump scalar magnetometer was used to measure the magnitude of the geomagnetic field at the satellite location. In addition, three orthogonal Fluxgate magnetometers measured the components of the vector field. The Cesium vapor magnetometer was accurate to approximately 1.5 nanotesla when working properly, but developed internal oscillations in its lamp circuitry which slightly degraded its accuracy. It was therefore used primarily to calibrate the fluxgates, whose accuracy was within 3 nanotesla in each axis (Langel, Berbert, and Jennings; 1981).

The data gathered by MAGSAT is being analyzed by scientists of the Goddard Space Flight Centre, the United States Geological Sur-

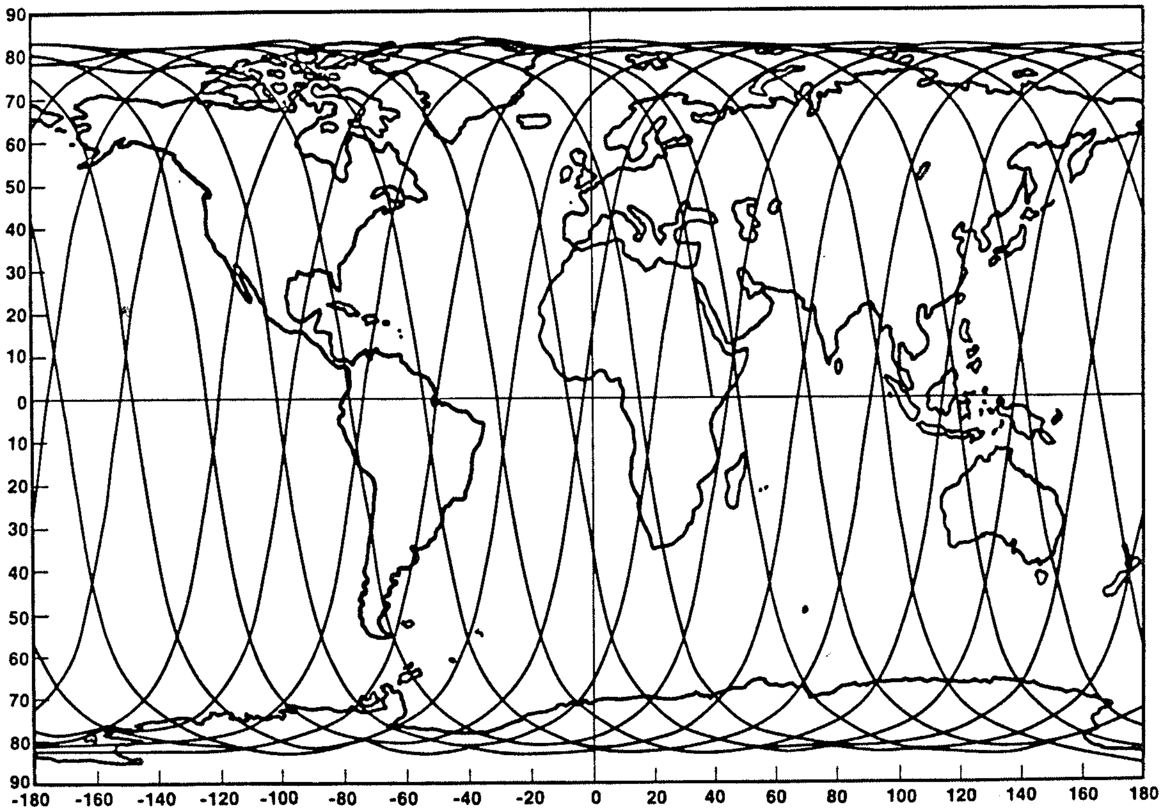

Figure 2.11: MAGSAT ground track for the first 24 hours. The gaps are filled in on successive orbits. (from Langel, Regan, and Murphy; 1977)

vey, and by investigators selected in response to a NASA Announcement of Opportunity. Langel (1980) details the investigators' projects. The data available to the author was known as Investigator-B (INV-B) data. The basic data set was contained on the so-called Chronicle tapes. These include all measured data and ephemeris information on separate files. The sampling rate for the Chronicle tapes was 8 samples per second in the case of the Cesium vapor magnetometer, and 16 samples per second for the fluxgates. Since many

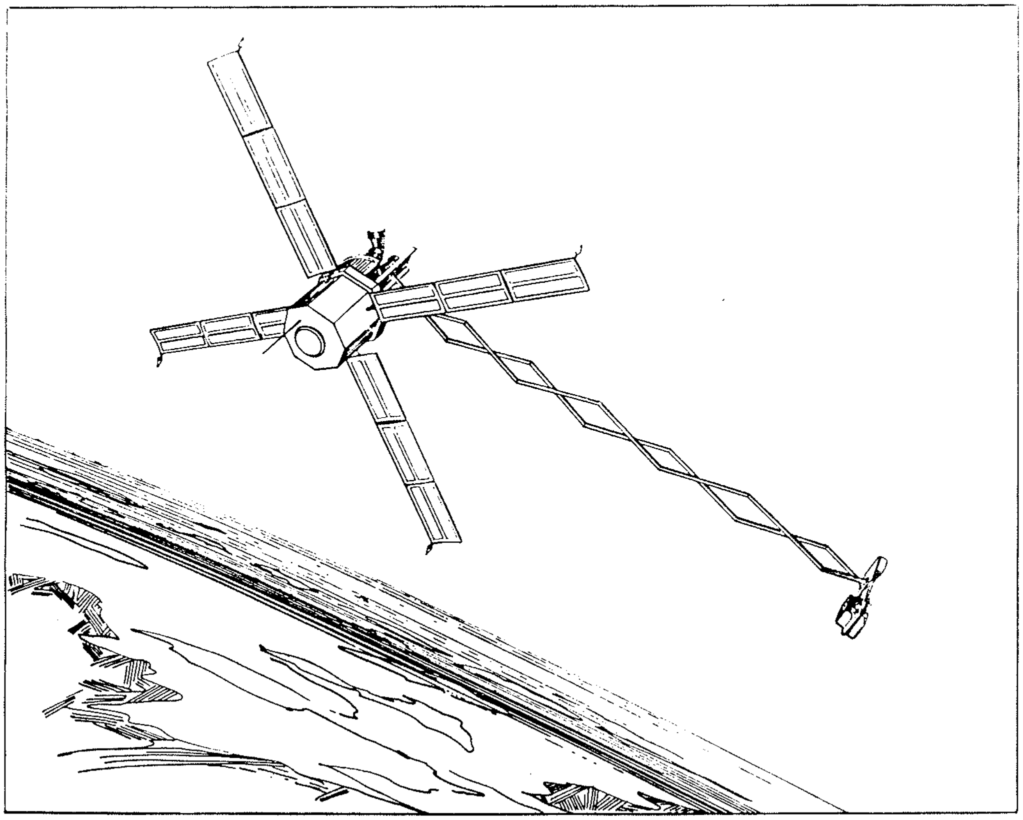

Figure 2.12: Artist's conception of MAGSAT in orbit. The magnetometers are located at the end of the 6 m boom to avoid ambient fields. (from Langel, Regan, and Murphy; 1977)

of the investigators did not require such a high sampling rate, the INV-B data included only every 40th scalar point, and every 80th vector point. As well as the scalar and vector magnetometer data, the INV-B tapes included the ephemeris data merged with the magnetic data, and a few calculated values to simplify the data processing steps. Those values included on the INV-B tapes applying to this study are summarized in Table 2.1.

The data was organized according to pass number. A pass was defined as having its starting point where the satellite changed from south-going to north-going. Some of the values are defined only for the ascending and descending nodes of the orbit. The ascending and descending nodes are defined as the points where the satellite crosses the ecliptic in a north-bound or south-bound direction, respectively.

TABLE 2.1

Partial Listing of Data Available on INV-B Tapes

Variable		Description
IPASS	-	pass number
ALONG(2)	-	geodetic longitude at ascending and descending nodes
IKP(2)	-	global magnetic activity Kp index at ascending and descending nodes
TZERO	-	epoch for spherical harmonic field model
GH(14,14)	-	13 degree/order spherical harmonic field model coefficients
GHT(8,8)	-	7 degree/order time derivatives of GH
LAT	-	geodetic latitude of satellite
LONG	-	geodetic longitude of satellite
RAD	-	geocentric radius of satellite orbit
MLT	-	magnetic local time (dawn or dusk)
INVLAT	-	invarient latitude (magnetic co-ordintes)
BS	-	scalar field from cesium magnetometer
BV	-	magnitude of vector field from fluxgates
X	-	North component of BV
Y	-	East component of BV
Z	-	Vertical component of BV
BVA	-	arithmetic mean of the 80 Chronicle points corresponding to this point
XA,YA,ZA	-	arithmetic means of the 80 Chronicle points
BMD	-	predicted scalar field from the GH and GHT spherical harmonic field coefficients
XM,YM,ZM	-	modelled vector components from GH and GHT

2.3 SATELLITE CRUSTAL MAGNETIC ANOMALY MAPS

The residual field left when estimates of the core and current fields are removed is called the crustal magnetic anomaly. An anomaly map is a contour map of the average anomaly field at the altitude of the satellite. It is important to realize that most satellite magnetic anomaly maps represent small changes in the field on a complicated surface defined by the satellite orbital altitude and the direction of the magnetic field at the location of the satellite. Since the main field is not vertical, effects seen on scalar anomaly maps must be projected down to the Earth's surface along its field direction. For maximum usefulness, anomaly maps are "reduced to a common elevation" and "reduced to a common inclination". The former removes effects of changes in the satellite altitude, and produces a map of the anomaly field at a specific altitude. The latter removes the effect of the changing field direction of the Earth, and produces a map of the anomaly field for a specific inclination. Generally, the inclination used is 90 degrees. The map is then called "reduced to the pole", and represents the anomaly that would be observed if the geomagnetic field were vertical everywhere.

Satellite anomaly maps are very recent and describe only very broad scale anomalies as compared with aeromagnetic anomaly maps. It was originally considered impossible to detect the extremely small variations of crustal origin in satellite data. While analyzing POGO data, Regan, Cain, and Davis (1975) discovered that crustal fields could be identified in the low altitude portions of the dataset. The map of Regan et al was partially contaminated by magnetospheric and ionospheric current systems (Regan, Handschumacher, and Sugiura; 1981), but the reality of the crustal origin has clearly been demonstrated (Langel, Coles, and Mayhew; 1980).

The POGO series of satellites, from which the map in Figure 2.13 was derived, had two severe limitations. First, the satellites were in a high orbit; most of the data is from altitudes in excess of 500 kilometres. Second, the data is of field magnitude only; the direction of the field was not recorded. MAGSAT was designed to alleviate both of these shortcomings. The lower altitude of the MAGSAT spacecraft increased the resolution by a factor of approximately two, and the field stength by a factor of between two and five. The vector magnetometers on board MAGSAT enabled the measurement of fields in directions other than the direction of the local geomagnetic field. Although initial results indicate that large scale crustal remanent magnetizations cannot be modelled using an equivalent point source technique (Galliher and Mayhew; 1982), the vector components are extremely useful in identifying current systems.

Figure 2.14 illustrates the preliminary MAGSAT north-polar scalar anomaly map prepared by Langel and distributed to investigators. Figure 2.15 illustrates the north-polar map prepared by Coles, Haines, Jansen van Beek, Nandi, and Walker (1982). All three poss-

Figure 2.13: North polar scalar anomaly map from POGO data. Contour interval is 2 nT. (from Langel, Berbert, and Jennings; 1981)

ess similarities, with considerably more detail in the MAGSAT maps. None of the three have been reduced to a common elevation, nor have they been reduced to a common inclination. In preparing their vec-

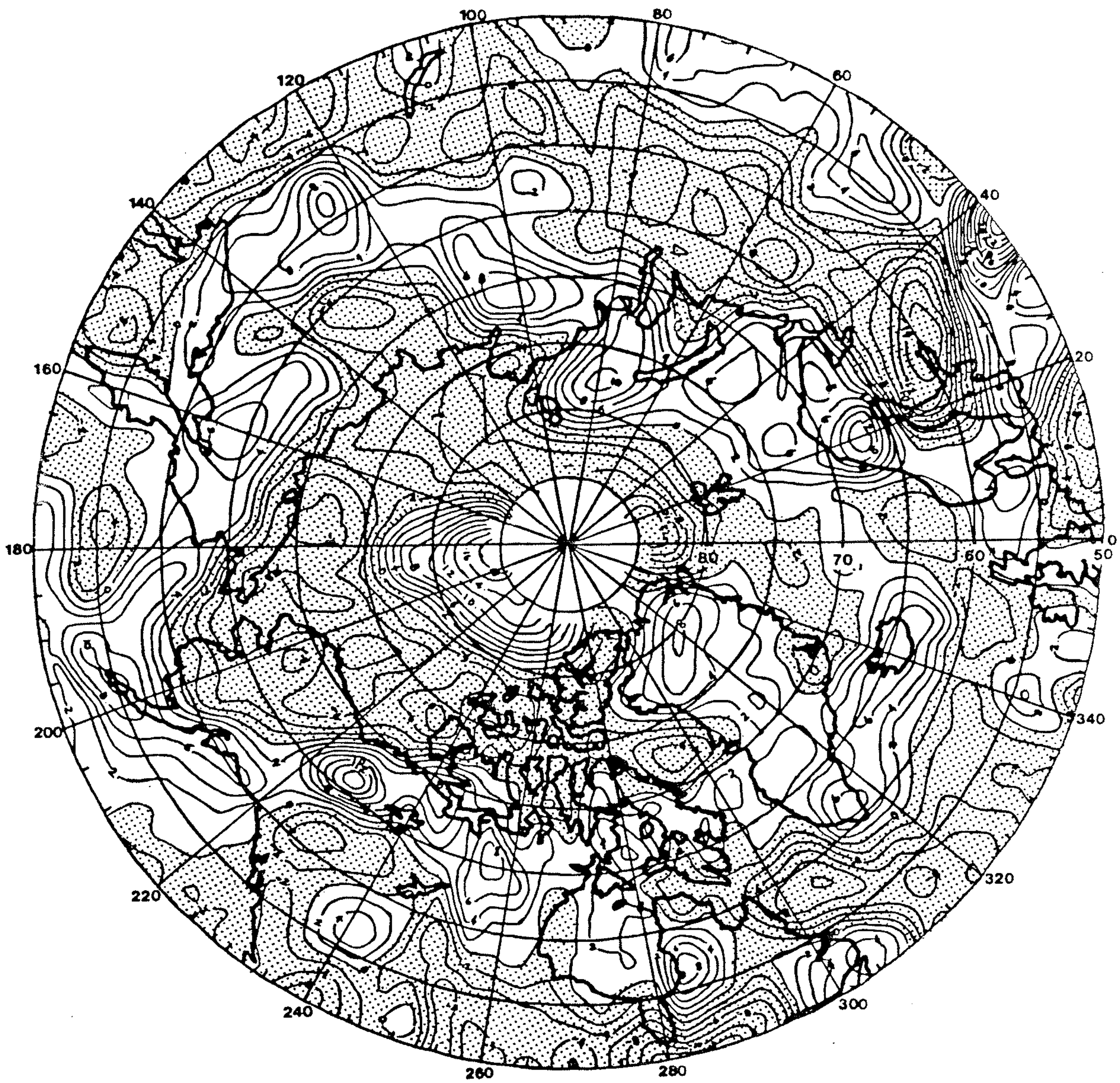

Figure 2.14: North polar scalar anomaly map from MAGSAT data supplied to investigators. Average altitude is 344 km. Contour interval is 2 nT. (Langel, Phillips, and Horner pre-print; 1982)

tor component maps for northern latitudes, Coles et al (1982) were very careful to avoid contamination from ionospheric and magnetospheric current systems. Their initial selection was on the basis of

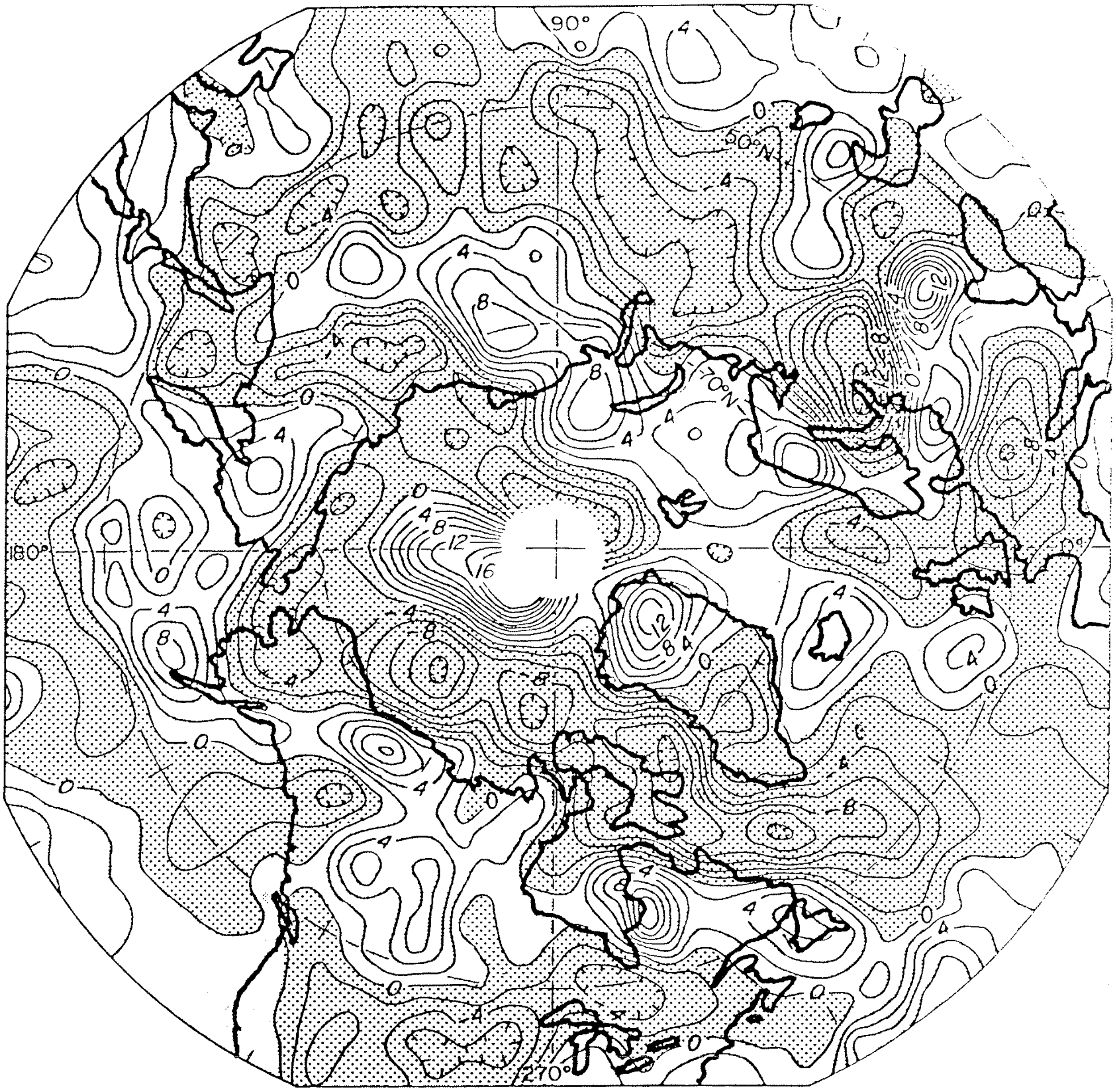

Figure 2.15: North polar scalar anomaly map from MAGSAT data. Average altitude is 430 km. Contour interval is 2 nT. (from Coles, Haines, Jansen van Beek, Nandi, and Walker; 1982)

the Kp index. Passes from 40 degrees north latitude, over the pole to 40 degrees north latitude again, were accepted only if they occurred during a nine hour interval during which Kp was equal to 1 or less. The map supplied to investigators (Figure 2.14) included data with Kp less than or equal to 33. The second screen of the Coles data made use of Canadian magnetic observatory data. If the range of magnetic activity recorded at the Fort Churchill observatory was considered too extreme at the time corresponding to a given satellite pass, the pass was rejected. Finally, the remaining passes were individually examined for consistency with neighbouring passes. Passes not showing patterns similar to neighbouring passes were rejected. As a result of their stringent data selection requirements, only 180 passes out of over 3000 possible were accepted.

The data processing stage was similar for each of the three maps. This included removing a spherical harmonic field model, a quadratic function representing magnetospheric currents, and linear trends representing inaccuracies in the first two removals. In their maps, Coles et al (1982) used a least-squares quadratic and no linear. The data was then gridded. Further processing consisted of eliminating data which was considered to be too far from the mean for a given grid cell. Finally, the data was contoured. The interpretation of such anomaly maps is not well developed. The anomaly map represents inaccuracies in the models used for the main and current fields, as well as petrologic changes in the Earth's crust, variations in the depth to Curie temperature, and variations in the magnetic susceptibility.

Chapter III

THE CHURCHILL-SUPERIOR BOUNDARY ZONE

3.1 GENERAL DESCRIPTION OF THE PROVINCES

The subdivision of the Canadian Shield into seven provinces and several sub-provinces is based primarily on overall differences in the internal structural trends and styles of folding observed. Where exposed, the position of the boundaries separating the various provinces is defined on the basis of truncation of structural features. Age determinations of rocks in the neighbourhood of the boundaries also plays a role in defining their locations. Where the boundaries are beneath the younger sedimentary cover, geophysical techniques have been used to trace their extent and position. Figure 3.1 is a simplified map of the provinces and sub-provinces of the Canadian Shield.

The Superior province is the largest of the tectonic subdivisions of the Canadian Shield. The oldest rocks found in the Superior province are generally volcanic and sedimentary rocks of Archean age. These formed in a series of easterly trending eugeoclines, and were last folded, faulted, and metamorphosed during the Kenoran orogeny, approximately 2.48 billion years ago. The Superior province is believed to be a remnant of an early Precambrian craton.

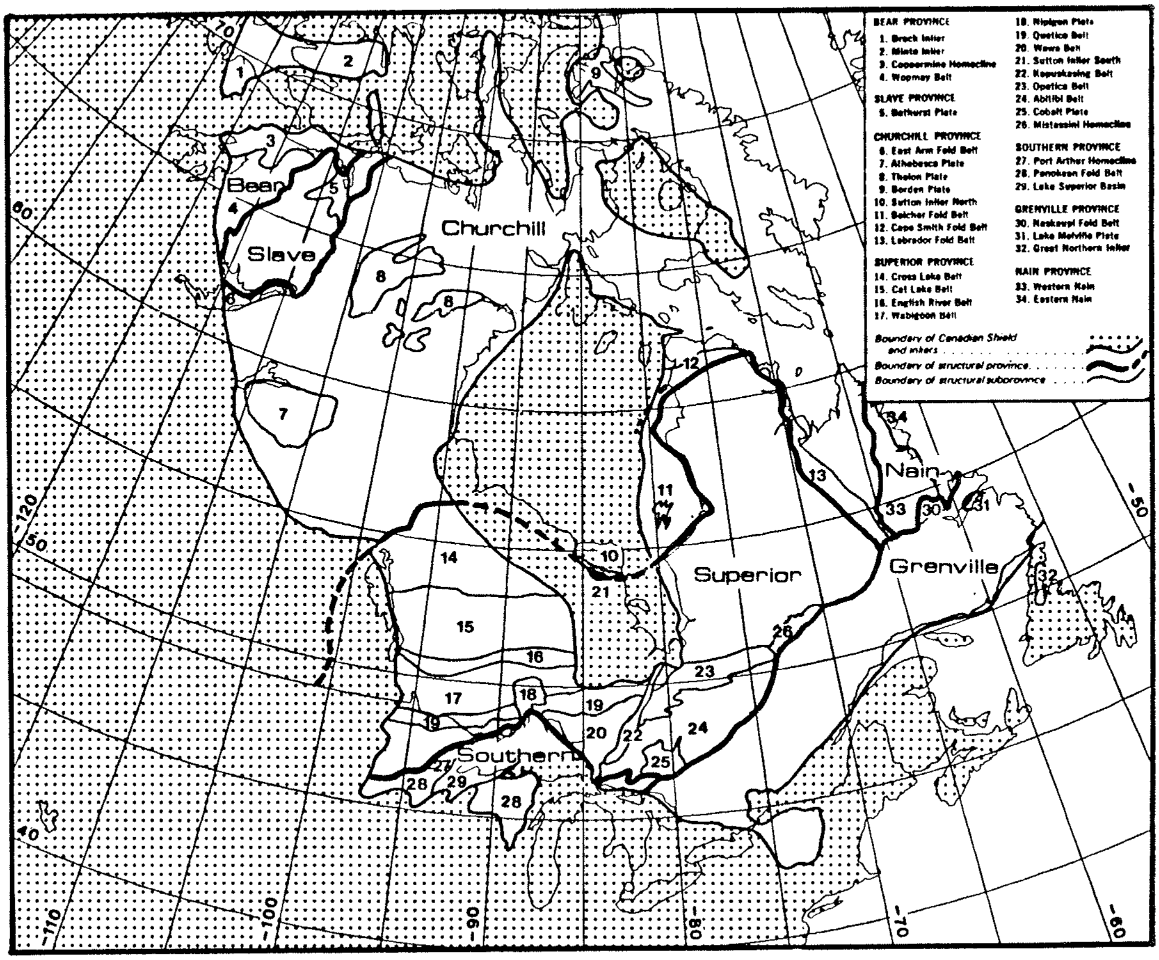

Figure 3.1: Structural Provinces of the Canadian Shield. (after Stockwell in: Douglas; 1970)

The Churchill province has some Archean rocks, most of which are mafic to intermediate volcanic flows and pyroclastics. Potassium-argon age determinations for most of the rocks in the Churchill province yield Hudsonian ages of approximately 1.735 billion years. Prior to the deposition of the Aphebian sediments, all of the Churchill province is thought to have been underlain by deformed Archean supracrustal and granitic rocks. A comprehensive discussion of the geological aspects of the two provinces may be found in Price and Douglas (1972) and Douglas (1970).

3.2 GEOPHYSICAL CHARACTERISTICS

Because of the economic importance and scientific interest, a considerable amount of research has been done on the boundary zone separating the Churchill and Superior provinces. The primary objectives of the geophysical studies undertaken recently have been to define the position, extent, and crustal structure of the zone. The characteristics of the boundary zone were originally established principally by regional geophysics, particularly aeromagnetic surveys. Recently, seismic and gravity studies have revealed much on the deep structure of the boundary zone.

3.2.1 Magnetic Studies

Green, Cumming, and Cedarwell (1979) compiled a magnetic anomaly map of southwestern Manitoba and southeastern Saskatchewan, primarily from aeromagnetic data obtained from oil companies. They identified three distinct magnetic regions:

1. An eastern region of high amplitude, E-W trending anomalies.
2. A central region of low the high amplitude, N-S striking anomalies.
3. A western region of relatively low amplitude anmomalies.

These were postulated to correspond with the magnetic anomaly patterns observed in profiles across the exposed boundary zone in northern Manitoba. Figure 3.2 illustrates the anomaly patterns observed, and the two profiles are illustrated in Figure 3.3.

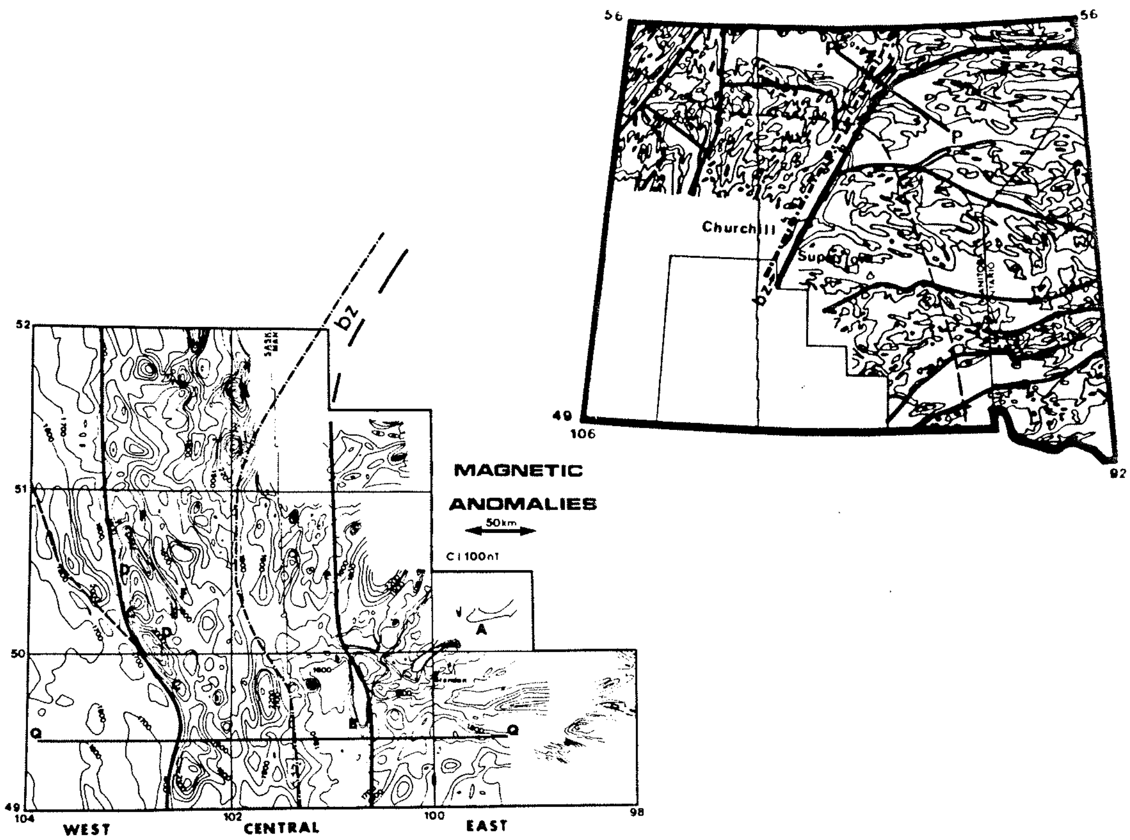

Figure 3.2: The Churchill-Superior boundary in southwestern Mantitoba. The two profiles P-P and Q-Q are illustrated in Figure 3.3. (from Green, Cumming, and Cedarwell; 1979)

Hall (1974) filtered existing aeromagnetic data to obtain the long- wavelength anomaly map illustrated in Figure 3.4. Although no immediately obvious correlation with the boundary zone is apparent,

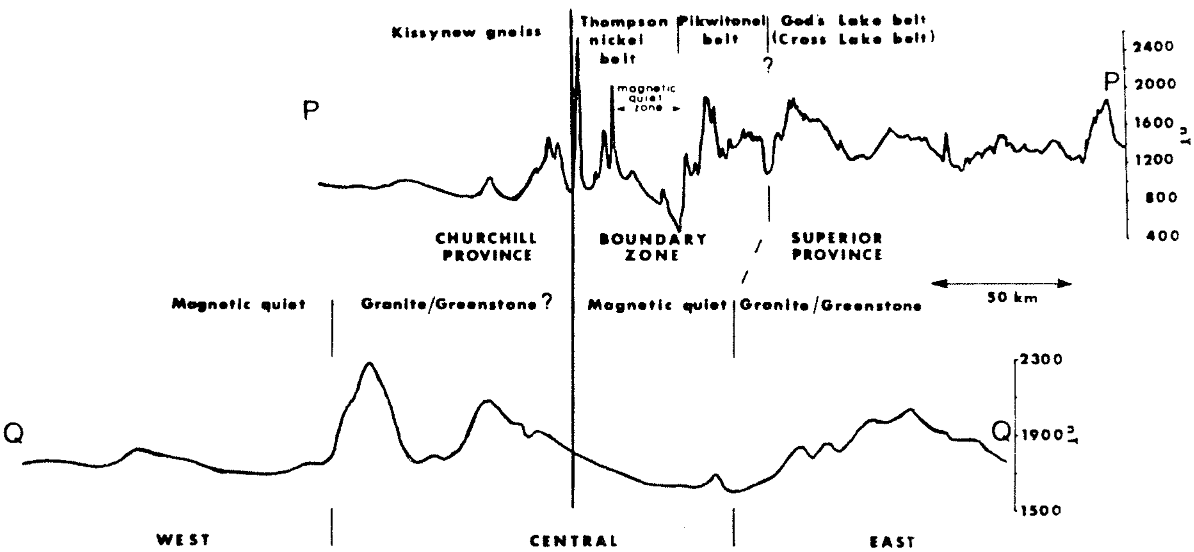

Figure 3.3: Aeromagnetic profiles of the Churchill-Superior boundary. Comparison of magnetic profiles P-P in northern Manitoba and Q-Q in southern Canada from Figure 3.2. Note the different scales on the ordinate axes of the two profiles. (from Green, Cumming, and Cedarwell; 1979)

the profile A-B plotted in Figure 3.5 illustrates the subtle change in amplitudes that occurs upon crossing the boundary zone. Relatively higher amplitude anomalies are more numerous on the Churchill side of the boundary, while lower amplitude anomalies are more prevalent on the Superior side.

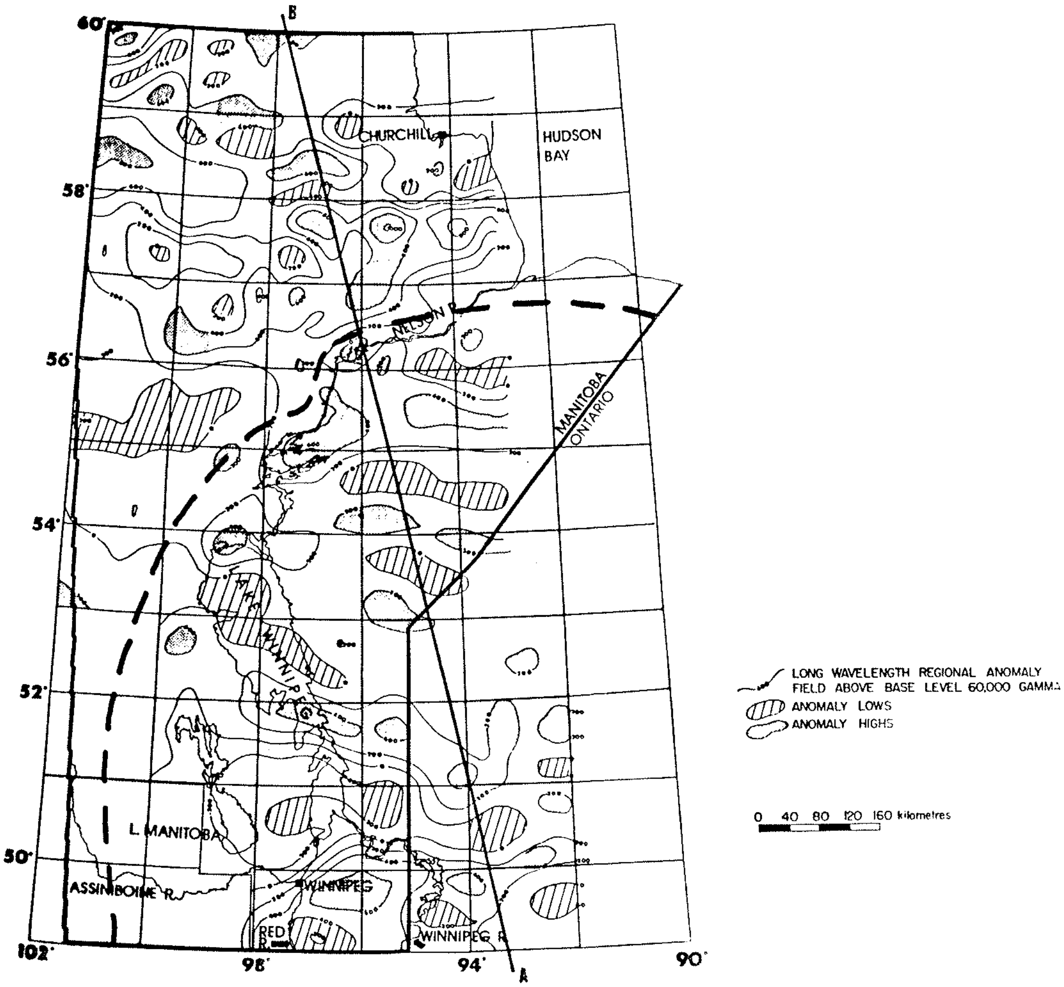

Figure 3.4: Long-wavelength aeromagnetic anomalies of Manitoba and northwestern Ontario. The broken line is the approximate location of the boundary zone separating the Churchill province to the north from the Superior province in the south-east. Profile A-B is shown in Figure 3.5. (after Hall; 1974)

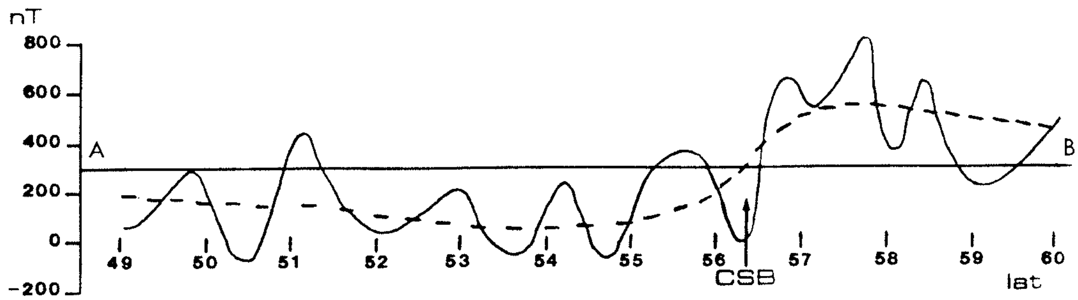

Figure 3.5: Long-wavelength aeromagnetic profile of the boundary. Anomaly profile A-B in Figure 3.4. Approximate location of Churchill-Superior boundary is shown with arrow. Trend of the anomaly profile is sketched in as dotted line.

3.2.2 Gravity Studies

Gibb and Thomas (1976) examined five gravity profiles, obtained from the published gravity maps of Canada. Two of the profiles were across the Churchill-Superior province boundary. All five profiles were found to be of a very similar nature and were interpreted as indicating a thicker, denser crust on the non-Superior side of the boundary. Thomas and Gibb (1977) examined two addtional profiles across the Cape Smith foldbelt (see Figure 3.1), and arrived at a similar model for the crustal structure. Mukhopadhyay and Gibb (1980) studied five gravity profiles across the Cape Smith foldbelt and the Belcher foldbelt of eastern Hudson Bay. Figure 3.7 compares the observed and calculated Bouguer gravity anomalies for one of the profiles, (illustrated in Figure 3.6), judged by Mukhopadhyay and Gibb to be representative of the crustal structure in the area.

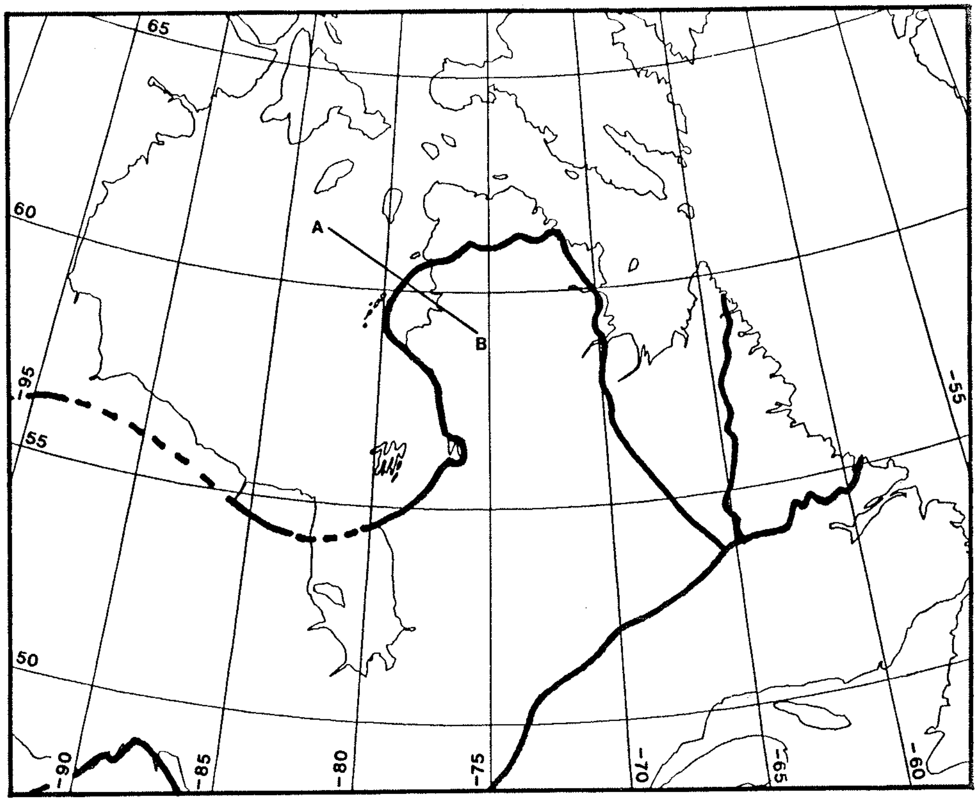

Figure 3.6: Gravity profile of Churchill-Superior boundary illustrated in Figure 3.7. This profile was considered representative of the crustal structure in the area. Approximate location of the province boundaries are taken from Figure 3.1. (after Mukhopadhyay and Gibb; 1980)

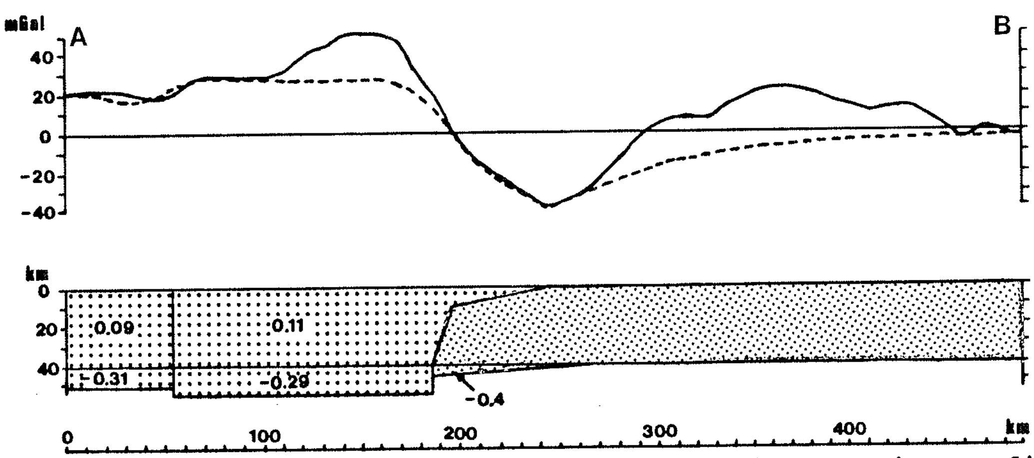

Figure 3.7: Churchill-Superior boundary model from gravity profile of Figure 3.6. Density contrasts are in g/cm^3, Superior province is on the right. Dash line is model signature. (after Mukhopadhyay and Gibb; 1980)

3.2.3 Seismic Studies

Seismic studies of the boundary zone structure have revealed the most detail. In July, 1977, the Consortium for Crustal Reconnaissance Using Seismic Techniques (CO-CRUST) group conducted a seismic study in southwestern Manitoba and southeastern Saskatchewan (Green et al; 1980). The location of their surveys is given in Figure 3.8, with their model of crustal structure in Figure 3.9. In conducting the survey, they used two reversed refraction - wide angle reflection profiles, as well as a much shorter 400% CDP near- vertical reflection survey. Figure 3.10 illustrates the CO-CRUST model merged with the results of Chandra and Cumming (1972). This profile clearly illustrates a step-like change in the thickness of the crust at a depth of approximately 45 kilometres, in agreement with the general structure proposed by Mukhopadhyay and Gibb (Figure 3.7).

Hall and Hajnal (1973) undertook a similar type of survey in northern Manitoba over the exposed part of the boundary zone. Their interpretations are summarized in Figure 3.12. Again, a thickening of the crust is evident on the Churchill side of the boundary. In particular, the lower crustal layer bounded by the Riel and Mohorovicic discontinuities thickens on the Churchill side.

Recently, DeLandro, Moon, and Green (1982) completed a detailed interpretation of the CO-CRUST data using ray-tracing techniques. Their interpretation has a gradual deepening of the Moho toward the Churchill side, with step-like changes in the depth of discontinuities in the upper crust. Their final crustal model is illustrated in Figure 3.13 (compare with Figure 3.9).

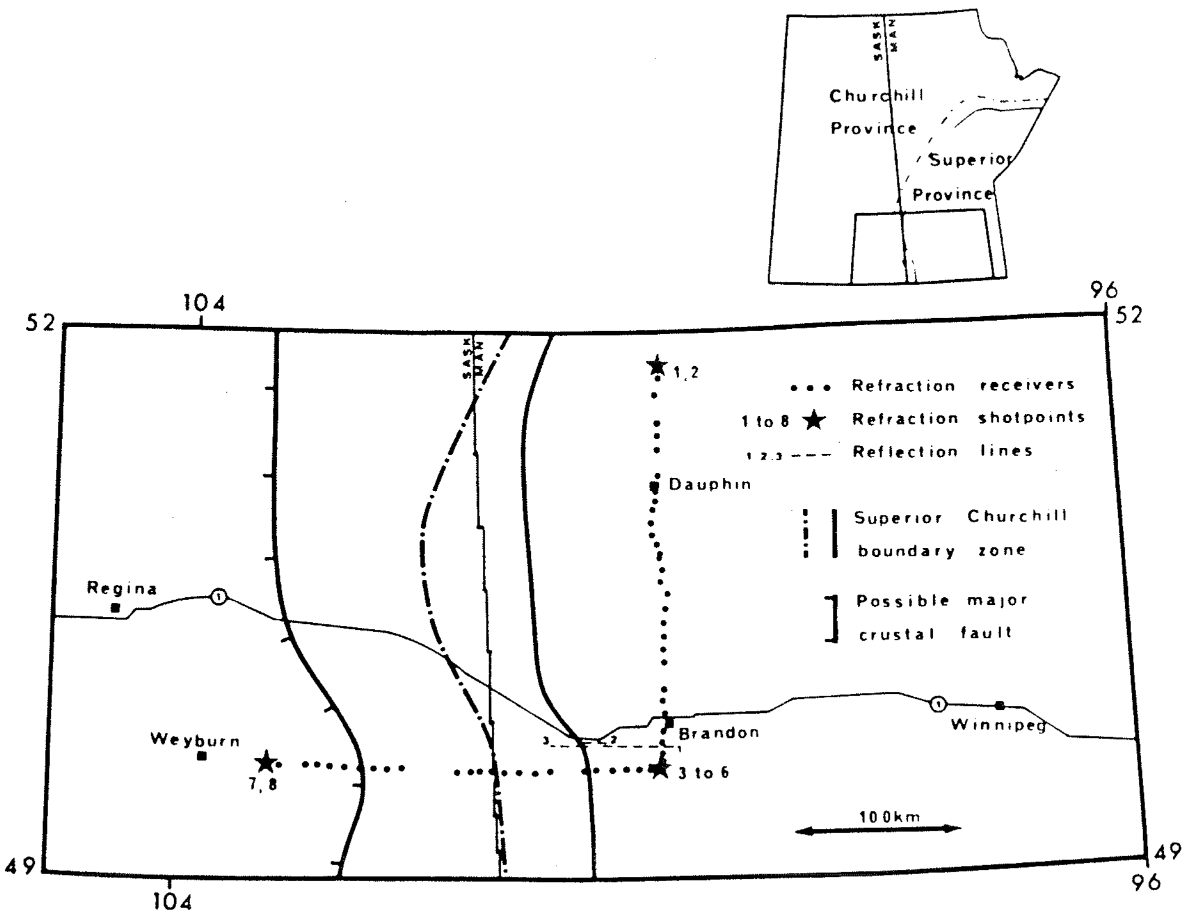

Figure 3.8: CO-CRUST survey lines. Locations of the CO-CRUST seismic surveys relative to the Churchill-Superior boundary zone. The boundary zone is that area bounded by the solid and dash-dot line. (from Green et al; 1980)

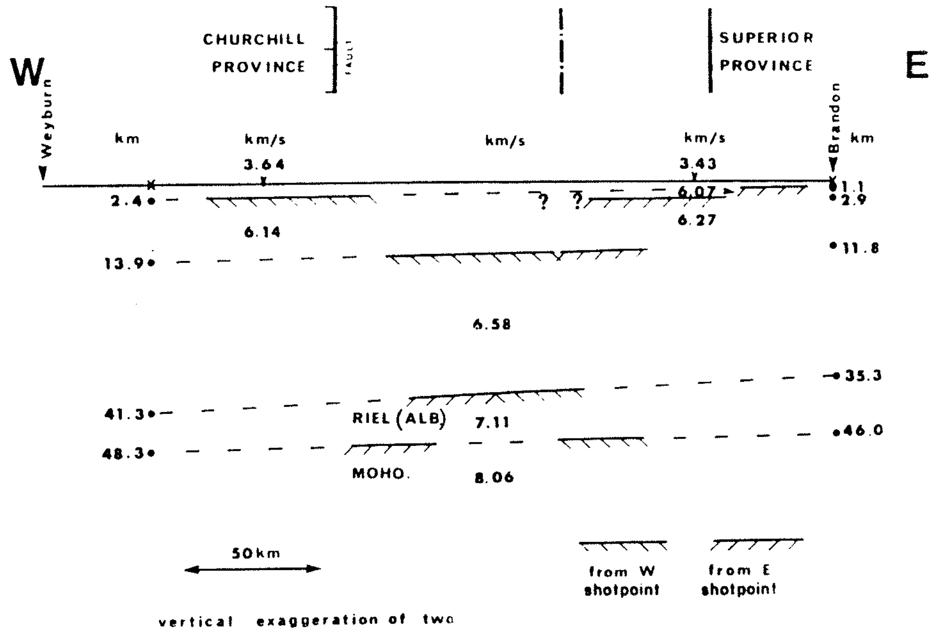

Figure 3.9: Churchill-Superior boundary model from CO-CRUST. Dipping layered model of the crustal structure determined from the CO-CRUST 1977 survey shown in Figure 3.8. (from Green et al; 1980)

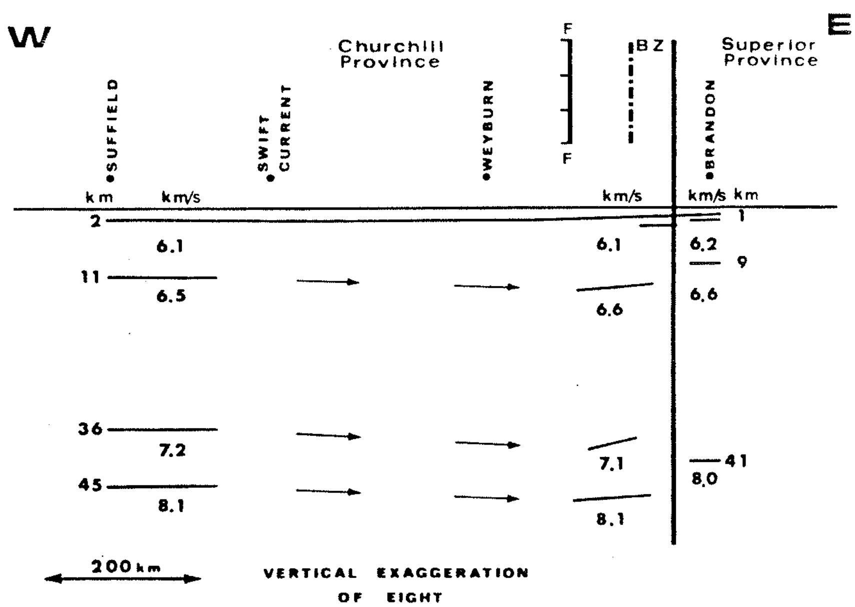

Figure 3.10: Crustal structure of provinces from CO-CRUST. Composite crustal structure from CO-CRUST and Chandra and Cumming (1972) models. (from Green et al; 1980)

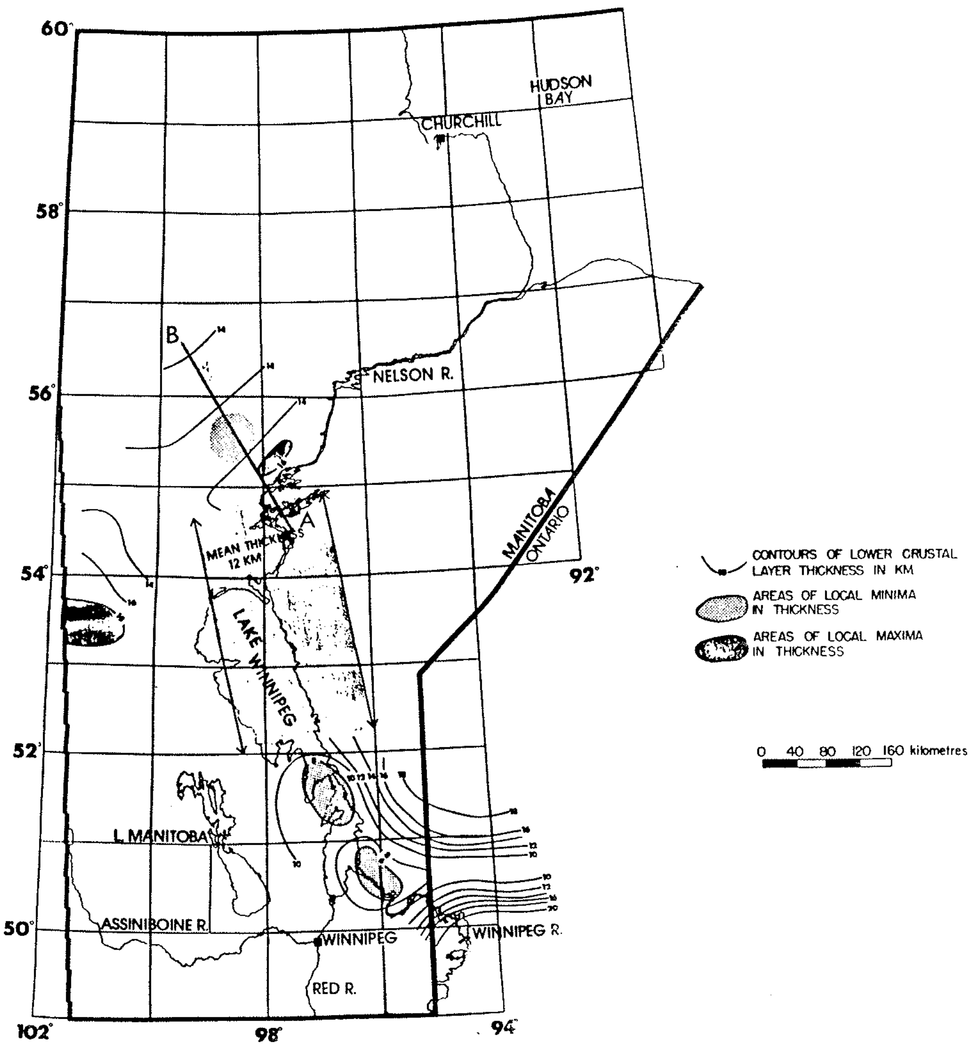

Figure 3.11: Thickness of the lower crustal layer in Manitoba. Profile A-B is illustrated in Figure 3.12. (from Hall; 1974)

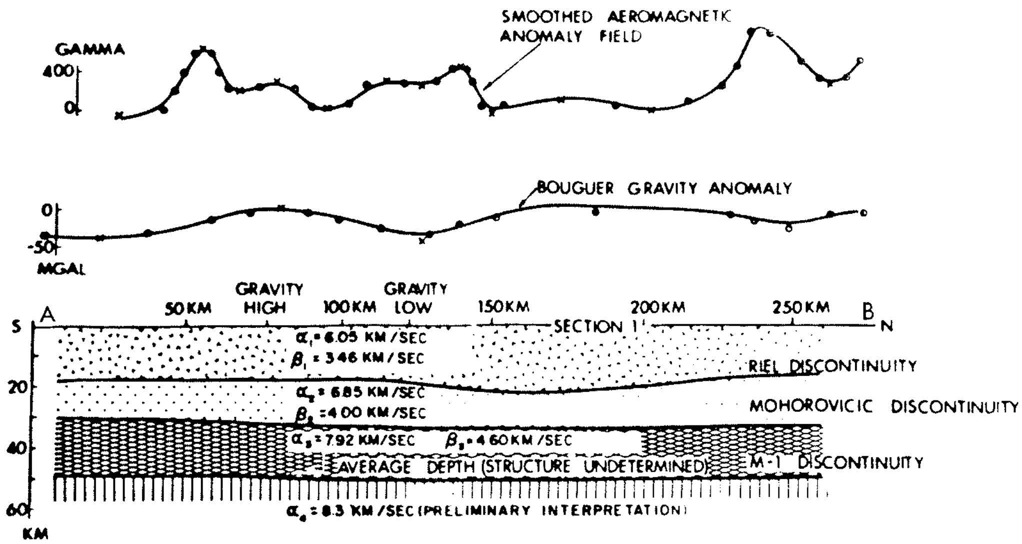

Figure 3.12: Crustal section across the Churchill-Superior boundary. Location of crustal section is illustrated in Figure 3.11. (from Hall and Hajnal; 1973)

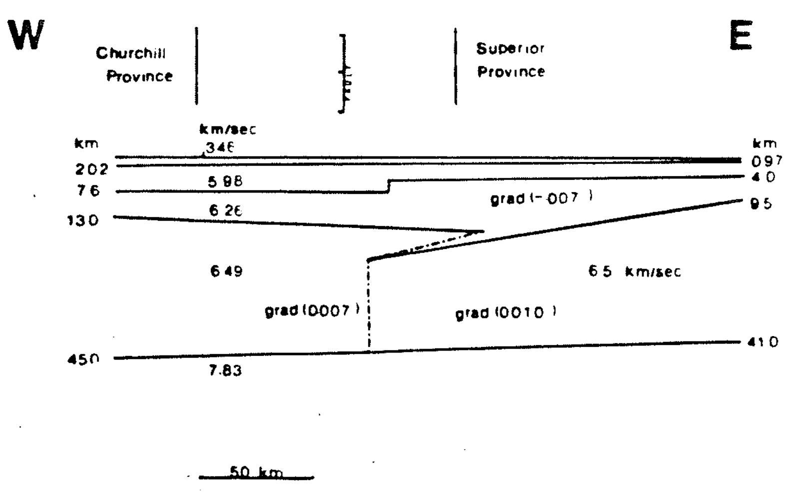

Figure 3.13: Ray-tracing model of the Churchill-Superior boundary. Crustal structure from the east-west profile of Figure 3.8. (from DeLandro, Moon, and Green; 1982)

Chapter IV

MODELLING CRUSTAL MAGNETIC ANOMALIES

Ku (1977) details a procedure for representing two or three dimensional solids of arbitrary shape as an array of equivalent-point dipoles. The method employed here is analagous to his development for rectangular prisms, with the exception that spherical prisms are used to define a magnetic body within the Earth's crust. The choice of spherical prisms rather than rectangular prisms is necessary since, in modelling the fields observed by a satellite, the Earth's curvature must be taken into consideration. Prisms are used instead of arbitrary shapes for computational simplicity.

4.1 THE MAGNETIC DIPOLE POTENTIAL

Figure 4.1 depicts the geometry involved in calculating anomaly fields due to a magnetic body. The magnetic scalar potential at P due to a single dipole at Q with magnetic dipole moment $\vec{M}$ is given by;

$$A = -\frac{\vec{M} \cdot \hat{R}}{4\pi R^2}$$

where $\hat{R}$ is the unit vector directed from P to Q. If Q is thought of as a point within a magnetic body of volume V, then the potential due to V is given by;

$$A = -\frac{1}{4\pi}\int_V \frac{\vec{J}\cdot\hat{R}}{R^2}\,dV$$

where $\vec{J}$ is the (uniform) magnetization of the body.

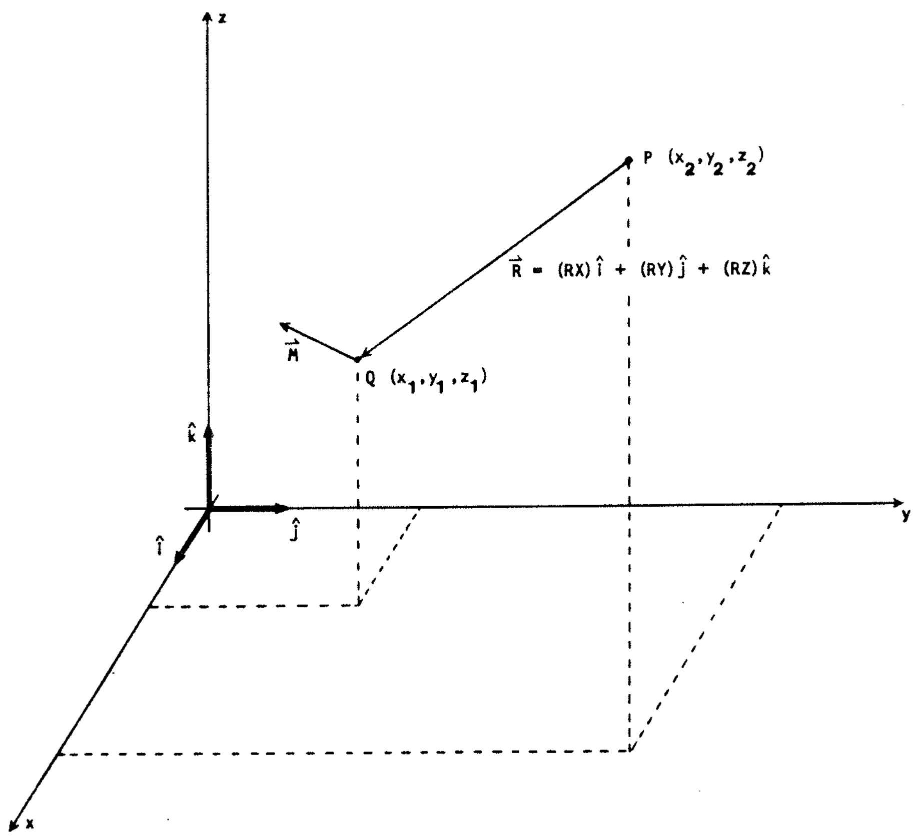

Figure 4.1: Geometry of Anomaly Calculations

If J_x, J_y, and J_z are the three components of magnetization, then;

$$A = -\frac{1}{4\pi}\int_V \frac{J_x\,(RX) + J_y\,(RY) + J_z\,(RZ)}{R^3}\,dV \qquad \ldots(1)$$

The three components of magnetic induction due to the body are taken to be the magnetic anomaly of the body. These are given as the negative directional derivatives of the magnetic potential A, multiplied by the permeability of free space;

$$\Delta X = -\mu_o \frac{\partial A}{\partial x_2} = \frac{\mu_o}{4\pi} \int_V \frac{\partial}{\partial x_2} \left\{ \frac{\vec{J} \cdot \vec{R}}{R^3} \right\} dV \qquad \ldots (2)$$

$$\Delta Y = -\mu_o \frac{\partial A}{\partial y_2} = \frac{\mu_o}{4\pi} \int_V \frac{\partial}{\partial y_2} \left\{ \frac{\vec{J} \cdot \vec{R}}{R^3} \right\} dV$$

$$\Delta Z = -\mu_o \frac{\partial A}{\partial z_2} = \frac{\mu_o}{4\pi} \int_V \frac{\partial}{\partial z_2} \left\{ \frac{\vec{J} \cdot \vec{R}}{R^3} \right\} dV$$

Differentiating the integrand of equation (1) with respect to x ;

$$\frac{\partial}{\partial x_2} \left\{ \frac{\vec{J} \cdot \vec{R}}{R^3} \right\} = \frac{\partial}{\partial x_2} \left\{ \frac{J_x (x_1 - x_2) + J_y (y_1 - y_2) + J_z (z_1 - z_2)}{\{(x_1 - x_2)^2 + (y_1 - y_2)^2 + (z_1 - z_2)^2\}^{3/2}} \right\}$$

$$= \frac{R^3 (-J_x) - \{J_x RX + J_y RY + J_z RZ\} \; \{3/2 \, (R^2)^{1/2} \; 2 (x_1 - x_2) (-1)\}}{R^6}$$

$$= \frac{J_x \{3 (RX)^2 - R^2\} + J_y \{3 (RX) (RY)\} + J_z \{3 (RX) (RZ)\}}{R^5} .$$

Substituting the above expression into equation (2) yields;

$$\Delta X = \frac{\mu_o}{4\pi} \int_V \frac{J_x \{3 (RX)^2 - R^2\} + J_y \{3 (RX) (RY)\} + J_z \{3 (RX) (RZ)\}}{R^5} dV.$$

Similarly;

$$\Delta Y = \frac{\mu_0}{4\pi} \int_V \frac{J_x\{3(RX)(RY)\} + J_y\{3(RY)^2 - R^2\} + J_z\{3(RY)(RZ)\}}{R^5} dV$$

$$\Delta Z = \frac{\mu_0}{4\pi} \int_V \frac{J_x\{3(RX)(RZ)\} + J_y\{3(RY)(RZ)\} + J_z\{3(RZ)^2 - R^2\}}{R^5} dV. \qquad \ldots(3)$$

Thus, the magnetic anomaly equations may be represented as a generalized equation;

$$\Delta F = \int f \; dV \qquad \ldots(4)$$

where f represents the integrand, dependent on the positions of P and Q, and on the magnetization vector $\vec{J}$.

4.2 GAUSS-LEGENDRE QUADRATURE

The function f of equation (4) may be numerically integrated in several ways. One such numerical integration technique is that of Gaussian quadrature. The simplest form of a quadrature problem is to construct an equality

$$\int_a^b f(x)\, dx = \sum_{i=1}^{n} w_i f(x_i) + T$$

where the truncation error T is as small as possible. This is accomplished by choosing the nodes x_i and weights w_i in such a way to make the approximation close enough that T may be neglected. In

Gauss-Legendre quadrature, the x_i are not equi-spaced, but are chosen so as to make the equation exact for a given polynomial of as high a degree as possible. This is achieved by normalizing the integration to the interval [-1,+1], and choosing the nodes x_1 , $x_2 \ldots x_n$ as the zeros of the Legendre polynomial of degree n. The weights w_1 , $w_2 \ldots w_n$ are then obtained by solving a set of n equations, and the approximation will be exact provided f is a polynomial of degree 2n-1 or less.

For example, let n=2, and use a dummy coefficient t;

$$\int_{-1}^{+1} f(t)\, dt \approx \sum_{i=1}^{2} w_i f(t_i)$$

$$\approx w_1 f(t_1) + w_2 f(t_2) \quad .$$

Suppose now that $f(t) = t^m$, where m = 0, 1, 2, 3. This leads to four exact equations (one for each function f);

$$0 = w_1 t_1^3 + w_2 t_2^3$$

$$2/3 = w_1 t_1^2 + w_2 t_2^2$$

$$0 = w_1 t_1 + w_2 t_2$$

$$2 = w_1 \cdot 1 + w_2 \cdot 1$$

Solving these equations gives $w_1 = w_2 = 1$, and $-t_1 = t_2 = 3^{-1/2}$. If the limits of integration are not [-1,+1], the transformation

$$x = \frac{(b-a)}{2} t + \frac{(b+a)}{2} \longrightarrow dx = \frac{(b-a)}{2} dt$$

yields;

$$\int_a^b f(x)\ dx = \frac{(b-a)}{2} \int_{-1}^{+1} f(t)\ dt \quad .$$

4.3 PHYSICAL SIGNIFICANCE OF THE GAUSSIAN QUADRATURE

In reducing an integration to a discrete summation, the magnetization of the body is treated as residing at discrete points rather than as a uniform distribution throughout the volume. The magnetization, then, is treated as a collection of point source dipoles located at the points within the prism dictated by the quadrature nodes. Thus, just as a spherical distribution of mass can be treated as a point mass at the sphere's centre, so can an arbitrarily shaped magnetic body be treated as a specified arrangement of dipole sources which are weighted in the manner dictated by Gaussian quadrature. Figure 4.2 illustrates a two dimensional circular sector containing a 2*2 array of dipoles, and their locations.

Note that in the limit as r approaches infinity and ϕ approaches zero, the circular sector and its dipoles become the rectangular array developed by Ku. In using three dimensional prisms, the dipoles are located at geocentric co-ordinates $(\rho_i, \phi_j, \lambda_k)$ where

$$\rho_i = \rho_a + \frac{\Delta\rho}{2} v_i$$

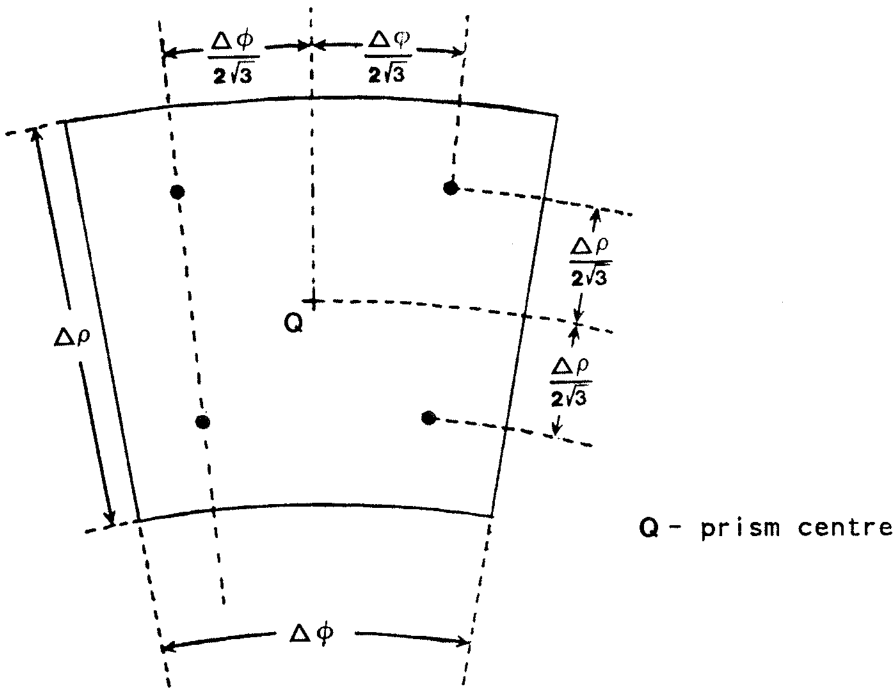

Figure 4.2: Dipole Locations in a Circular Sector

$$\phi_j = \phi_Q + \frac{\Delta \phi}{2} v_j$$

$$\lambda_k = \lambda_Q + \frac{\Delta \lambda}{2} v_k$$

where $i,j,k = 1,2$

and $v_m = \frac{(-1)^m}{\sqrt{3}}$, the Gaussian nodes.

In rectangular prisms, and for 2*2*2 arrays of dipoles, the weighting parameters are both equal to 1, i.e. each dipole represents an equal portion of the total volume element. However, in using spherical prisms, the volume element is not made up of eight equal portions. Rather, the outer and low latitude dipoles of a spherical prism represent a proportionally larger volume of the prism. This is accounted for in the summation by using the volume element $\Delta\rho\ \Delta\phi\ \Delta\lambda\ \rho_i^2 \sin\phi_j$ instead of $\Delta\rho\ \Delta\phi\ \Delta\lambda\ \rho_Q^2 \sin\phi_Q$. Again, in the limit as the spherical prism becomes rectangular, the arc-length positions of the dipoles are as Ku depicts.

4.4 EQUIVALENT DIPOLE SOURCES AND SPHERICAL PRISMS

The generalized anomaly equation (4) is a volume integration over a magnetic body of volume V. If this body is taken to be a volume element of a sphere, then equation (4) becomes;

$$\Delta F(P,Q) = \int\int\int f(P,Q)\ \{\rho^2 \sin\phi\ d\rho\ d\phi\ d\lambda\}$$

$$= \int\int\int g(P,Q)\ d\rho\ d\phi\ d\lambda$$

where ρ, ϕ, and λ are as shown in Figure 4.3 and

$g(P,Q) = f(P,Q)\ \rho^2 \sin\phi$.

Applying Gauss-Legendre quadrature to the above equation;

$$\Delta F(P,Q) = \frac{\Delta\lambda}{2}\sum_{k=1}^{n}\left[\frac{\Delta\phi}{2}\sum_{j=1}^{n}\left\{\frac{\Delta\rho}{2}\sum_{i=1}^{n} g(P,Q')\ w_i\right\} w_j\right] w_k$$

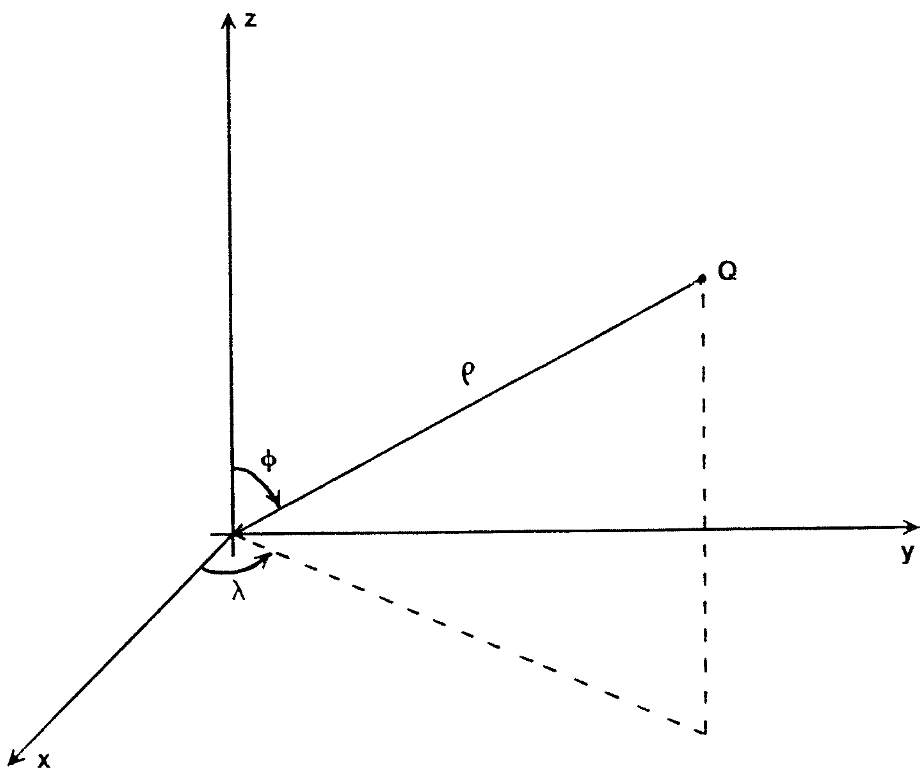

Figure 4.3: Geometry for Spherical Prisms

where $Q' = (\rho_i, \phi_j, \lambda_k)$, the co-ordinates of subdivision for the quadrature. For n = 2;

$$\Delta F(P,Q) = \frac{\Delta\rho\ \Delta\phi\ \Delta\lambda}{8} \sum_{k=1}^{2}\sum_{j=1}^{2}\sum_{i=1}^{2} f(\rho_i, \phi_j, \lambda_k, Q) \quad \rho_i^2 \sin\phi_j$$

and $\rho_i = \rho_Q + \dfrac{v_i \Delta \rho}{2}$

$$\phi_j = \phi_Q + \frac{v_j \Delta \phi}{2}$$

$$\lambda_k = \lambda_Q + \frac{v_k \Delta \lambda}{2} \qquad \ldots (5)$$

where $(\rho_Q, \phi_Q, \lambda_Q)$ are the co-ordinates of the centre of the prism of dimension $\Delta\rho$, $\Delta\phi$, $\Delta\lambda$, and $v_1 = -3^{-\frac{1}{2}}$, $v_2 = 3^{-\frac{1}{2}}$, the Gauss-Legendre quadrature coefficients. Thus, equations (3) become;

$$\Delta X = C_1 \sum_{i,j,k}^{2} C_2 \{J_x [3(RX_{ijk})^2 - R_{ijk}^2] + J_y 3 RX_{ijk} RY_{ijk} + J_z 3 RX_{ijk} RZ_{ijk}\}$$

$$\Delta Y = C_1 \sum_{i,j,k}^{2} C_2 \{J_x 3 RX_{ijk} RY_{ijk} + J_y [3(RY_{ijk})^2 - R_{ijk}^2] + J_z 3 RY_{ijk} RZ_{ijk}\}$$

$$\Delta Z = C_1 \sum_{i,j,k}^{2} C_2 \{J_x 3 RX_{ijk} RZ_{ijk} + J_y 3 RY_{ijk} RZ_{ijk} + J_z [3(RZ_{ijk})^2 - R_{ijk}^2]\}$$

where

$$C_1 = \frac{\mu_0}{4\pi} \frac{\Delta\rho \; \Delta\phi \; \Delta\lambda}{8}$$

$$C_2 = \rho_i^2 \sin\phi_j \quad R_{ijk}^{-5} \qquad \ldots (6)$$

where $\vec{R}_{ijk}$ is the separation vector from the observation point to the dipole corresponding to i,j,k in the prism, having x, y, and z components RX_{ijk}, RY_{ijk}, and RZ_{ijk} respectively. These components, and their resultant, will thus depend upon which of the eight dipoles is being considered, where the dipoles have co-ordinates $(\rho_i, \phi_j, \lambda_k)$ given by equations (5).

4.5 THE COMPUTER ALGORITHM

The method employed in the computer program involves defining a three-dimensional arrangement of spherical prisms at or below the Earth's surface in geodetic or "map" co-ordinates. The anomaly due to the specified arrangement is calculated at each point on a two-dimensional observation grid at a specified altitude. Both the prism grid and the observation grid are approximately spherical, being defined in geodetic co-ordinates.

All calculations are carried out in the Earth-fixed cartesian co-ordinate system having origin at the centre of the Earth, z-axis coincident with the north rotational axis, and x-axis through the Greenwich meridian. The Earth's magnetic field vector is calculated at each prism centre using the MGS481#2 spherical harmonic model obtained from the MAGSAT Investigator B tapes. The magnetization of the prism is assumed to be entirely induced, and is then calculated as;

$$\vec{J} = \left\{\frac{k}{k+1}\right\} \frac{\vec{B}}{\mu_o}$$

where k is the susceptibility of the prism

$\vec{B}$ is the Earth's field at the prism centre

and μ_o is the permeability of free space .

The vector anomaly components for a single dipole of the prism are calculated at each observation grid location, and the component anomalies summed over the eight dipoles. The procedure is then repeated for each prism in the arrangement.

The scalar anomaly is obtained in one of two ways. Strictly, the scalar anomaly will be the dot product of the vector anomaly at a given observation point with a unit vector in the direction of the Earth's main field at that point. This involves calculating the Earth's field at each point of the observation grid, which may be costly in terms of computing time. Alternatively, the Earth's field may be calculated at the centre of the observation grid, and then assumed to have the same north, east, and vertical components over the entire grid. The validity of this assumption will, of course, depend on the size and location of the observation grid.

Program SPEPS (Spherical Prism Equivalent Point Source) (Appendix A) is a refinement of an earlier program SPHPRISM (Hall and Miller; 1980). The method employed is similar to that of von Frese, Hinze, Braile, and Luca (1981) with the exception that their procedure accomodates a changing susceptibility within the body. As in Ku's approach (1977), von Frese et al (1981) utilize arbitrary shapes made up of l*m*n arrays of dipoles. As well, their technique uses geocentric co-ordinates thoughout, rather than geodetic, geocentric, and Earth-fixed.

4.6 CHARACTERISTICS OF THE MODELLING TECHNIQUE

It can be seen from equations (3) that the anomaly calculation involves the product of magnetization and volume. The anomaly fields, then, contain an ambiguity involving these two quantities; a small volume with large magnetization "looks" the same as a larger volume with a smaller magnetization. This, of course, is within certain limits. The areal extent of a magnetic body may be limited according to the shape and extent of the target anomaly, but the depth and magnetization are mutually indeterminant for satellite observed fields. In most applications, the ambiguity is dealt with by setting one or other of the depth and magnetization at a fixed value, and calculating the variation required in the unfixed quantity to model the fields observed. Mayhew and Galliher (1982) , for example, calculated the magnetization distribution required to model the observed MAGSAT anomaly field, based on a uniform 40 kilometre thick magnetic crust. One may just as easily fix the magnetization at, say, 5 amperes per metre, and calculate the depth variations required to model the field.

Chapter V

THE MAGSAT SIGNATURE OF THE CHURCHILL-SUPERIOR BOUNDARY

Since the Churchill and Superior provinces are structurally very different, it was proposed that the boundary should give rise to a magnetic expression or "signature" which ought to be observable in MAGSAT data. Comparing Figures 2.3 and 3.1, it is apparent that, with the exception of the Circum-Ungava foldbelt, the Churchill-Superior boundary is very nearly coincident with the locus of maximum auroral activity. The large anomaly centred over the east coast of Hudson Bay (Figures 2.13 to 2.15) precluded examination of data in that region for the purposes of boundary studies. Thus, only data west of -80 degrees longitude could be considered. The problem of eliminating current effects, then, was the primary consideration in attempting to identify a crustal boundary signature.

5.1 DATA SELECTION

The INV-B dataset contained over 3400 passes of data. Initial data selection was on the basis of latitude and longitude of the satellite. Data points outside of the area bounded by 40 to 80 degrees north latitude and by -140 to -50 degrees east longitude were deleted in the formation of a new dataset. Secondly, data was eliminated on the basis of the Kp index of global magnetic activity. Although intended primarily for low latitudes, the Kp index was the only measure available with which to judge magnetic activity. Passes having ascending or descending node Kp indices of greater than 10 were rejected. Passes for further consideration were then selected from this set according to their proximity to the Churchill-Superior boundary. Two groups were created:

1. Dusk passes - having descending longitude of between 70 and 102 degrees.
2. Dawn passes - having descending longitude of between -120 and -95 degrees.

The two sets contained 64 and 41 passes respectively. The two groups were further subdivided on the basis of whether or not they crossed the boundary between -98 and -80 degrees east longitude. Thus, four datasets were created:

1. Dusk Hits
2. Dusk Misses
3. Dawn Hits
4. Dawn Misses

The purpose in creating the four separate datasets was to isolate effects of the ionospheric currents. If observed signatures were due to currents, the Hits should be similar to the Misses, and the Dawn passes similar, but of oposite polarity, to the Dusk passes. Conversly, if effects were due to the bcundary, the Dawn Hits would

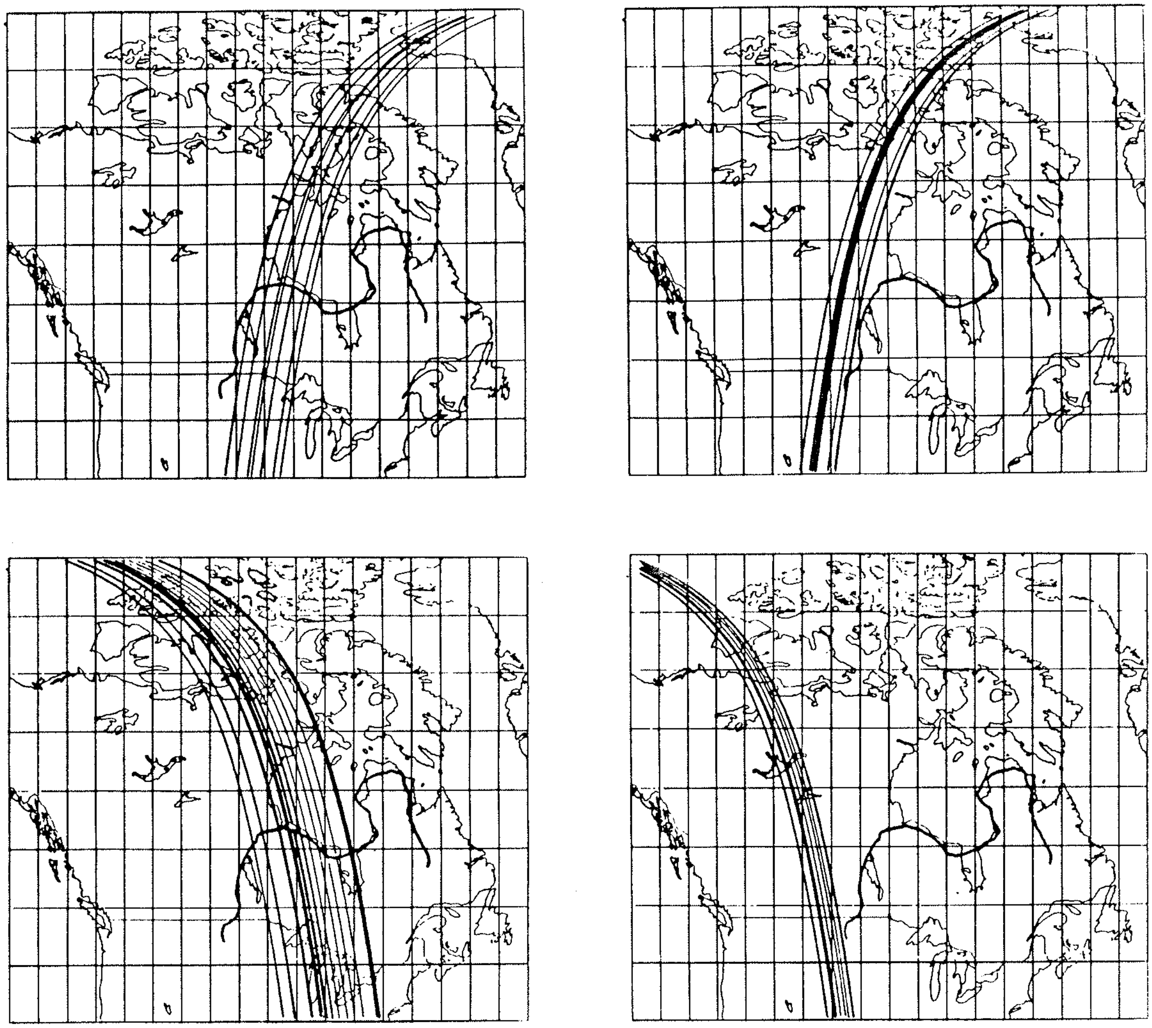

Figure 5.1: Dawn Hits, Dawn Misses, Dusk Hits, and Dusk Misses. Latitude-longitude plots of the passes accepted for further processing. The four datasets are named as Dusk or Dawn and as Hits or Misses in accordance with magnetic local time of the pass, and whether or not the pass crosses the Churchill-Superior boundary (illustrated as the heavy line in the centre of the plots). Dawn passes are at top, Hits are on the left. Plots are on a 5 degree Cartesian grid.

resemble the Dusk Hits, and the Misses of both types would not necessarily resemble each other or the Hits.

Plots of the North, East, Vertical, and Scalar anomalies of each of the passes in the above four datasets were then examined. In view of the effects of Birkeland currents (Chapter 2), particular attention was given to the East component anomaly. Passes having horizontal components judged too severe in their fluctuation were rejected. The vertical anomalies of the remaining passes were intercompared for similarity in both amplitude and character of variation. Any passes not displaying characteristics similar to the others in the dataset were rejected. Of the 45 passes remaining of the over 3400, 19 were Dusk Hits, 8 were Dawn Hits, 10 were Dawn Misses, and 8 were Dusk Misses. Figure 5.1 illustrates the latitude-longitude plots of the passes accepted for further processing. As can be seen from Figure 5.1, the selected passes are evenly spaced across the boundary. As well, they are well distributed temporally, the four datasets spanning 143, 122, 131, and 122 days respectively. Short term current systems, then, are not well represented. Only long term current systems and crustal sources have a significant contribution to the datasets. As noted by Coles et al (1982), the dusk passes were considerably quieter than the dawn passes. Initial data selection was for Kp=0, but this allowed only two dawn passes to be considered.

5.2 DATA PROCESSING

Since the ever-present Birkeland currents affect the horizontal components to the greatest degree, all further processing utilized the vertical component only. The vertical anomaly fields examined were the result of subtracting the modelled vertical component (ZM in Table 2.1) from the 80 Chronicle point average vertical measurements (ZA in Table 2.1). The 80 point average fields were chosen to avoid difficulties arising in anomalous points and very short-term variations due to currents extremely local to the satellite. To simplify further processing, geodetic latitude was chosen as the abscissa, and was given a uniform latitude increment of 0.25 degrees. All INV-B measurements were then interpolated using a modified cubic spline to conform with this latitude increment. (The original increment was approximately 0.3 degrees, but varied with latitude.)

Several processing options were then applied in various combinations. A least-squares polynomial function was fit to the individual passes, and then subtracted from them. A Butterworth bandpass filter of various pass bands was applied to the data. "Static corrections" were applied to align the Hits according to the specific latitude at which they crossed the boundary and, finally, the arithmetic mean (stack) of the datasets was computed. The most successful of the various combinations is outlined below:

1. A least squares linear function was removed from the raw anomalies. The linear function served to remove random effects

of long-wavelength anomalies due to magnetospheric current systems, and to correct for variations in the altitude of the satellite. Many authors remove a least-squares quadratic to improve internal consistency in the data. A quadratic function was found to remove too much signal on data of such a short extent (40 degrees latitude).

2. The traces were bandpass filtered. The Butterworth filtering process involved filtering forward through the trace, then filtering in reverse. This forced the endpoint of the trace (at 80 deg. lat.) to be equal to zero, inducing high amplitude, short wavelength artificial anomalies at the end of the traces. Removing the linear trend prior to filtering alleviated this problem considerably. The passband used allowed "wavelengths" of from 5 degrees latitude to 90 degrees latitude to be retained, and thus acted as a "high-cut" filter.
3. The Hits were static corrected such that the Churchill-Superior boundary was located at 56 degrees latitude on the resulting plots.
4. The linearly adjusted, filtered, static shifted traces were then stacked to produce an average trace for each of the four datasets.

The various stages of processing are summarized in Figures 5.2 to 5.5.

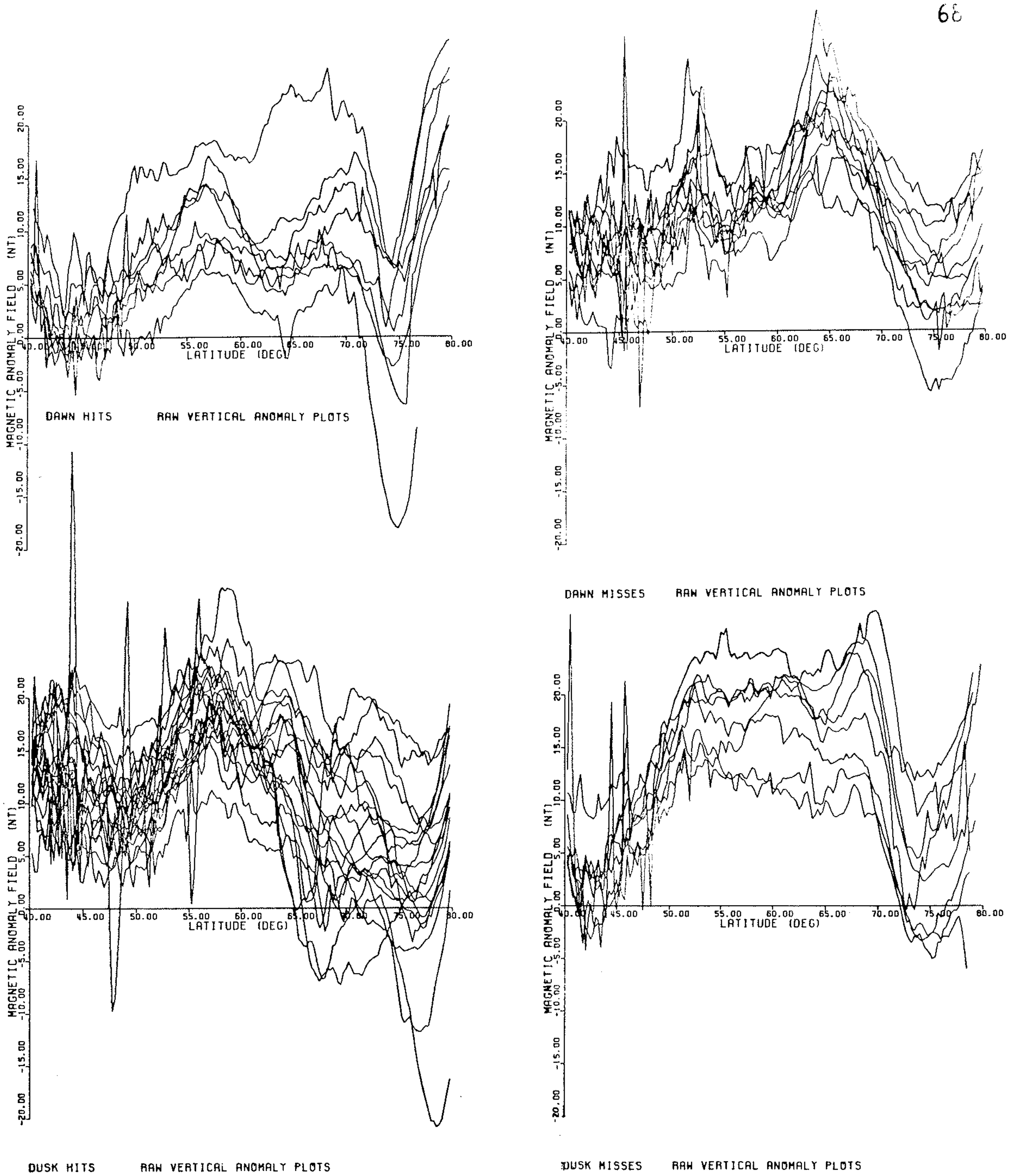

Figure 5.2: Raw anomaly plots for the four datasets. The residuals were obtained by removing the MGS481#2 spherical harmonic field model from the 80 point Chronicle averages for the vertical component.

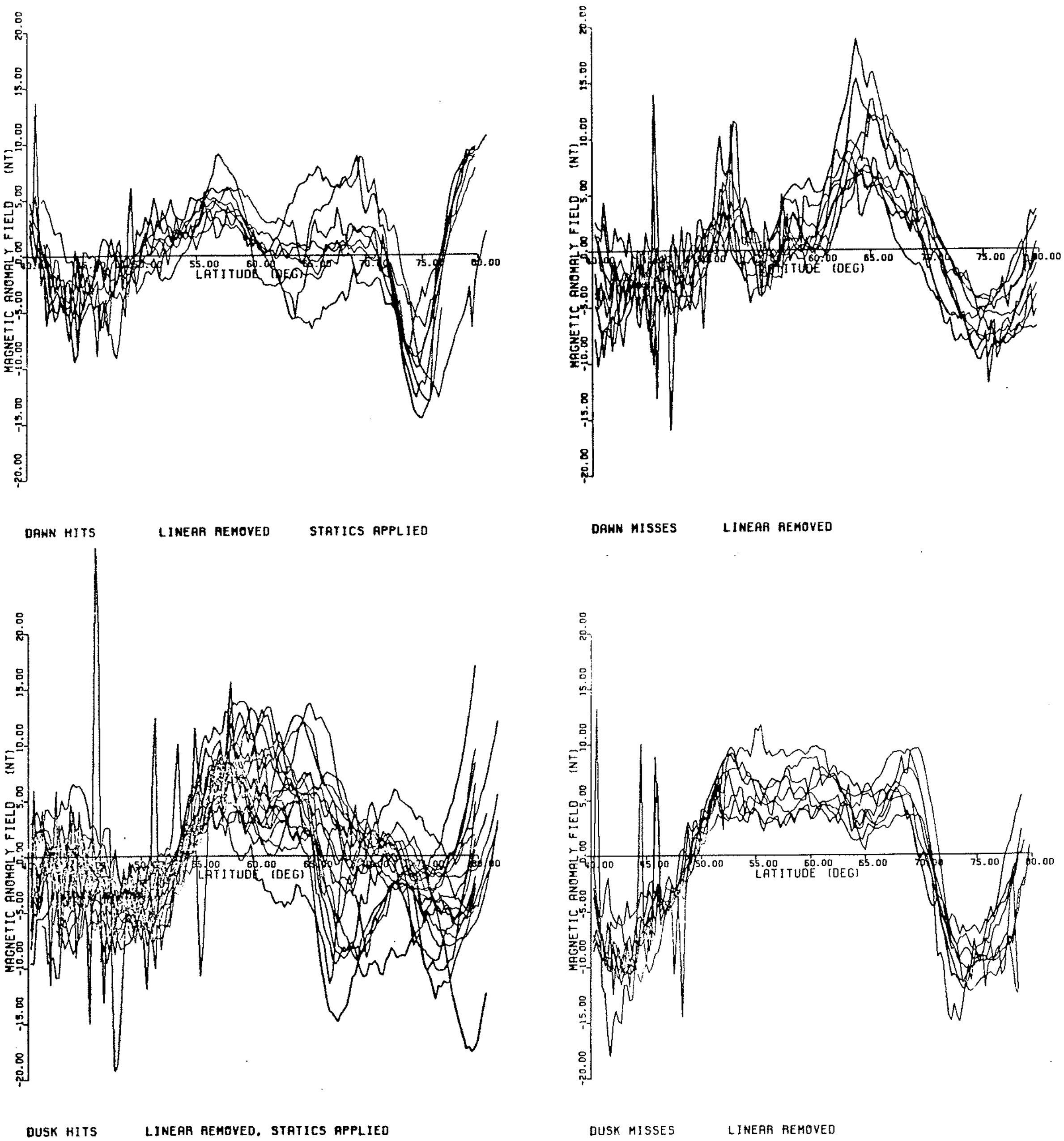

Figure 5.3: Raw anomalies with linear removed. Vertical anomalies of Figure 5.2 with least-squares linear fit individually calculated and removed. "Static corrections" have been applied to the Hits such that the Churchill-Superior boundary occurs at 56 degrees latitude.

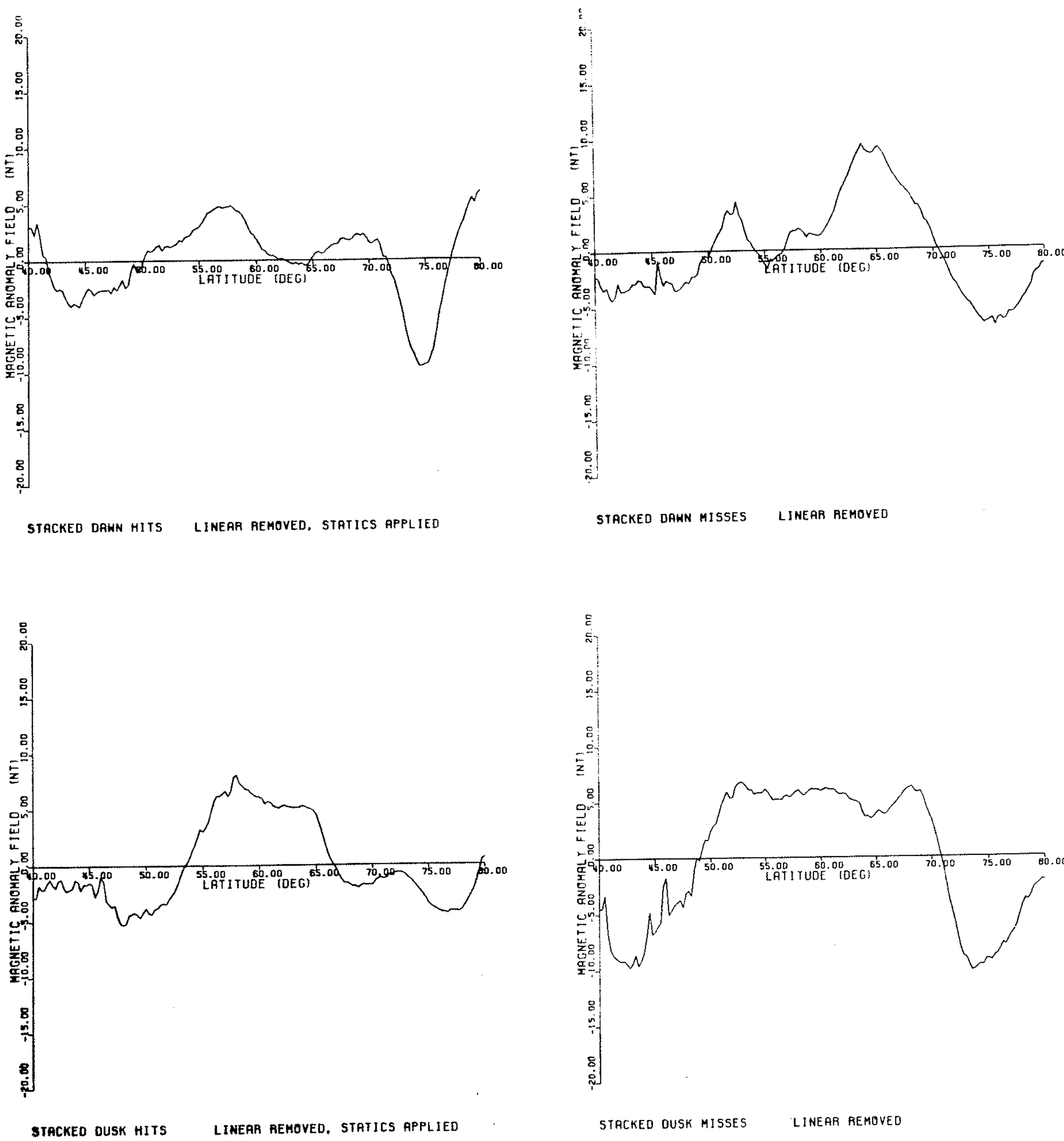

Figure 5.4: Average anomaly profiles. Stacked vertical anomalies of Figure 5.3.

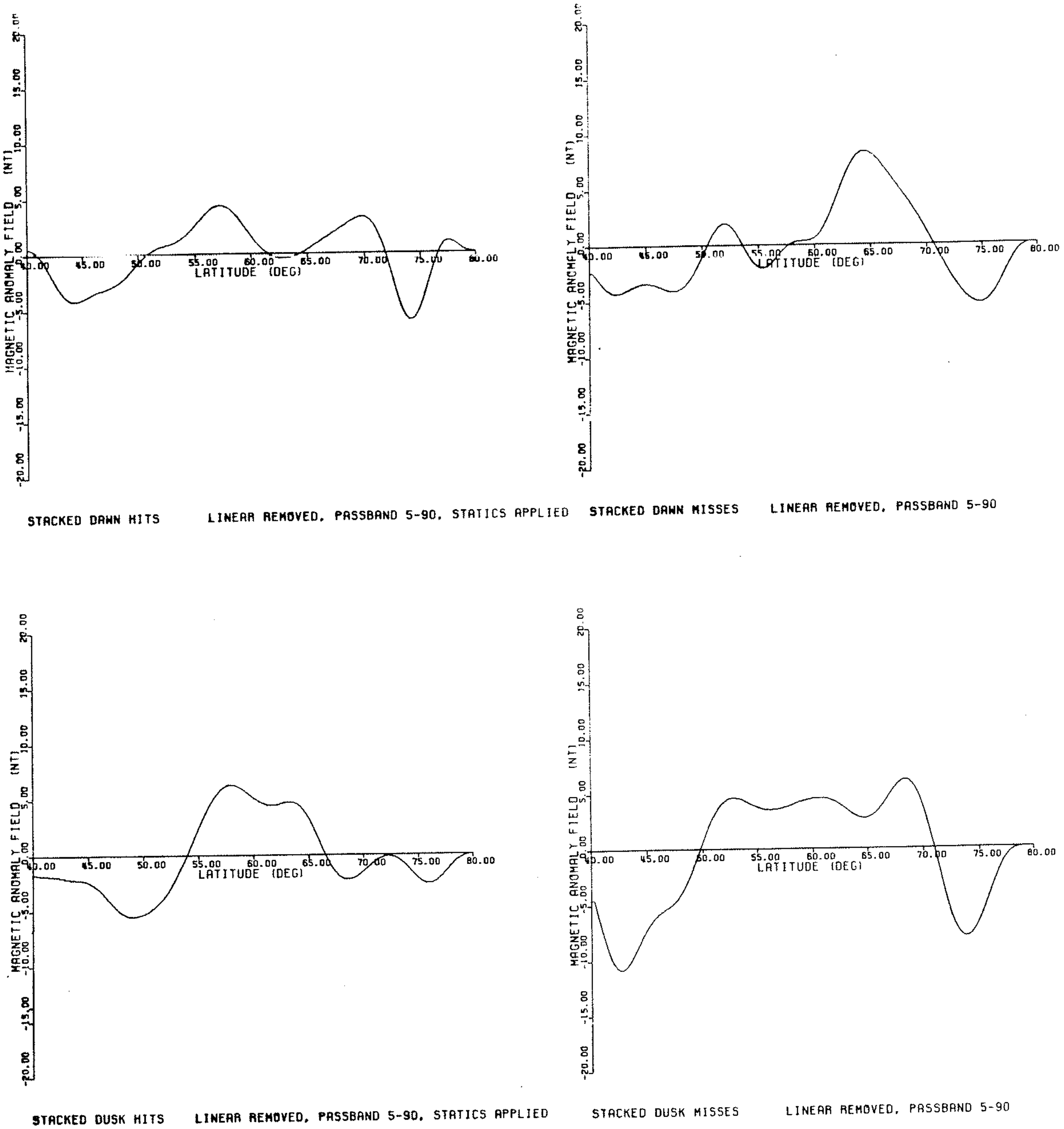

Figure 5.5: Filtered average anomaly profiles. As in Figure 5.4, with a Butterworth bandpass filter applied to individual profiles prior to stacking. The passband allowed "wavelengths" of from 5 degrees to 90 degrees latitude to be retained.

5.3 SIGNATURE INTERPRETATION

As mentioned earlier, ionospheric currents formed the most significant obstacle in detecting a boundary signature. As an additional test designed to reveal current sources, the four datasets were plotted against magnetic latitude instead of geodetic latitude. As discussed in Chapter 2, the ionospheric current systems are a virtually permanent feature of high latitudes, and are distributed according to magnetic local time and magnetic latitude. Stacking the profiles according to magnetic latitude would tend to reinforce any current signatures present. As can be seen from Figure 5.6, this procedure had the effect of "compressing" the anomaly profiles, but did not significantly alter their relative differences. This, then, suggests the differences and similarities observed are probably related to crustal structure, and are not influenced greatly by ionospheric currents.

The Dawn Hits and Dusk Hits were then merged into one dataset and processed together to produce the Churchill-Superior boundary (CSB) signature illustrated in Figure 5.7. Due to the large differences in their spatial positions (Figure 5.1), it is expected that the CSB Hits will have a great deal of variation except where they cross the boundary, adjusted to be 56 degrees latitude. Stacking the Dawn with the Dusk traces would also tend to cancel effects from current systems, due to the reversal in polarity detailed in Chapter 2. The CSB Hits signature bears little resemblence to either of the Misses

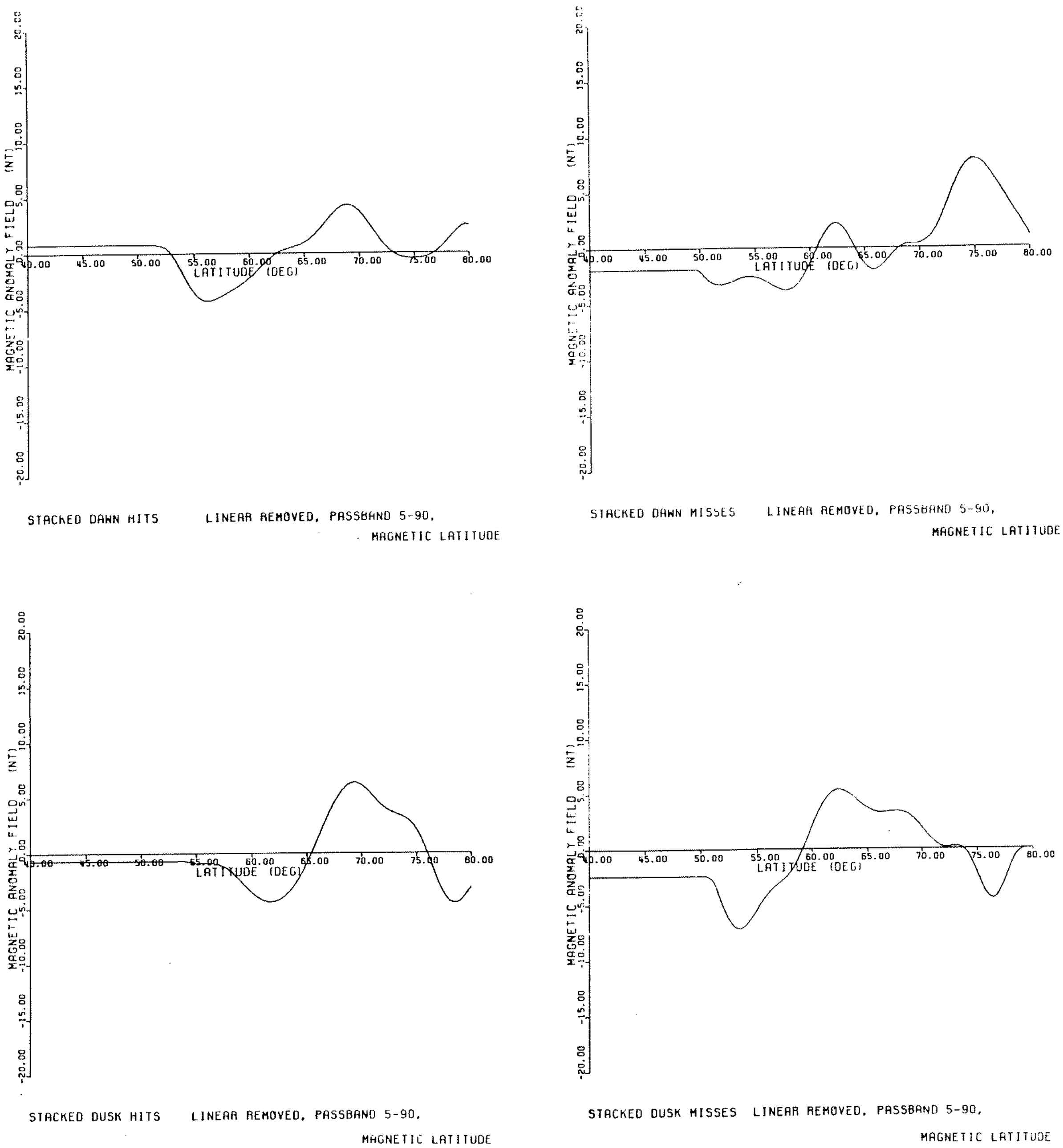

Figure 5.6: Magnetic latitude profiles of average filtered traces. Current signatures should occur at the same magnetic latitude on the four plots, with reversed polarity in the dawn and dusk datasets. The Churchill-Superior boundary occurs at approximately 67 degrees magnetic latitude.

datasets. Note particularly the latitude of the crossover and the peak at approximately 57 degrees. This signature, then, is taken to be the result of a change in crustal structure encountered at, or near, the Churchill-Superior boundary.

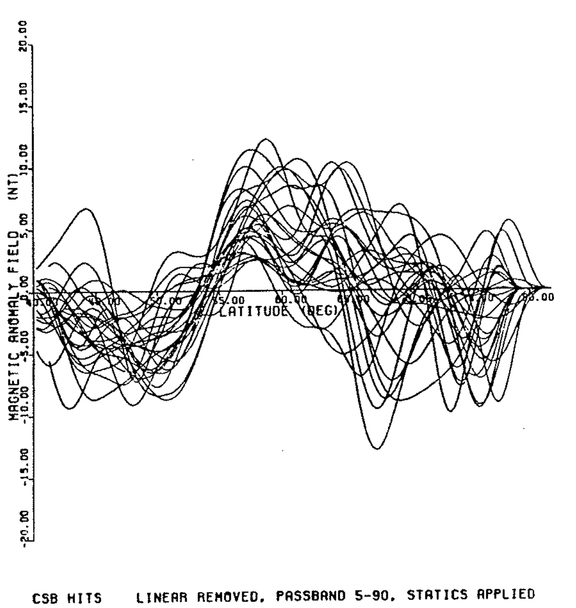

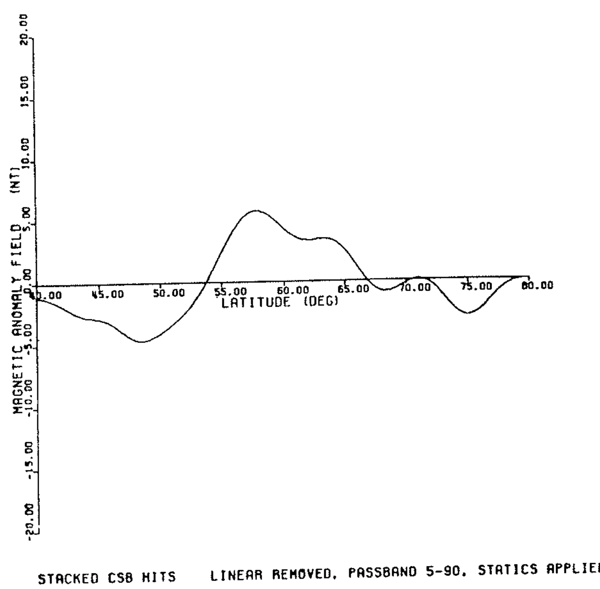

Figure 5.7: Churchill-Superior boundary MAGSAT signature. Both Dawn and Dusk Hits of Figure 5.3 filtered and stacked. Large variations except near 56 degrees (CSB latitude) are expected.

Modelling the CSB signature employed the program SPEPS (Appendix A). As outlined in Chapter 4, this program utilized the Spherical Prism Equivalent Point Source technique. In view of the various models of the boundary structure from both gravity and seismic results (Chapter 3), a step-like discontinuity was used to approximate the crustal structure. The simplified model involved defining the susceptibility in the region confined by a Riel-like boundary above and a Moho-like boundary below. The susceptibility value was such that the magnetization of the layer was approximately 5 amperes per metre. The thickness of this magnetic layer was then altered, as was the size and location of the step. In order to eliminate edge effects, the two provinces were represented as "infinite" hemispherical plates having a boundary at 55 degrees latitude. The step-like changes were arranged to increase the thickness of the magnetic layer on the Churchill side of the boundary; a step up in the Riel, or a step down in the Moho. The average thickness of the layer (no step) was varied between 20 and 2 kilometres, and the depth to Riel was varied between 20 and 0 kilometres. Figure 5.8 illustrates such a model, incorporating a four kilometre step down in the Moho and an average magnetic layer thickness of 12 kilometres.

Since the MAGSAT signatures had a least-squares linear fit removed, the anomaly profiles were relative to an artificial zero. This effect was mimicked in the modelling procedure by calculating the field due to a uniform magnetic layer without the step, and subtracting this field from the field calculated for the layer incorporating the step. The uniform layers used corresponded to the average thickness of the step layers. The uniform layer anomaly fields were essentially a linear bias. It was found that the depth of the magnetic layer could not be discriminated once this bias was re-

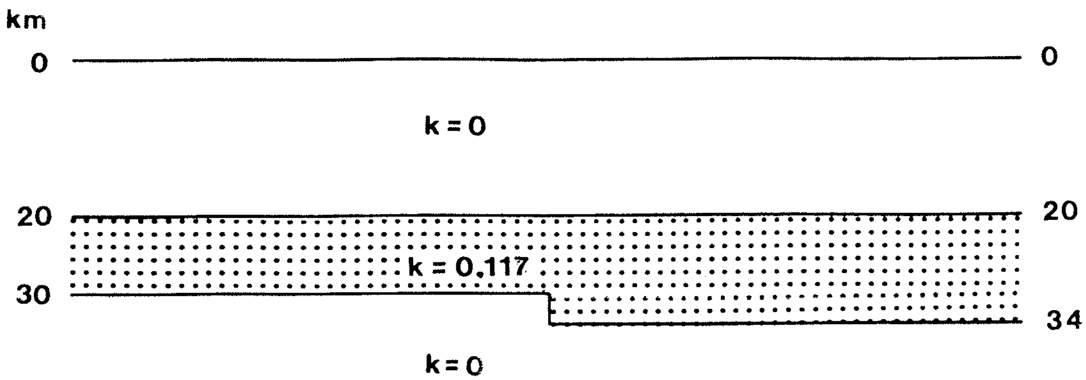

Figure 5.8: Simple crustal model of the Churchill-Superior boundary. The Churchill province is on the right. The susceptibility of 0.117 gives rise to a magnetization of 5.00 amperes per metre for an induction field of 60,000 nanotesla.

moved; a magnetic step-layer at the surface produced virtually the same amplitude anomaly as a step-layer 30 kilometres deep. As well, a step up in the Riel gave the same result as a step down in the Moho. The amplitude of the modelled signature, however, was sensitive to the size of the step; a four kilometre step produced an anomaly approximately twice the amplitude of a two kilometre step. The bias level of the uniform layer signature gives an indication of the thickness of the magnetic layer. A twenty kilometre uniform layer having a magnetization of approximately 5 amperes per metre produced a bias field of approximately 17 nanotesla. The lack of sensitivity to depth of magnetization is to be expected since the observation altitude is 400 kilometres.

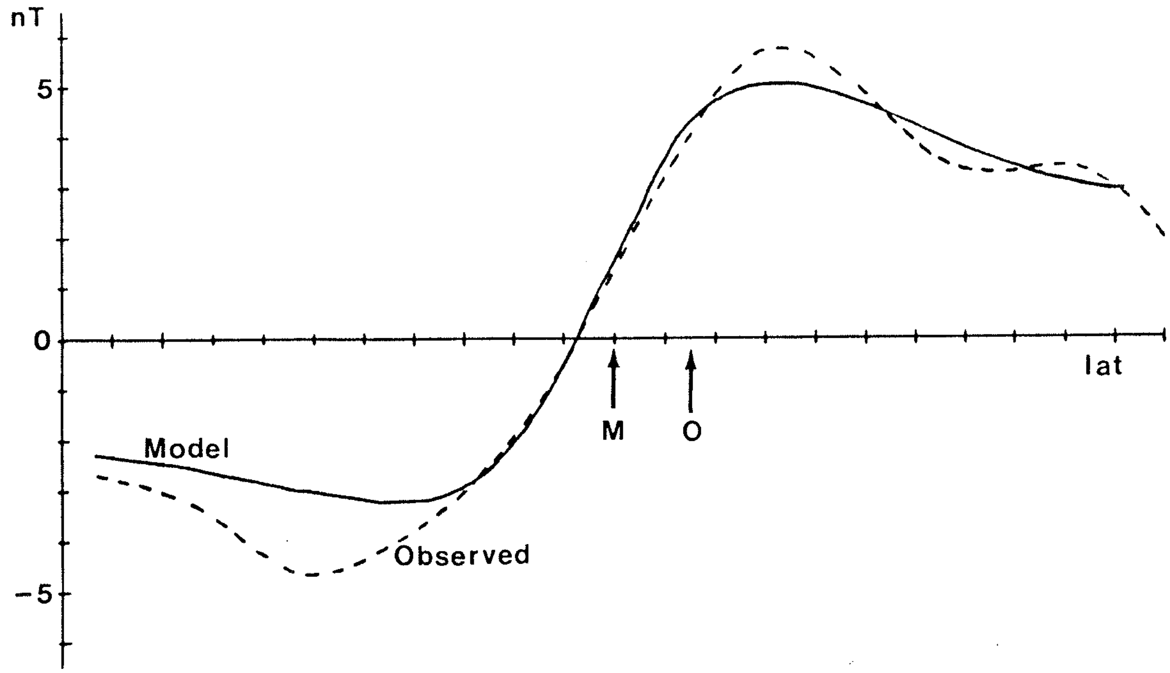

Figure 5.9: Modelled boundary signature. Four kilometre step signature compared with stacked CSB Hits of Figure 5.7. The boundary occurs at the points marked M and O for the modelled and observed boundaries respectively. The horizontal scale is marked at 1 degree intervals.

Figure 5.9 illustrates the observed CSB signature and the model signature resulting from a 4 kilometre step-like thickening of the magnetic layer on the Churchill side of the boundary. A best fit is obtained by mis-aligning the location of the boundary for the two signatures. This implies that if the boundary is to be modelled as a step-like change in magnetic layer thickness, the step should occur approximately 200 kilometres south of the surface-observed boundary. Since the gravity and seismic results that include a step-like change have this change occurring north of the surface-observed boundary, it is apparent that the magnetic step may not reflect the physical structure of the boundary. However, the amplitude and character of the signature are well correlated to the four kilometre step signature, implying that the model is valid, although not necessarily accurate in spatial location.

In order to address the problem of the thickness of the magnetic layer, a closer examination of the linear trends removed is in order. Figure 5.10 illustrates both the stacked raw anomaly plots of Figure 5.2 and the average of the linear trends removed from the profiles of Figure 5.2 to produce Figure 5.4. These average linear trends were obtained by superimposing Figures 5.10 and 5.4, and tracing the location of the abscissa axes from Figure 5.4 to Figure 5.10. Figure 5.11 illustrates the arithmetic mean of the four linear trends of Figure 5.10. This is very nearly a DC bias of approximately 11 nanotesla. If the magnetization is fixed at 5 amperes per metre, a uniform magnetic thickness of 12 kilometres is required to produce a field of 11 nanotesla. Thus, the model of Figure 5.8 best reflects the character and amplitude of the observed anomaly, as well as the mean DC bias observed due to the average magnetic thickness of the layer.

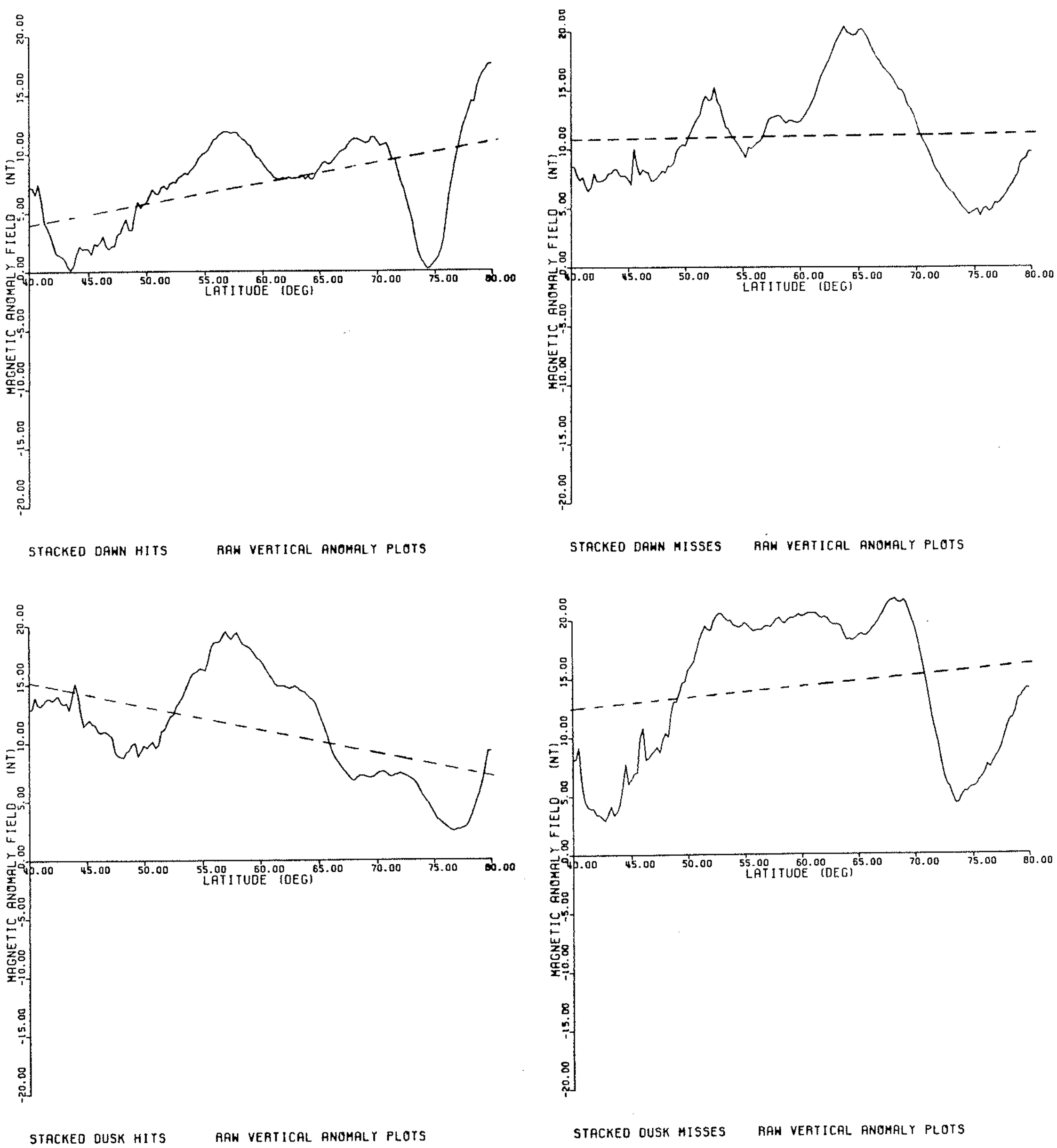

Figure 5.10: Linear trends of the raw anomaly profiles. The dotted line reflects the mean of the individual linear trends removed from the raw data of Figure 5.2.

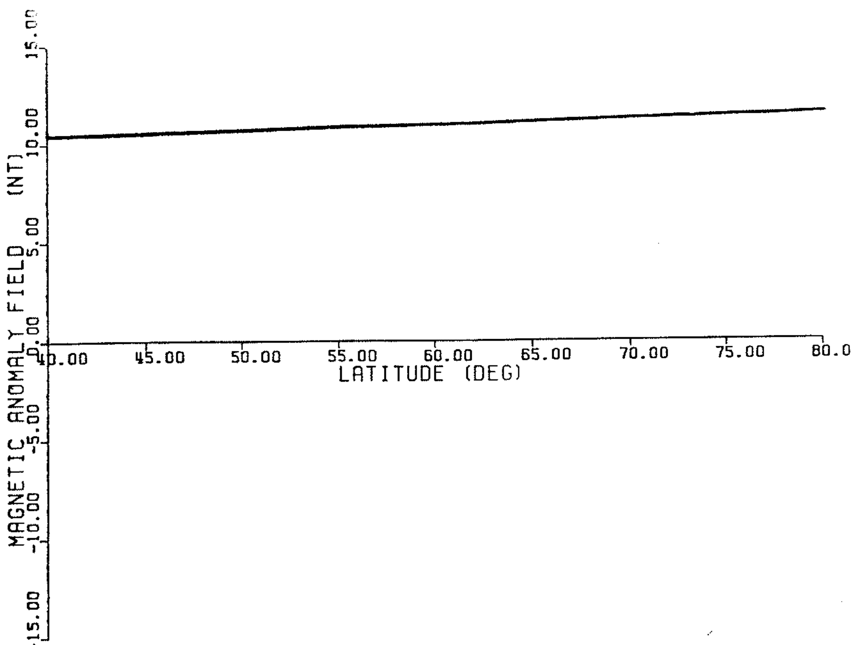

Figure 5.11: Mean linear trend of entire dataset. The nearly DC bias was obtained by finding the mean of the four linear trends of Figure 5.10. This reflects the average artificial zero all anomaly profiles are referenced to.

Chapter VI

THE UNGAVA ANOMALY

As mentioned in Chapter 5, the Churchill-Superior boundary could not be examined east of -80 degrees longitude due to the large anomaly centred over the east coast of Hudson Bay. This anomaly over the Ungava Peninsula effectively dominated all anomaly profiles in the area, preventing the study of the boundary signature. The anomaly itself, however, was studied in an attempt to identify its source.

6.1 POGO AND MAGSAT ANOMALY MAPS

In order to determine whether the Ungava anomaly was crustal related or had its origin elsewhere, maps from the POGO satellites were compared with those from MAGSAT. Figures 6.1 to 6.3 illustrate the anomaly pattern for the Canadian Shield, redrawn from Figures 2.13 to 2.15. Since the location of the anomaly is relatively fixed on the three maps, it is unlikely that the anomaly is the result of inaccuracies in the field models or some long term current system. The anomaly appears to be of a wavelength too small to be core-generated (Bullard; 1967) and, thus, must have its origin in the crust. Detailed aeromagnetic anomaly maps of the Ungava Peninsula do not reflect the presence of any strongly magnetic body, implying that the source of the anomaly is probably in the lower crust.

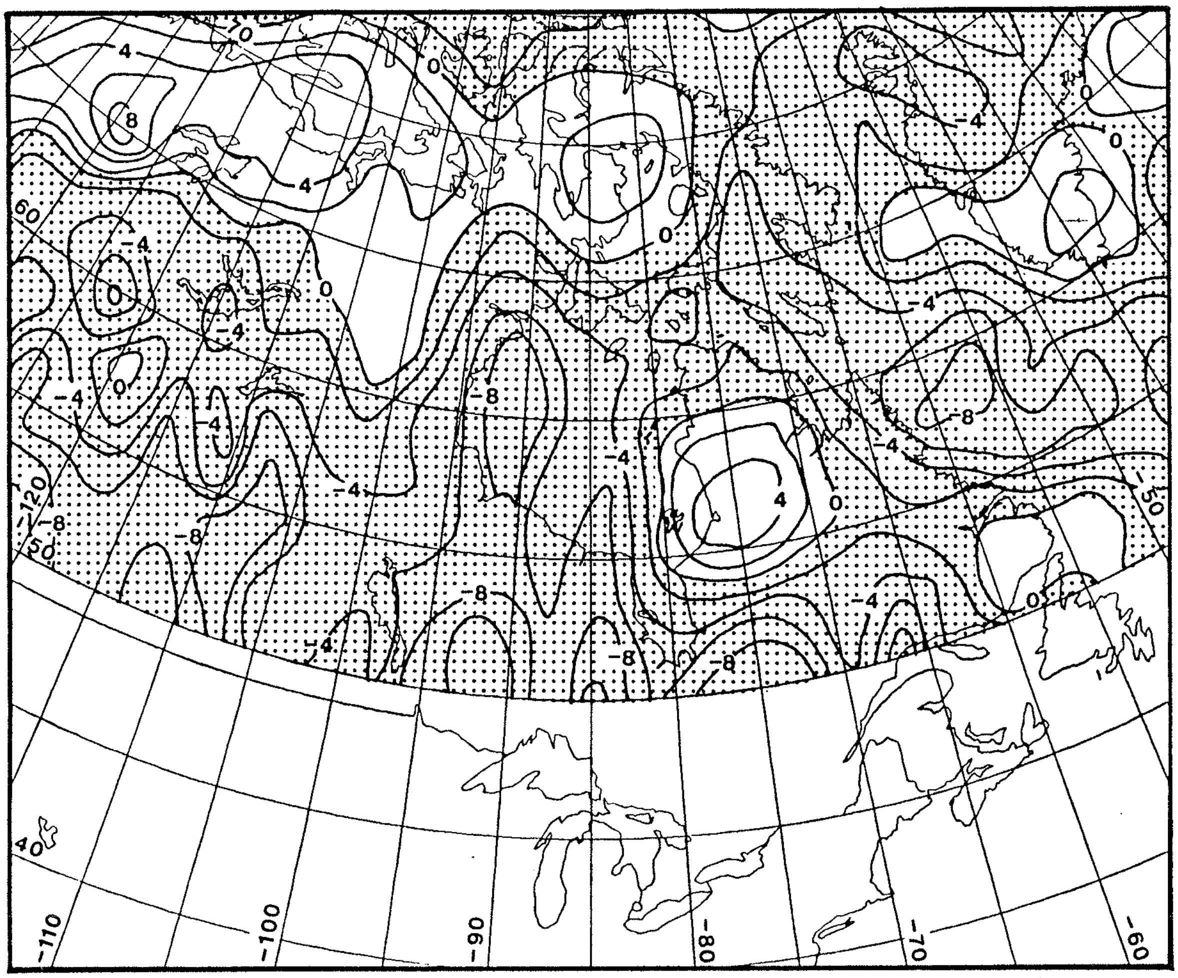

Figure 6.1: POGO Anomaly Map of the Canadian Shield. Contour interval is 2 nT. (redrawn from Figure 2.13)

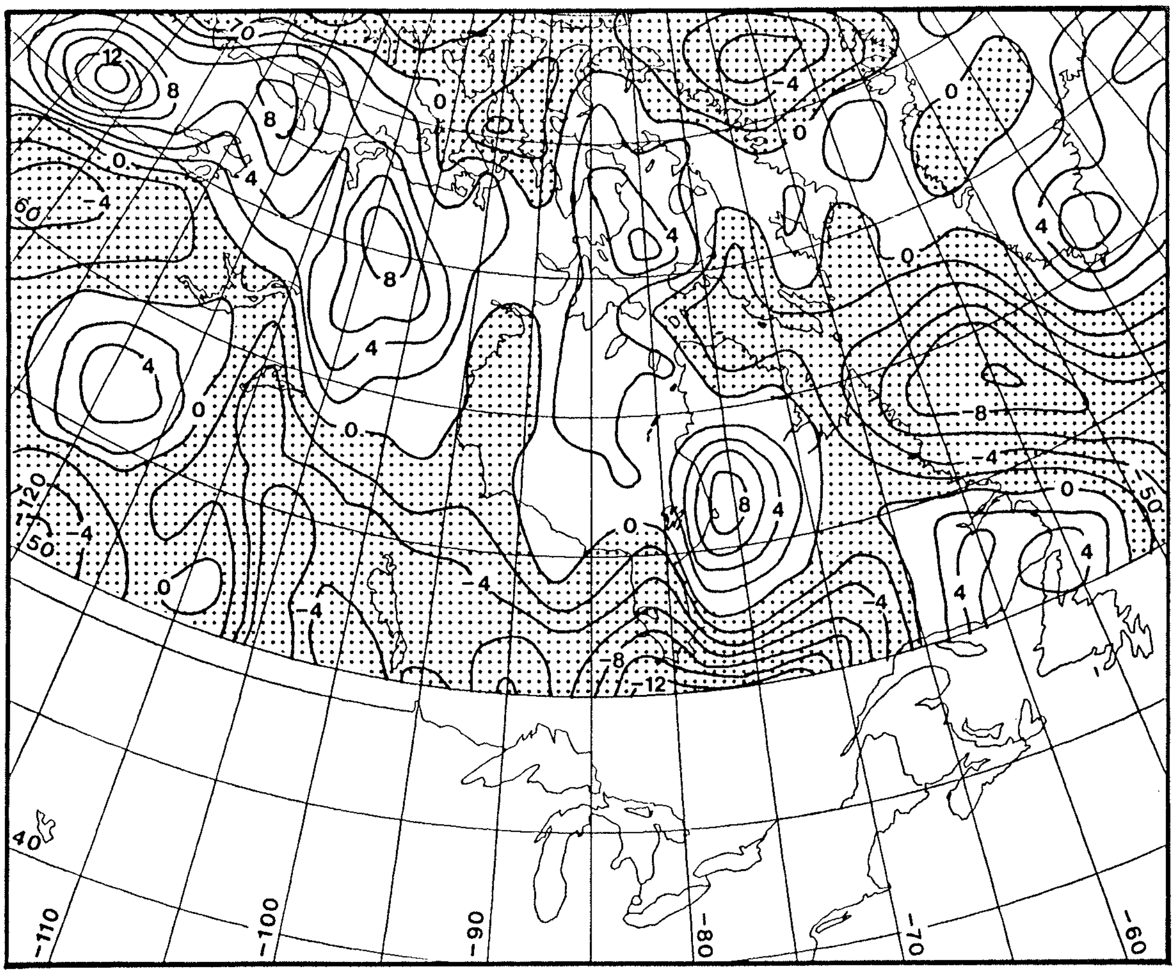

Figure 6.2: MAGSAT Anomaly Map of the Canadian Shield. Contour interval is 2 nT. (redrawn from Figure 2.14)

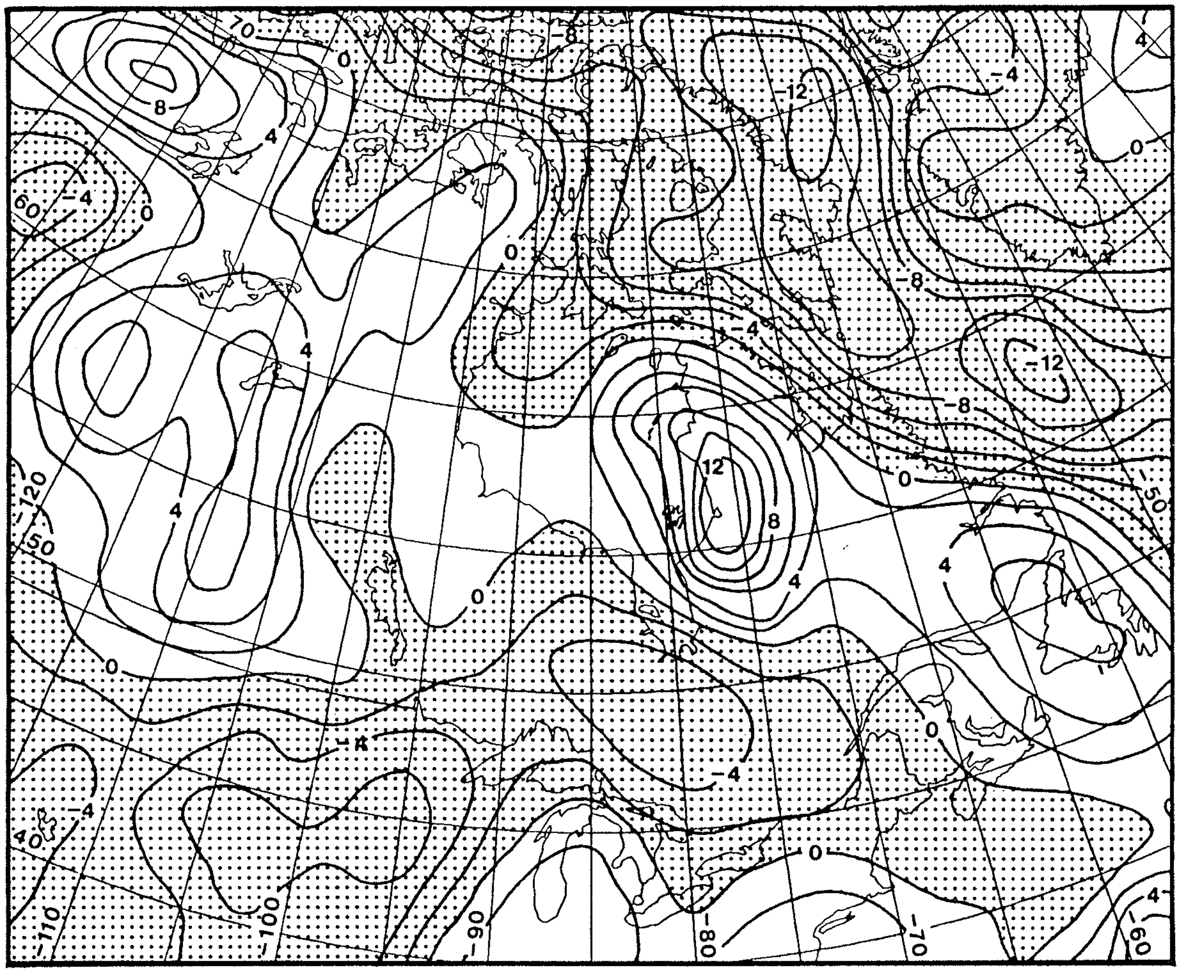

Figure 6.3: MAGSAT Anomaly Map of the Canadian Shield. Contour interval is 2 nT. (redrawn from Figure 2.15)

6.2 GRAVITY ANOMALIES IN THE AREA

Figure 6.4 illustrates the gravity anomaly pattern of the Ungava Peninsula. A north-northeast trending series of relative highs extend from midway between the Belcher Islands and Richmond Gulf to the Cape Smith foldbelt near the tip of the Ungava Peninsula. The high midway between the Belcher Islands and Richmond Gulf has been modelled by Mukhopadhyay and Gibb (1980) as being near-surface in origin, extending to only 6 or 8 kilometres in depth. Since the magnetic source must be in the lower crust, that particular gravity source must be distinct from the magnetic source. In their paper, Mukhopadhyay and Gibb modelled the Churchill-Superior boundary and the crustal structure of the Circum-Ungava foldbelt, and did not fully investigate the relatively minor gravity anomalies on the Superior side of the boundary zone.

Chandler and Schwartz (1980) suggested the Richmond Gulf is an aulocagen structure. Their analysis was further supported by detailed geological mapping and a geochronological study of the region (Chandler; 1982). If their proposed model is accurate, the lower crust would be expected to have undergone a considerable amount of activity at that time, possibly giving rise to an above-average magnetization in the lower crust. Wasilewski and Fountain (1982), from a study of the Ivrea Zone of northern Italy, suggested that mafic and ultramafic magmas formed the parent material for an extremely magnetic layer at the base of the zone, proposed to be a

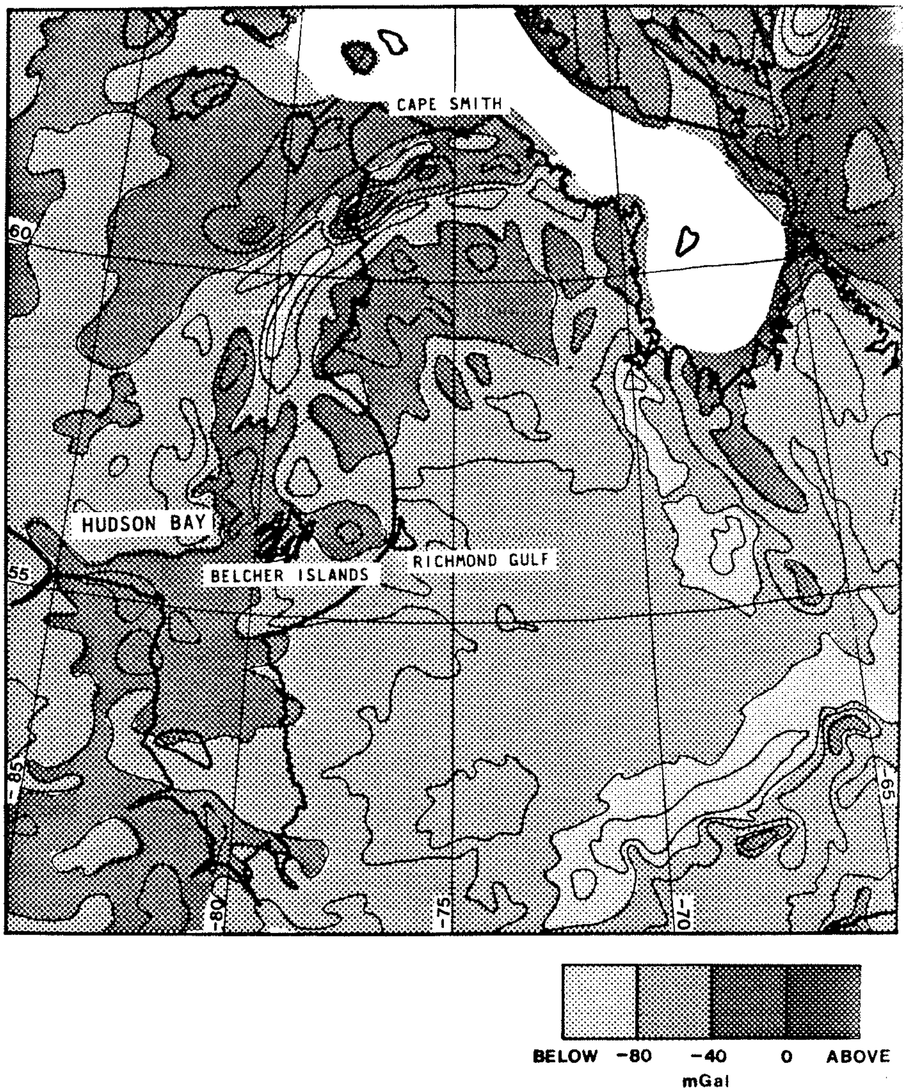

Figure 6.4: Gravity anomalies of the Ungava Peninsula. Bouguer on land, freeair offshore. Contour interval is 20 mGal. (after the GMS 80-1 Gravity Map of Canada; 1980)

cross-section of continental crust. They suggest that emplacement of this two kilometre thick layer may have occurred within a continental extensional environment, or at deep levels within a continental margin orogenic zone. It is conceivable, then, that there exists a relatively thin layer of highly magnetic material deep in the crust which would not necessarily be revealed in either low-level magnetic or in gravity data.

6.3 MODELLING THE UNGAVA ANOMALY

The modelling procedure was undertaken in an effort to determine if the Ungava anomaly was related to the nearby Churchill-Superior boundary. The modelling made use of the program SPEPS (Appendix A), which employs an equivalent point source technique incorporating spherical prisms. The maps of Coles et al (1982) were used as targets in the modelling procedure. Initial attempts at modelling restricted the location of the prisms to the Circum-Ungava foldbelt and the Richmond Gulf area. It was found that no combination of prisms so arranged gave rise to the observed anomaly.

Figure 6.6 illustrates one model used to describe the anomaly field of Figure 6.5. The thickness of the prisms is 36 kilometres, and their susceptibilities are +0.17 and -0.02, giving rise to magnetizations of approximately +5.2 and -1.0 amperes per metre. As mentioned in Chapter 5, the modelling procedure is relatively insensitive to changes in depth, and the models have an inherent ambiguity in thickness/magnetization. The same results, then, can be obtained from several models.

The gravity models of Mukhopadhyay and Gibb (1980) have the deep crustal position of the boundary occurring up to 400 kilometres west

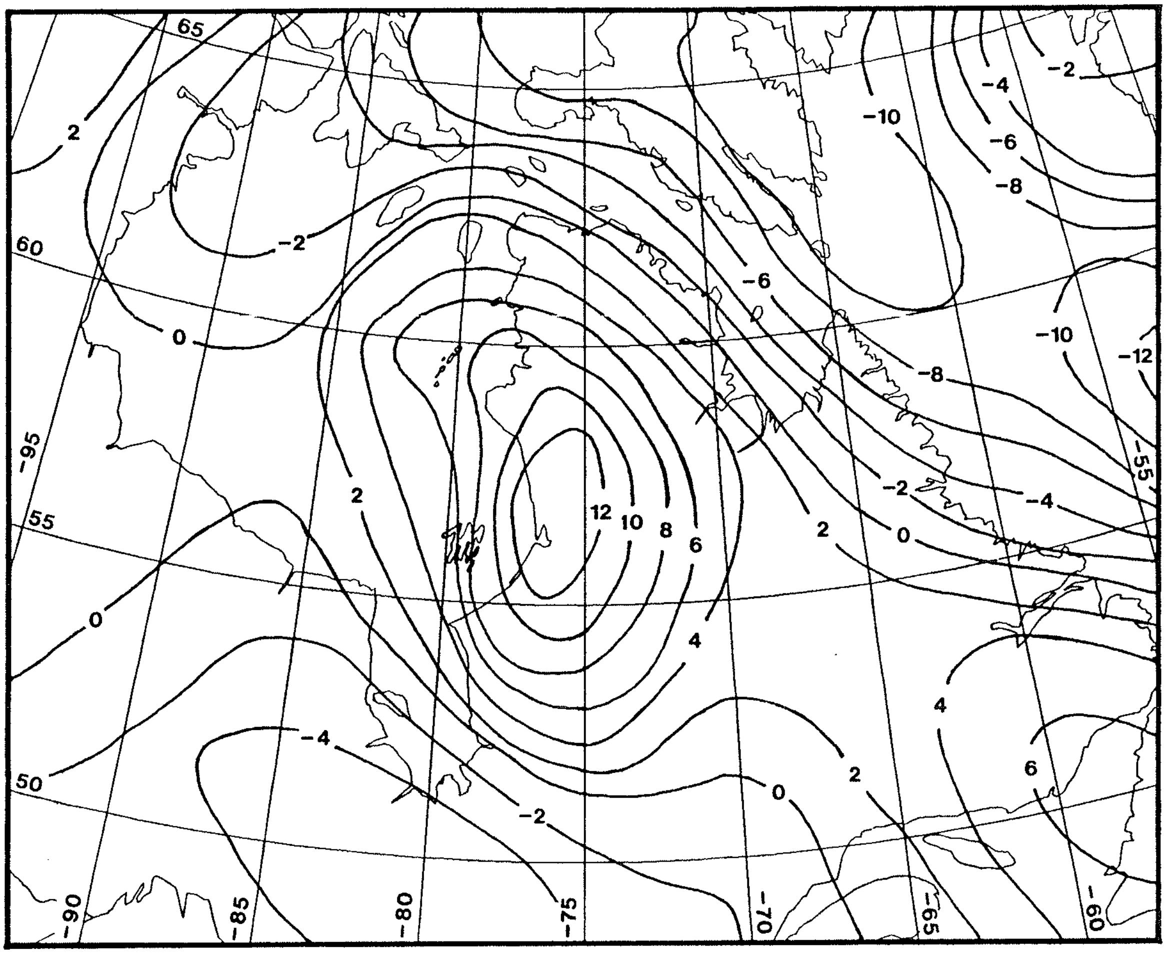

Figure 6.5: Scalar Anomaly Map of the Ungava Peninsula. Contour interval is 2 nT. (from Coles et al; 1982)

of the east coast of Hudson Bay. The magnetic anomaly sources are clearly nowhere near the boundary structure if their model is accurate. The anomaly sources, then, appear to be unrelated to the crustal structure of the boundary zone, but may be related to the tectonic regime that created the boundary.

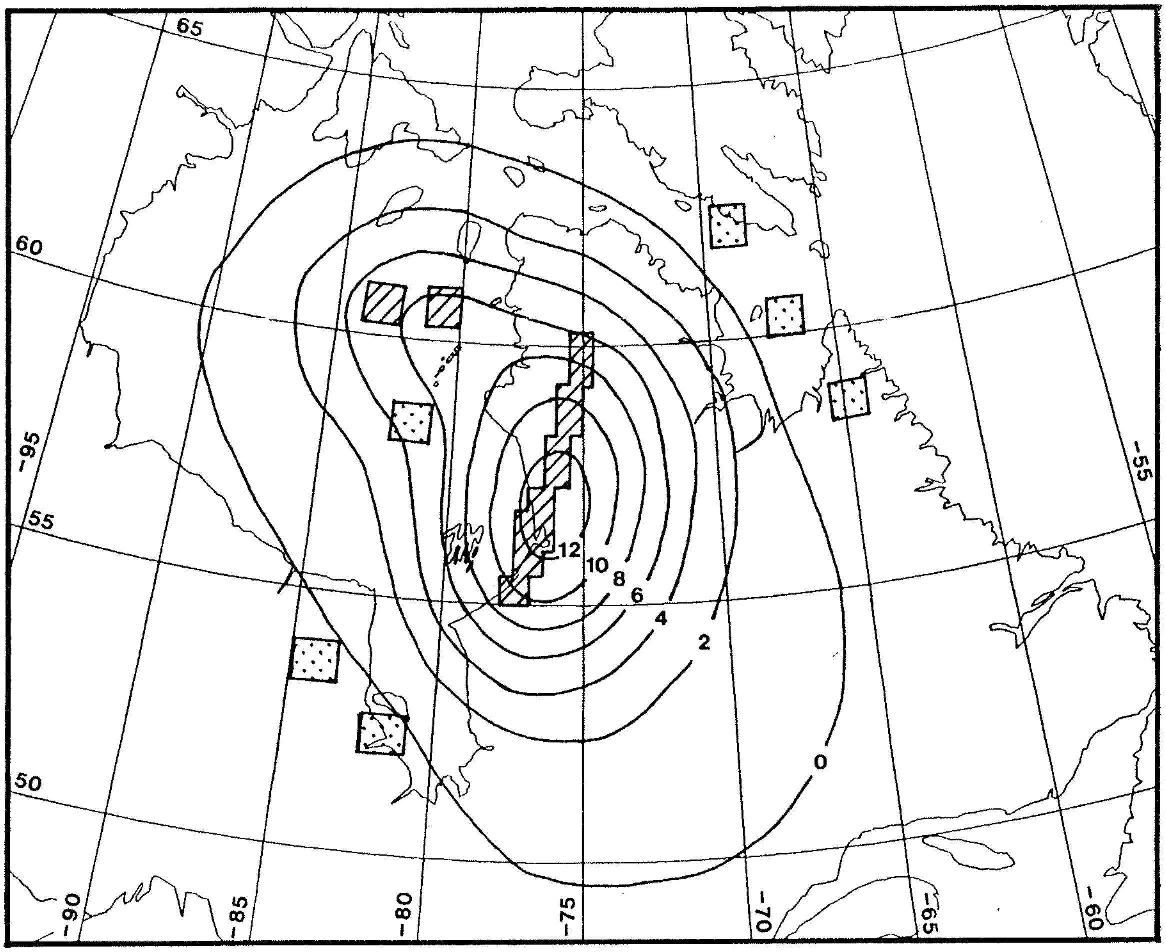

Figure 6.6: Prismatic model and calculated Ungava anomaly field. Spherical prisms are 36 km in thickness having magnetizations of approx. +5.2 and -1.0 . The negative magnetization (dot pattern) serves to model the influence of the neighbouring lows. Contour interval is 2 nT.

Chapter VII

CONCLUSIONS

Results of the Churchill-Superior boundary study indicate that a change in geophysical characteristics at or near the boundary zone gives rise to a magnetic signature in MAGSAT satellite magnetic data. This change was successfully modelled as a step-like increase in the thickness of a lower crustal magnetic layer. The size of the step was determined to be approximately 4 kilometres, which is in good agreement with gravity models of the boundary by Gibb and Thomas (1976), and by Mukhopadhyay and Gibb (1980). The average thickness of the magnetic layer was determined to be approximately 12 kilometres, in good agreement with seismic results of Hall and Hajnal (1973). The location of the step was indicated to be approximately 150 kilometres south of the surface-observed boundary. This result does not agree with the various seismic and gravity models, wherein the step-like change generally occurs approximately 50 kilometres north of the observed boundary. The inconsistency implies that the step-model, although explaining the character and amplitude of the observed signature, fails to adequately model its position and probably does not reflect the physical properties of the boundary structure. A gradually sloping change in thickness would serve to broaden the signature, possibly modelling the position better. The depth of the layer and whether the step occurred in the Riel or Moho could not accurately be determined from the modelling procedure. Magnetic studies indicate that satellite observed fields have their source in the lower crust, however, and this is assumed to be the case here.

The results of the Ungava Anomaly study indicate a deep crustal source for the anomaly which is probably unrelated to the boundary structure. The anomaly source may be related to tectonic effects experienced by the lower crust in the formation of the Richmond Gulf aulocagen structure.

LIST OF REFERENCES

Alldredge, L.R. and C.O. Stearns, 1974. A discussion of sources and description of the Earth's magnetic field and its secular variations. Journal of Geomagnetism and Geoelectricity, 26, pp.393-404.

Andreasen, G.E. and I. Zietz, 1969. Magnetic fields for a 4X6 prismatic model. U.S.G.S. Professional paper 666.

Araki, T., T. Iyemori, S. Tsunomura, T. Kamei, and H. Maeda, 1982. Detection of an ionospheric current for the preliminary impulse of the geomagnetic sudden commencement. Geophysical Research Letters, 9, pp.341-344.

Baragar, W.R.A. and C.G. Lamontagne, 1980. The Circum-Ungava Belt in eastern Hudson Bay: The geology of Sleeper Islands and parts of the Ottawa and Belcher Islands; in Current Research, Part A, Geological Survey of CanadA, Paper 80-1A, pp. 89-94.

Baragar, W.R.A. and M. Piche, 1982. The Circum-Ungava Belt of eastern Hudson Bay: The geology of the Ottawa Islands and the Cape Smith region; in Current Research, Part A, Geological Survey of Canada, Paper 82-1A, pp.11-15.

Bates, A. and D.H. Hall, 1975. Upper mantle structure in southern Saskatchewan and western Manitoba from Project Edzoe. Canadian Journal of Earth Sciences, 12, pp.2134-2144.

Berry, M.J., 1973. Structure of the crust and upper mantle in Canada. Tectonophysics, 20, pp.183-201.

Bullard, E.C., 1967. The removal of trend from magnetic surveys. Earth and Planetary Science Letters, 2, pp.293-300.

Bullard, E.C. and H. Gellman, 1954. Homogeneous dynamos and terrestrial magnetism. Philosophical Transactions of the Royal Astronomical Society of London A, 247, pp.213.

Cain, J.C., 1979. Main field and secular variation. Reviews of Geophysics and Space Physics, 17, pp.273-277.

Cain, J.C. and R.A. Langel, 1980. The geomagnetic survey by the polar Orbiting Geophysical Observatories OGO-2 and OGO-4, 1965-1967. Goddard Space Flight Centre Report X-612-68-502.

Chandler, F.W., 1982. The structure of the Richmond Gulf graben and the geological environments of lead-zinc mineralization and of iron-manganese formations in the Nastapoka Group, Richmond Gulf area, New QuebecNorthwest Territories; in Current Research, Part A, Geological Survey of Canada, Paper 82-1A, pp.1-10.

Chandler, F.W. and E.J. Schwarz, 1980. Tectonics of the Richmond Gulf area, northern Quebec - a hypothesis; in Current Research, Part C, Geological Survey of Canada, Paper 80-1C, pp.59-68.

Chandra, N.N. and G.L. Cumming, 1972. Seismic refraction studies in western Canada. Canadian Journal of Earth Sciences, 9, pp.1099-1109.

Coles, R.L., 1973. Relationships between measured rock magnetizations and interpretations of longer wavelength anomalies in the Superior province of the Canadian shield. Ph.D. Thesis, University of Manitoba.

Coles, R.L., 1979. Some comparisons among geomagnetic field models, obervatory data, and airborne magnetometer data: Implications for broad scale anomaly studies over Canada. Journal of Geomagnetism and Geoelectricity, 31, pp.459-478.

Coles, R.L., G.V. Haines, and W. Hannaford, 1981. Broad-scale magnetic anomalies over central and eastern Canada: a discussion. Canadian Jounal of Earth Sciences, 18, pp.657-661.

Coles, R.L., G.V. Haines, G. Jansen van Beek, A. Nandi, and J.K. Walker, 1982. Magnetic anomaly maps from 40 N to 83 N derived from MAGSAT satellite data. Geophysical Research Letters, 9, pp.281-284.

Coons, J.J., E.M. Greville, D. Brown, and J.H. Berbert, 1980. MAGSAT investigator-B tape generation program requirements. Goddard Space Flight Centre Report CSC/TM-80/6178.

DeLandro, W., 1981. Deep seismic sounding in southern Manitoba and Saskatchewan. M.Sc. Thesis, University of Manitoba.

DeLandro, W., W. Moon, and A.G. Green, 1982. Seismic structure of Superior-Churchill precambrian boundary zone (COCRUST 77). The University of Manitoba Centre for Precambrian Studies Publication Number 59.

Douglas, R.J.W. (Ed.), 1970. Geology and Economic Minerals of Canada. Ottawa: Geological Survey of Canada.

Dunlop, D.J., 1974. Thermal enhancement of magnetic susceptibility. Journal of Geophysics, 40, pp.439-451.

Elsasser, W.M., 1946a. Induction effects in terrestrial magnetism. Part I. Theory. Physical Review, 69, pp.106-116.

Elsasser, W.M., 1946b. Induction effects in terrestrial magnetism. Part II. The secular variation. Physical Review, 70, pp.202-212.

Emilia, D.A., 1973. Equivalent sources used as an analytic base for processing total magnetic field profiles. Geophysics, 38, pp.339-348.

Fougere, P.F., 1963. Spherical harmonic analysis. Journal of Geophysical Research, 68, pp.1131-1139.

Franck, S., 1982. Ascending droplets in the Earth's core. Physics of the Earth and Planetary Interiors, 27, pp.249-254.

Frey, H., 1982a. MAGSAT scalar anomalies and major tectonic boundaries in Asia. Geophysical Research Letters, 9, pp.299-302.

Frey, H., 1982b. MAGSAT scalar anomaly distribution: the global perspective. Geophysical Research Letters, 9, pp.277-280.

Galliher, S.C. and M.A. Mayhew, 1982. On the possibility of detecting large-scale crustal remanent magnetization with MAGSAT vector magnetic anomaly data. Geophysical Research Letters, 9, pp.325-328.

Garland, G.D., 1979. Introduction to Geophysics (Mantle, Core, and Crust). Philadelphia: W.B. Saunders Company.

Gerald, C.F., 1978. Applied Numerical Analysis. Reading, Massachusetts: Addison-Wesley.

Gibb, R.A. and M.D. Thomas, 1976. Gravity signature of fossil plate boundaries in the Canadian Shield. Nature, 262, pp.199-200.

Gibb, R.A., M.D. Thomas, and M. Mukhopadhyay, 1980. Proterozoic sutures in Canada. Geoscience Canada, 7, pp.149-154.

Green, A.G., 1981. Results of a seismic reflection survey across the fault zone between the Thompson nickel belt and the Churchill tectonic province, northern Manitoba. Canadian Journal of Earth Sciences, 18, pp.13-25.

Green, A.G., G.L. Cumming, and D. Cedarwell, 1979. Extension of the Superior-Churchill boundary zone into southern Canada. Canadian Journal of Earth Sciences, 16, pp.1691-1701.

Green, A.G., O.G. Stephenson, G.D. Munn, E.R. Kanasewich, G.L. Cumming, Z. Hajnal, J.A. Mair, and G.F. West, 1980. Cooperative seismic surveys across the Superior-Churchill boundary zone in southern Canada. Canadian Journal of Earth Sciences, 17, pp.617-632.

Hall, D.H., 1971. Geophysical determination of deep crustal structure in Manitoba. The Geological Association of Canada, Special Paper No.9, pp.83-88.

Hall, D.H., 1974. Long wavelength aeromagnetic anomalies and deep crustal magnetization in Manitoba and northwestern Ontario, Canada. Journal of Geophysics, 40, pp.403-430.

Hall, D.H., 1977a. Overview of geophysics, Churchill province. Paper No.1, University of Manitoba Centre for Precambrian Studies Annual Report, pp.6-23.

Hall, D.H., 1977b. Partial melting and mineral stability boundaries and their bearing on the seismic exploration of the lithosphere in Canada. Canadian Journal of Earth Sciences, 14, pp.2638-2650.

Hall, D.H. and Z. Hajnal, 1973. Deep seismic crustal studies in Manitoba. Bulletin of the Seismological Society of America, 63, pp.885-910.

Hall, D.H. and T. Millar, 1980. Magnetic signatures of subprovinces in the Canadian Shield and MAGSAT data. [abstr.]. Int. Geol. Congr. Abstr. - Congr. Geol. Int., Resumes, 26, p.822.

Hastings, D.A., 1982. Preliminary correlations of MAGSAT anomalies with tectonic features of Africa. Geophysical Research Letters, 9, pp.303-306.

Hide, R., 1982. On the role of rotation in the generation of magnetic fields by fluid motions. Philosophical Transactions of the Royal Society of London, 306, pp.223-234.

Hughes, T.J., D.W. Oldenburg, and G. Rostoker, 1979. Interpretation of auroral oval equivalent current flow near dusk using inversion techniques. Journal of Geophysical Research, 84, pp.450-456.

Hughes, T.J., and G. Rostoker, 1977. Current flow in the magnetosphere and ionosphere during periods of moderate activity. Journal of Geophysical Research, 82, pp.2271-2282.

Hughes, T.J. and G. Rostoker, 1979. A comprehensive model current system for high-latitude magnetic activity - I. The steady state system. Geophysical Journal of the Royal Astronomical Society, 58, pp.525-569.

Hughes, T.J., D.D. Wallis, J.R. Burrows, and M.D. Wilson, 1982. Model predictions of magnetic pertubations observed by MAGSAT in dawn-dusk orbit. Geophysical Research Letters, 9, pp.357-360.

Iijima, T., N. Fukushima, and R. Fujii, 1982. Transverse and parallel geomagnetic pertubations over the polar regions observed by MAGSAT. Geophysical Research Letters, 9, pp.369-372.

Klumpar, D.M. and D.M. Greer, 1982. A technique for modelling the magnetic pertubations produced by field -aligned current systems. Geophysical Research Letters, 9, pp.361-364.

Krause, F., 1982. Progress in dynamo theory: kinematic and dynamic models. Philosophical Transactions of the Royal Society of London, 306, pp.255-260.

Krutikhovskaya, Z.A. and I.K. Pashkevich, 1977. Magnetic model for the Earth's crust under the Ukrainian Shield. Canadian Journal of Earth Sciences, 14, pp.2718-2728.

Ku, C.C., 1977. A direct computation of gravity and magnetic anomalies caused by 2- and 3-dimensional bodies of arbitrary shape and arbitrary magnetic polarization by equivalent-point method and a simplified cubic spline. Geophysics, 42, pp.610-622.

Langel, R.A., 1980. MAGSAT scientific investigations. Johns Hopkins Applied Physics Laboratory Technical Digest, 1, pp.214-277.

Langel, R.A., 1982. The magnetic Earth as seen from MAGSAT, initial results. Geophysical Research Letters, 9, pp.239-242.

Langel, R.A., S.I. Bensusen, R.D. Regan, W.M. Davis, and J.C. Cain, 1975. High latitude magnetic anomaly maps. EOS (Transactions of the American Geophysical Union), 56, p.356.

Langel, R.A., J. Berbert, and T. Jennings, 1981. MAGSAT data processing: an interim report for investigators. NASA Technical Report.

Langel, R.A., R.L. Coles, and M.A. Mayhew, 1980. Comparisons of magnetic anomalies of lithospheric origin measured by satellite and airborne magnetometers over western Canada. Canadian Journal of Earth Sciences, 17, pp.876-887.

Langel, R.A., and R.H. Estes, 1982. A geomagnetic field spectrum. Geophysical Research Letters, 9, pp.250-253.

Langel, R.A., G. Ousley, J. Berbert, J. Murphy, and M. Settle, 1982. The MAGSAT mission. Geophysical Research Letters, 9, pp.243-245.

Langel, R.A, J.D. Phillips, and R.J. Horner, 1982. Initial scalar magnetic anomaly map from MAGSAT. Geophysical Research Letters, 9, pp.269-272.

Langel, R.A., R.D. Regan, and J.P. Murphy, 1977. MAGSAT: a satellite for measuring near Earth magnetic fields. Goddard Space Flight Centre Report X-922-77-199.

Langel, R.A., C.C. Schnetzler, J.D. Phillips, and R.J. Horner, 1982. Initial vector magnetic anomaly map from MAGSAT. Geophysical Research Letters, 9, pp.272-276.

Levy, E.H., 1979. Dynamo magnetic field generation. Reviews of Geophysics and Space Physics, 17, pp.277-281.

Longacre, M.B., W.J. Hinze, and R.R.B. von Frese, 1982. A satellite magnetic model of northeastern South American aulacogens. Geophysical Research Letters, 9, pp.318-321.

Mayhew, M.A., 1976. A method of inversion of satellite magnetic anomaly data. Goddard Space Flight Centre Report X-922-77-260.

Mayhew, M.A. and S.C. Galliher, 1982. An equivalent layer magnetization model for the United States derived from MAGSAT data. Geophysical Research Letters, 9, pp.311-313.

Mayhew, M.A., B.D. Johnson, and R.A. Langel, 1980. An equivalent source model of the satellite-altitude magnetic anomaly field over Australia. Earth and Planetary Science Letters, 51, pp.189-198.

Mukhopadhyay, M. and R.A. Gibb, 1981. Gravity anomalies and deep structure of eastern Hudson Bay. Tectonophysics, 72, pp.43-60.

Nagata, T., 1965. Main characteristics of recent geomagnetic secular variation. Journal of Geomagnetism and Geoelectricity, 17, pp.263-276.

Pakiser, L.C. and I. Zietz, 1965. Transcontinetal crustal and upper mantle structure. Reviews of Geophysics, 3, pp.505-520.

Peddie, N.W., 1980. International geomagnetic reference field 1980. U.S. Geological Survey Report.

Pollack, H.N. and D.S. Chapman, 1977. On the regional variations of heat flow, geotherms, and lithospheric thickness. Tectonophysics, 38, pp.279-296.

Potemra, T.A., 1980. Studies of auroral field-aligned currents with MAGSAT. Johns Hopkins Applied Physics Laboratory Technical Digest, 1, pp.228-232.

Potemra, T.A., F.F. Mobley, and L.D. Eckard, 1980. The geomagnetic field and its measurment: introduction and magnetic field satellite (MAGSAT) glossary. Johns Hopkins Applied Physics Laboratory Technical Digest, 1, pp.162-170.

Price, R.A. and R.J.W. Douglas (editors), 1972. Variations in tectonic styles in Canada. The Geological Association of Canada, Special Paper No. 11.

Regan, R.D., J.C. Cain, and W.M. Davis, 1975. A global magnetic anomaly map. Journal of Geophysical Research, 80, pp.794-802.

Regan, R.D., D.W. Handschumacher, and M. Sugiura, 1981. A closer examination of the reduction of satellite magnetometer data for geological studies. Journal of Geophysical Research, 86, pp.9567-9573.

Ritzwoller, M.H. and C.R. Bentley., 1982. MAGSAT magnetic anomalies over Antarctica and the surrounding oceans. Geophysical Research Letters, 9, pp.285-288.

Rostoker, G. and T.J. Hughes, 1979. A comprehensive model current system for high-latitude magnetic activity - II. The substorm component. Geophysical Journal of the Royal Astronomical Society, 58, pp.571-581.

Sailor, R.V., A.R. Lazarewicz, and R.F. Brammer, 1982. Spatial resolution and repeatability of MAGSAT crustal anomaly data over the Indian Ocean. Geophysical Research Letters, 9, pp.289-292.

Shuey, R.T., D.R. Schellinger, E.H. Johnson, and L.G. Alley, 1973. Aeromagnetics and the transition between the Colorado Plateau and the Basin Range province. Geology, 1, pp.107-110.

Stacey, F.D., 1969. Physics of the Earth. New York: John Wiley and Sons, Inc.

Stroud, A.H. and D. Secrest, 1966. Gaussian Quadrature Formulas. New Jersey: Prentice-Hall.

Talwani, M., 1965. Computation with the help of a digital computer of magnetic anomalies caused by bodies of arbitrary shape. Geophysics, 30, pp.797-817.

Telford, W.M., L.P. Geldart, R.E. Sheriff, and D.A. Keys., 1976. Applied Geophysics. Cambridge: Cambridge University Press.

Thomas, M.D. and R.A. Gibb, 1977. Gravity anomalies and deep structure of the Cape Smith foldbelt, northern Ungava, Quebec. Geology, 5, pp.169-172.

von Frese, R.R.B., W.J. Hinze, and L.W. Braile, 1981. Spherical Earth gravity and magnetic anomaly analysis by equivalent point source inversion. Earth and Planetary Science Letters, 53, pp.69-83.

von Frese, R.R.B., W.J. Hinze, L.W. Braile, and A.J. Luca, 1981. Spherical-Earth gravity and magnetic anomaly modeling by Gauss-Legendre quadrature integration. Journal of Geophysics, 49, pp.234-242.

Wasilewski, P. and D.M. Fountain, 1982. The Ivrea zone as a model for the distribution of magnetization in the continental crust. Geophysical Research Letters, 9, pp.333-336.

Wasilewski, P. and M.A. Mayhew, 1982. Crustal xenolith magnetic properties and long wavelength anomaly source requirements. Geophysical Research Letters, 9, pp.329-332.

Wasilewski, P. and E. Padovani, 1980. Magnetization in the lower crust. EOS (Transactions of the American Geophysical Union), 61, pp.222.

Wickens, A.J., 1971. Variations in lithospheric thickness in Canada. Canadian Journal of Earth Sciences, 8, pp.1154-1162.

Zanetti, L.J. and T.A. Potemra, 1982. Correlated Birkeland current signatures from the TRIAD and MAGSAT magnetic field data. Geophysical Research Letters, 9, pp.349-352.

Zeitz, I., E.R. King, W. Geddes, and E.G. Lidiak, 1966. Crustal study of a continental strip from the Atlantic Ocean to the Rocky Mountains. Geological Society of America Bulletin, 77, pp.1427-1448.

Zmuda, A.J., 1973. The geomagnetic field and its harmonic description. Geomagnetism and Aeronomy, 13, pp.929-939.

Appendix A

PROGRAM SPEPS

Following is program SPEPS (Spherical Prism Equivalent Point Source), a refinement of an earlier version (Hall and Millar; 1980). The program computes the North, East, Vertical, and Scalar anomaly fields for a given prismatic body in a spherical Earth. Useful references include Ku (1977), and von Frese, Hinze, Braile, and Luca (1981).

```
// EXEC FORTHCLG,SIZE=512K,LSIZE=512K
//FORT.SYSPRINT DD DUMMY
//FORT.SYSIN DD *
C**
C** ################################################################
C** ##                       PROGRAM SPEPS                        ##
C** ##           (SPHERICAL PRISM EQUIVALENT POINT SOURCE)        ##
C** ##   THIS PROGRAM COMPUTES THREE-COMPONENT MAGNETIC ANOMALIES   ##
C** ##   DUE TO AN ARRANGEMENT OF SPHERICAL PRISMS, EACH CONTAINING ##
C** ##   A 2X2X2 ARRAY OF EQUIVALENT DIPOLE SOURCES ARRANGED        ##
C** ##   ACCORDING TO GAUSSIAN QUADRATURE.                          ##
C** ################################################################
C**
      COMMON /OBGRID/ FORGE,FORGN,FDELTE,FDELTN,FELEV
      COMMON /FIELDS/ FLDNOR,FLDEST,FLDVRT,FLDSCA
      COMMON /PRISMS/ LOCBLK
      COMMON /GRID/ IROWMT,ILVLMT
C**
      DIMENSION FLDNOR(35,35),FLDEST(35,35),FLDVRT(35,35)
      DIMENSION FLDSCA(35,35)
      DIMENSION TITLE(20)
      DIMENSION BLKDIM(3),BLKMAG(3),SUSCEP(9),IPDIM(9)
      DIMENSION LOCBLK(50,50,10), IROWMT(50,10),ILVLMT(10)
C**
C** ################################################################
C** ##                       INPUT CARDS                          ##
C** ##   CARDS 1 TO 3 DEFINE A FIELD OBSERVATION GRID.  MAGNETIC    ##
C** ##   FIELDS ARE CALCULATED AT GRID POINTS ON THE 2-D GRID ABOVE ##
C** ##   THE EARTH'S SURFACE.   CARDS 4 TO 6 DEFINE A 3-D PRISM     ##
C** ##   GRID WITHIN THE EARTH.  PRISMS ARE LOCATED WITH THEIR      ##
C** ##   TOP SOUTH-WEST CORNER ON THE GRID POINTS.                  ##
C** ##   FIELDS ARE CALCULATED ONLY FOR PRISMS WITHIN A PRESCRIBED  ##
C** ##   WINDOW.   THE FOLLOWING SET OF CARDS DEFINE THE ARRAY      ##
C** ##   LOCBLK.  THIS ARRAY REPRESENTS THE PRISM GRID.  A DIGIT    ##
C** ##   BETWEEN 1 AND 9 AT LOCATION LOCBLK(I,J,K) REPRESENTS A     ##
C** ##   PRISM OF TYPE 1 TO 9 LOCATED WITH ITS TOP SOUTH-WEST VERTEX##
C** ##   AT THE POSITION "I" GRID POINTS EAST, "J" GRID POINTS      ##
C** ##   NORTH, AND "K" GRID POINTS DOWN FROM THE PRISM GRID ORIGIN.##
C** ##   THE NEXT TWO CARDS DEFINE THE PRISM "TYPE" REFERRED TO BY  ##
C** ##   THE DIGIT IN THE LOCBLK ARRAY.   THE LAST TWO CARDS GIVE   ##
C** ##   I/O DESTINATIONS FOR THE THREE COMPONENTS AND THE TOTAL    ##
C** ##   FIELD, AND A TITLE FOR THE DATA.                           ##
C** ##------------------------------------------------------------##
      DUMMY=1.
C** ##------------------------------------------------------------##
C** ##  FIELD OBSERVATION GRID                                      ##
C** ##                                                              ##
C** ##  CARD 1     FORGE  -  EAST LONGITUDE OF ORIGIN FOR FIELD     ##
C** ##                       CALCULATION GRID                       ##
C** ##             FORGN  -  GEODETIC NORTH LATITUDE OF FIELD GRID  ##
C** ##                       ORIGIN                                 ##
C** ##             FDELTE -  E - W FIELD GRID SPACING IN DEGREES    ##
C** ##             FDELTN -  N - S FIELD GRID SPACING IN DEGREES    ##
C** ##             FELEV  -  KILOMETRE ALTITUDE OF FIELD GRID       ##
C** ##        FORMAT(5F10.0)                                        ##
C** ##                                                              ##
C** ##  CARD 2     NFEAST -  NUMBER OF GRID POINTS IN E-W DIRECTION ##
C** ##             NFNORT -  NUMBER OF GRID POINTS IN N-S DIRECTION ##
C** ##        FORMAT(2I4)                                           ##
C** ##                                                              ##
C** ##  CARD 3     HORIZN -  ANY PRISMS LOCATED BEYOND HORIZN ARE   ##
C** ##                       IGNORED IN THE CALCULATION OF FIELDS   ##
C** ##                       UNITS ARE KILOMETRES                   ##
```

```
C** ##        FORMAT(F10.0)                                             ##
C** ##--------------------------------------------------------------------##
      DUMMY=2.
C** ##--------------------------------------------------------------------##
C** ##  PRISM GRID                                                        ##
C** ##                                                                    ##
C** ##  CARD 4     GORGE  -  EAST LONGITUDE OF THE PRISM GRID ORIGIN ##
C** ##             GORGN  -  NORTH LATITUDE OF THE PRISM GRID ORIGIN ##
C** ##             GORGV  -  KILOMETRE ALTITUDE OF THE ORIGIN (+ UP) ##
C** ##             GDELTE -  E - W GRID SPACING                         ##
C** ##             GDELTN -  N - S GRID SPACING                         ##
C** ##             GDELTV -  VERTICAL GRID SPACING                      ##
C** ##      FORMAT(6F10.0)                                              ##
C** ##                                                                    ##
C** ##  CARD 5     NMEAST -  NUMBER OF GRID POINTS IN E-W DIRECTION  ##
C** ##             NMNORT -  NUMBER OF GRID POINTS IN N-S DIRECTION  ##
C** ##             NMDOWN -  NUMBER OF GRID POINTS IN VERTICAL DIR.  ##
C** ##      FORMAT(3I4)                                                 ##
C** ##                                                                    ##
C** ##  CARD 6     IWINDW -  WEST-MOST GRID POINT TO BE CONSIDERED   ##
C** ##             IWINDE -  EAST-MOST   "    "    "  "     "        ##
C** ##             IWINDS -  SOUTH-MOST  "    "    "  "     "        ##
C** ##             IWINDN -  NORTH-MOST  "    "    "  "     "        ##
C** ##      FORMAT(4I4)                                                 ##
C** ##--------------------------------------------------------------------##
      DUMMY=3.
C** ##--------------------------------------------------------------------##
C** ##  LOCBLK ARRAY                                                      ##
C** ##                                                                    ##
C** ##  CARD 7          K  -  LEVEL NUMBER IN 3-D ARRAY                 ##
C** ##      FORMAT(I3)                                                  ##
C** ##                                                                    ##
C** ##  CARD 8          J  -  NUMBER OF THE EAST-WEST RUNNING ROW     ##
C** ##                        (ROWS ARE NUMBERED FROM THE SOUTH END) ##
C** ##              ITYPE-   TYPE CODE IS PLACED IN CARD COLUMN I+4 ##
C** ##                        TO PLACE A PRISM OF THAT TYPE IN        ##
C** ##                        LOCATION I,J,K  OF THE PRISM GRID       ##
C** ##      FORMAT(I3,1X,76I1)                                          ##
C** ##  CARDS 9,10,11 ETC. AS CARD 8                                     ##
C** ##                                                                    ##
C** ##   CONTINUE WITH CARD 8 FORMAT UNTIL THE LEVEL IS DESCRIBED,  ##
C** ##   THEN ENTER "J" AS "999".  PROCEED WITH LEVELS 2,3,4, ETC.  ##
C** ##   FOLLOWING THE SAME FORMAT UNTIL THE 3-D PRISM GRID IS       ##
C** ##   DESCRIBED, THEN ENTER "K" AS "999" TO TERMINATE INPUT.      ##
C** ##                                                                    ##
C** ##--------------------------------------------------------------------##
      DUMMY=4.
C** ##--------------------------------------------------------------------##
C** ##                                                                    ##
C** ##  OUTPUT DESTINATION                                                ##
C** ##                                                                    ##
C** ##  CARD LAST-1                                                       ##
C** ##             IOFLAG   -  999 ==> QUIT                             ##
C** ##             IOXMAG   -  DESTINATION CODE FOR NORTH COMPONENT   ##
C** ##             IOYMAG   -       "       "    "  EAST       "      ##
C** ##             IOZMAG   -       "       "    "  VERTICAL   "      ##
C** ##             IOSMAG   -       "       "    "   SCALAR ANOMALY   ##
C** ##         FORMAT 5I4                                               ##
C** ##               ABOVE CODES ARE AS FOLLOWS;                       ##
C** ##                  1 --> WRITE DATA AND TITLE TO UNIT 8          ##
C** ##                  2 -->   "    "    "    "    "  "  9           ##
C** ##                 11 -->   "    "    "    "    " UNITS 6 AND 8   ##
C** ##                 12 -->   "    "    "    "    "  "    "  "  9   ##
C** ##                                                                    ##
```

```
C** ##  CARD LAST   TITLE - TITLE FOR THE ANOMALY DATA                  ##
C** ##      FORMAT(20A4)                                                 ##
C** ##                                                                   ##
C** ##   CONTINUE REPEATING THE ABOVE SET OF TWO  CARDS TO DEFINE        ##
C** ##   ALL DESIRED DATA DESTINATIONS AND THEIR TITLES, THEN            ##
C** ##   ENTER IOFLAG AS 999 TO END                                      ##
C** ##                                                                   ##
C** #####################################################################
C**
      DATE=1980.0
C**
C**
C**  READ IN OBSERVATION GRID INFORMATION
      READ(5,50) FORGE,FORGN,FDELTE,FDELTN,FELEV
      READ(5,51) NFEAST,NFNORT
      READ(5,50) HORIZN
C**  ECHO OBSERVATION INPUT
      WRITE(6,60) FORGE,FORGN,FELEV,FDELTE,FDELTN,NFEAST,NFNORT,HORIZN
C**
C**  READ IN PRISM GRID INFORMATION
      READ(5,50) GORGE,GORGN,GORGV,GDELTE,GDELTN,GDELTV
      READ(5,51) NMEAST,NMNORT,NMDOWN
      DO 10 K=1,NMDOWN
      ILVLMT(K)=0
      DO 10 J=1,NMNORT
      IROWMT(J,K)=0
      DO 10 I=1,NMEAST
   10 LOCBLK(I,J,K)=0
      READ(5,51) IWINDW,IWINDE,IWINDS,IWINDN
      CALL BLKIN(NMEAST,NMNORT,NMDOWN)
      READ(5,*) (IPDIM(I),I=1,9)
      READ(5,*) (SUSCEP(I),I=1,9)
C**  ECHO PRISM GRID INPUT
      WRITE(6,61) GORGE,GORGN,GORGV,GDELTE,GDELTN,GDELTV,NMEAST,NMNORT,
     &            NMDOWN,IWINDW,IWINDE,IWINDS,IWINDN
      CALL BLKOUT(NMEAST,NMNORT,NMDOWN)
      WRITE(6,62) (I,IPDIM(I),SUSCEP(I),I=1,9)
C**
C**  READ IN DATA DESTINATION INFORMATION
  100 CONTINUE
      READ(5,51) IOFLAG,IOXMAG,IOYMAG,IOZMAG,IOSMAG
      IF(IOFLAG.EQ.9999) GO TO 999
      READ(5,52) TITLE
C**
C**  ZERO MODEL FIELD ARRAYS
C**
      DO 11 N=1,NFNORT
      DO 11 NN=1,NFEAST
      FLDNOR(N,NN)=0.0
      FLDEST(N,NN)=0.0
      FLDVRT(N,NN)=0.0
   11 FLDSCA(N,NN)=0.0
C**
C**
C**
C**  LOOP OVER PRISMS
C**
      DO 12 KK=1,NMDOWM
      IF(ILVLMT(KK).EQ.0) GO TO 101
      BLKALT=GORGV-(KK-1)*GDELTV
C**
      DO 13 JJ=1,NMNORT
      IF(JJ.GT.IWINDN.OR.JJ.LT.IWINDS) GO TO 102
      IF(IROWMT(JJ,KK).EQ.0) GO TO 102
```

```
      BLKLAT=GORGN+(JJ-1)*GDELTN
C**
      DO 14 II=1,NMEAST
      ITYPE = LOCBLK(II,JJ,KK)
      IF(II.GT.IWINDE.OR.II.LT.IWINDW) GO TO 103
      IF(ITYPE.EQ.0) GO TO 103
      CALL SIZE(IPDIM(ITYPE),BLKDIM,GDELTN,GDELTE)
      BLKLNG=GORGE+(II-1)*GDELTE
      CNTALT=BLKALT-BLKDIM(3)/2.
      CNTLAT=BLKLAT+BLKDIM(1)/2.
      CNTLNG=BLKLNG+BLKDIM(2)/2.
C**
      CALL SOURCE(CNTLAT,CNTLNG,CNTALT,BLKDIM,NFEAST,NFNORT,
     &              HORIZN,DATE,SUSCEP(ITYPE))
C**
  103 CONTINUE
   14 CONTINUE
  102 CONTINUE
   13 CONTINUE
  101 CONTINUE
   12 CONTINUE
C**
      CALL PRTOUT(FLDNOR,NFEAST,NFNORT,TITLE,IOXMAG,FDELTE,FDELTN)
      CALL PRTOUT(FLDEST,NFEAST,NFNORT,TITLE,IOYMAG,FDELTE,FDELTN)
      CALL PRTOUT(FLDVRT,NFEAST,NFNORT,TITLE,IOZMAG,FDELTE,FDELTN)
      CALL PRTOUT(FLDSCA,NFEAST,NFNORT,TITLE,IOSMAG,FDELTE,FDELTN)
      GO TO 100
C**
  999 CONTINUE
C**
C**-----------------------------------------------------------------
C**                                                         FORMATS
   50 FORMAT(8F10.0)
   51 FORMAT(10I4)
   52 FORMAT(20A4)
   60 FORMAT(/////' ',5X,'OBSERVATION GRID:',/' ',10X,'ORIGIN:',/' ',
     & 15X,F7.2,' DEGREES EAST LONGITUDE',/' ',15X,F7.2,' DEGREES',
     & ' NORTH LATITUDE',/' ',15X,F7.2,' KILOMETRE ALTITUDE',/' ',
     & 10X,'SPACING:',/' ',12X,'E-W',F7.3,' DEG. EAST LONG.',/' ',12X,
     & 'N-S',F7.3,' DEG. NORTH LATITUDE',/' ',10X,'DIMENSION:',/' ',12X,
     & 'E-W',I7,' GRID POINTS',/' ',12X,'N-S',I7,' GRID POINTS'/' ',10X,
     & 'LIMIT BEYOND WHICH FIELDS ARE NOT CALCULATED: ',F10.3,' KM.')
   61 FORMAT(/////' ',5X,'PRISM GRID:',/' ',10X,'ORIGIN:',/' ',
     & 15X,F7.2,' DEGREES EAST LONGITUDE',/' ',15X,F7.2,' DEGREES',
     & ' NORTH LATITUDE',/' ',15X,F7.2,' KILOMETRE ALTITUDE',/' ',
     & 10X,'SPACING:',/' ',12X,'E-W',F7.3,' DEG. EAST LONG.',/' ',12X,
     & 'N-S',F7.3,' DEG. NORTH LATITUDE',/' ',11X,'DOWN',F7.3,
     & ' KILOMETRES',/' ',10X,'DIMENSION:',/' ',12X,
     & 'E-W',I7,' GRID POINTS',/' ',12X,'N-S',I7,' GRID POINTS',/' ',
     & 12X,'VERT',I6,' GRID POINTS',/////' ',10X,'WINDOW IN PRISM GRID:'
     &,/' ',12X,'WEST LIMIT =',I3,10X,'EAST LIMIT =',I3,10X,
     & 'SOUTH LIMIT =',I3,10X,'NORTH LIMIT =',I3)
   62 FORMAT('1',10X,'PRISM TYPE    DIMENSION CODE    SUSCEPTIBILITY',//
     &       /' ',9(14X,I2,11X,'0',I5,12X,F7.5,//' '))
      STOP
      END
      SUBROUTINE SIZE(ICODE,BLKDIM,GDELTN,GDELTE)
C** ##############################################################
C** ##                   SUBROUTINE SIZE                        ##
C** ##                                                          ##
C** ##    CALCULATES DIMENSIONS OF PRISM FROM 6 DIGIT CODE      ##
C** ##                                                          ##
C** ##    E.G.  ICODE=010203   ===>   BLKDIM(1)=01*GDELTN       ##
C** ##                                 BLKDIM(2)=02*GDELTE      ##
```

```
C** ##                                    BLKDIM(3)=03.0                  ##
C** ####################################################################
C**
      DIMENSION BLKDIM(3)
      II=ICODE/10000
      JJ=(ICODE-II*10000)/100
      KK=ICODE-II*10000-JJ*100
      BLKDIM(1)=FLOAT(II)*GDELTN
      BLKDIM(2)=FLOAT(JJ)*GDELTE
      BLKDIM(3)=FLOAT(KK)
      RETURN
      END
      SUBROUTINE SOURCE(CNTLAT,CNTLNG,CNTALT,BLKDIM,NFEAST,NFNORT,
     &              HORIZN,DATE,SUSCEP)
C**
C** ####################################################################
C** ##                                                                ##
C** ##               EQUIVALENT SOURCE SPHERICAL PRISM                ##
C** ##                                                                ##
C** ##            COMPUTES THE MAGNETIC ANOMALY FIELD DUE TO AN       ##
C** ##      ARRAY OF 8 DIPOLES WITHIN A SPHERICAL PRISM WITH CENTRE   ##
C** ##      GIVEN BY CNTLAT (NORTH LATITUDE), CNTLNG (EAST LONG),     ##
C** ##      AND CNTALT (DEPTH  - NEGATIVE DOWN)                       ##
C** ##                                                                ##
C** ##            THE VOLUME IS REPRESENTED BY A 2*2*2 ARRAY          ##
C** ##      OF EQUIVALENT DIPOLE SOURCES ARRANGED ACCORDING TO        ##
C** ##      GAUSSIAN QUADRATURE.                                      ##
C** ##                                                                ##
C** ##        CO-ORDINATE SYSTEMS USED;                               ##
C** ##          FIXED EARTH                                           ##
C** ##            -CARTESIAN SYSTEM WITH ORIGIN AT EARTH'S CENTRE     ##
C** ##            X DIRECTION - THRU INTERSECTION OF EQUATOR AND      ##
C** ##                          GREENWICH MERIDIAN                    ##
C** ##            Z DIRECTION - COINCIDENT WITH NORTH ROTATIONAL      ##
C** ##                          AXIS                                  ##
C** ##                                                                ##
C** ##          GEODETIC                                              ##
C** ##            -GEOGRAPHIC "MAP" SYSTEM                            ##
C** ##            GEOGRAPHIC LATITUDE  (-90 TO +90)                   ##
C** ##            EAST LONGITUDE       (0 TO 360)                     ##
C** ##            ALTITUDE             (POSITIVE UP)                  ##
C** ##                                                                ##
C** ##         GEOCENTRIC                                             ##
C** ##            -SPHERICAL SYSTEM WITH ORIGIN AT EARTH CENTRE       ##
C** ##            GEOCENTRIC CO-LATITUDE   - PHI                      ##
C** ##            EAST LONGITUDE           - LAMBDA                   ##
C** ##            RADIAL DISTANCE          - RHO                      ##
C** ##                                                                ##
C** ##         TOPOCENTRIC                                            ##
C** ##            -LOCAL CARTESIAN SYSTEM WITH ORIGIN ON EARTH        ##
C** ##            SURFACE                                             ##
C** ##            CO-ORDS ARE ALIGNED WITH NORTH, EAST, AND           ##
C** ##            VERTICAL (POSITIVE DOWN)                            ##
C** ##                                                                ##
C** ##                                                                ##
C** ##                                                                ##
C** ##     REF:-  CHAO C KU, GEOPHYSICS, VOL 42, NO 3 1977            ##
C** ##            P 610-622                                           ##
C** ##                                                                ##
C** ####################################################################
C**
      COMMON /OBGRID/ FORGE,FORGN,FDELTE,FDELTN,FELEV
      COMMON /FIELDS/ FLDNOR,FLDEST,FLDVRT,FLDSCA
C**
```

```
      DIMENSION FLDNOR(35,35),FLDEST(35,35),FLDVRT(35,35),FLDSCA(35,35)
      DIMENSION BLKDIM(3),BLKMAG(3),GAUSSV(2)
C**
      REAL JX,JY,JZ
C**
      DATA GAUSSV/.57735027,-.57735027/
      DATA CON/.0174533/
      DATA ITIME/0/,ITIME2/0/
C**
C**+++++++++++++++++++++++++++++++++++++++++++++++++++++++++++++++++++++++
C**+++++++++++++++++++++++++++++++++++++++++++++++++++++++++++++++++++++++
C**                     DEFINITION OF VARIABLES
C**
C**       CNTLAT, CNTLNG, CNTALT - GEODETIC CO-ORDS OF PRISM CENTRE
C**
C**       BLKDIM(3) - GEODETIC NORTH (DEG LAT), EAST (DEG LONG),
C**                   AND VERTICAL (KM DEPTH) DIMENSIONS OF PRISM
C**
C**       JX, JY, JZ  -  FIXED EARTH COMPONENTS OF MAGNETIZATION
C**                    MAGNETIZATION VECTOR HAS UNITS AMP/METRE
C**
C**       GAUSSV(2)  - CO-ORD'S OF INTERVAL LOCATIONS FOR GAUSSIAN
C**                    QUADRATURE
C**
C**
C**
C**+++++++++++++++++++++++++++++++++++++++++++++++++++++++++++++++++++++++
C**+++++++++++++++++++++++++++++++++++++++++++++++++++++++++++++++++++++++
C**
C**   FIND CENTRE OF PRISM IN GEOCENTRIC CO-ORDS
      CALL DETCEN(CNTLAT,CNTLNG,CNTALT,CRHO,CPHI,CLAMDA)
C**   CHECK TO ENSURE PRISM IS SMALL ENOUGH FOR OBSERVATION HEIGHT
      IF(ITIME2.GT.0) GO TO 101
      DEPTH=BLKDIM(3)
      SNLENG=CRHO*BLKDIM(1)*CON
      WIDTH=CRHO*SIN(CPHI*CON)*BLKDIM(2)*CON
      BIG=DEPTH
      IF(SNLENG.GT.BIG) BIG=SNLENG
      IF(WIDTH.GT.BIG) BIG=WIDTH
      BIG=BIG*GAUSSV(1)
      IF(BIG.GT.FELEV) WRITE(6,60) BIG,FELEV
      IF(BIG.GT.FELEV) ITIME2=1
  101 CONTINUE
C**
C**   FIND INDUCED MAGNETIZATION  AS ;  J = (K/((K+1)*MU)) * B
C**   CONFAC=(10**-9)/(4*PI*10**-7)
C**   10**-9    - CONVERT B TO TESLA FROM NANOTESLA
C**   4*PI*10**-7  -  PERMEABILITY OF FREE SPACE
      CONFAC=(.01/(4.*3.14159))*SUSCEP/(SUSCEP+1.)
      CALL IGRF(DATE,2,CRHO,CPHI,CLAMDA,CNMAG,CEMAG,CVMAG,CTMAG)
      PMAGN=CNMAG*CONFAC
      PMAGE=CEMAG*CONFAC
      PMAGV=CVMAG*CONFAC
C**   ROTATE COMPONENTS OF MAGNITIZATION VECTOR TO FIXED EARTH
C**   CO-ORD SYSTEM
C**
      CALL VECTRA(CRHO,CPHI,CLAMDA,PMAGN,PMAGE,PMAGV,
     &            JX,JY,JZ,+1)
C**
C**   FIND REFERENCE MAIN FIELD FOR SCALAR ANOMALY CALCULATION
C**   USE IGRF MAIN FIELD AT CENTRE OF OBS. GRID AND ASSUME IT TO BE
C**   CONSTANT OVER THE ENTIRE OBSERVATION GRID.
      CGALT=FELEV
      CGLAT = FORGN + 0.5*NFNORT*FDELTN
```

```
      CGLNG = FORGE + 0.5*NFEAST*FDELTE
      CALL DETCEN(CGLAT,CGLNG,CGALT,CGRHO,CGPHI,CGLAM)
      CALL IGRF(DATE,2,CGRHO,CGPHI,CGLAM,REFNOR,REFEST,REFVRT,REFTOT)
C**   SET UP FOR GAUSSIAN QUADRATURE
C**   INTEGRATION LIMITS;
      CONST1=(BLKDIM(3) * BLKDIM(2)*CON * BLKDIM(1)*CON) / 8.
C**   CONVERSION FACTORS;
C**   CONVERT ANOMALY EQUATION TO TESLA FROM AMP*TURN/METRE
C**   I.E. FROM ANOMALY IN H TO AN ANOMALY IN B  (MULTIPLY BY MU.ZERO)
C**   CONVERT ANOMALY EQUATION TO NANOTESLA FROM TESLA  (10**9)
C**   CONFAC= MU * 10**9  = 4*PI*10**-7 * 10**9  = 4*PI*100
C**   DIVIDE BY 4*PI ACCORDING TO S.I. EQUATION ;  CONFAC = 100
      CONST1 = CONST1*100.
C**
      H2 = HORIZN*HORIZN
C**
C**-------------------------------------------------------------------
C**                                   LOOP OVER FIELD OBSERVATION POINTS
C**   FIND POSITION OF POINT IN EARTH-FIXED CO-ORDINATES
      OBSALT=FELEV
      DO 10 JF=1,NFNORT
      OBSLAT=(JF-1)*FDELTN+FORGN
      DO 11 IF=1,NFEAST
      OBSLNG=(IF-1)*FDELTE+FORGE
C**   FIND FIXED EARTH CO-ORDS OF THIS FIELD OBSERVATION POINT
      CALL DETCEN(OBSLAT,OBSLNG,OBSALT,OBSRHO,OBSPHI,OBSLAM)
      CALL CENFIX(OBSRHO,OBSPHI,OBSLAM,OBSX,OBSY,OBSZ,+1)
C**   ANOMALY FIELDS;
      XANOM=0.0
      YANOM=0.0
      ZANOM=0.0
      SCANOM=0.0
C**------------------------------------------------------------
C**                                   LOOP OVER 8 DIPOLES IN PRISM
      DO 12 I=1,2
C**   GEODETIC CO-ORDS FOR TOP OR BOTTOM FOUR DIPOLES;
      DIPALT = CNTALT + (BLKDIM(3)/2.)*GAUSSV(I)
      DO 12 J=1,2
C**   NORTH OR SOUTH FOUR;
      DIPLAT = CNTLAT + (BLKDIM(1)/2.)*GAUSSV(J)
      DO 12 K=1,2
C**   EAST OR WEST FOUR;
      DIPLNG = CNTLNG + (BLKDIM(2)/2.)*GAUSSV(K)
C**   FIND GEOCENTRIC AND EARTH-FIXED CO-ORDS OF THIS DIPOLE
      CALL DETCEN(DIPLAT,DIPLNG,DIPALT,DIPRHO,DIPPHI,DIPLAM)
      CALL CENFIX(DIPRHO,DIPPHI,DIPLAM,DIPX,DIPY,DIPZ,+1)
C**
C**   FIND COMPONENTS OF SEPARATION VECTOR FROM OBS. PNT. TO DIPOLE
      RX = DIPX - OBSX
      RY = DIPY - OBSY
      RZ = DIPZ - OBSZ
      R2 = RX*RX +RY*RY +RZ*RZ
      R5 = R2*R2*SQRT(R2)
C**
C**   CHECK IF PRISM IS BEYOND SPECIFIED HORIZON
      IF(R2.GT.H2) GO TO 100
C**   CONSTANT FOR GAUSSIAN QUADRATURE IN SPHERICAL CO-ORDINATES;
      CONST2 = (CONST1 * DIPRHO*DIPRHO * SIN(DIPPHI*CON)) / R5
C**
C**   CALCULATE ANOMALY FIELDS AND SUM INTO TOTAL ANOMALY DUE TO THIS
C**   PRISM
      XANOM=XANOM + CONST2*(JX*((3.*RX*RX)-R2)+JY*3.*RX*RY+JZ*3.*RX*RZ)
      YANOM=YANOM + CONST2*(JX*3.*RX*RY+JY*((3.*RY*RY)-R2)+JZ*3.*RY*RZ)
      ZANOM=ZANOM + CONST2*(JX*3.*RX*RZ+JY*3.*RY*RZ+JZ*((3.*RZ*RZ)-R2))
```

```
   12 CONTINUE
C**   TRANSFORM ANOMALOUS FIELD VALUES AT THIS OBSERVATION POINT TO
C**   TOPOCENTRIC COMPONENTS
      CALL VECTRA(OBSRHO,OBSPHI,OBSLAM,  ANOMN,ANOME,ANOMV,
     &            XANOM,YANOM,ZANOM, -1)
C**   SUM INTO FIELD VALUES FOR THIS LOCATION AND OTHER PRISMS
      FLDNOR(JF,IF)=FLDNOR(JF,IF)+ANOMN
      FLDEST(JF,IF)=FLDEST(JF,IF)+ANOME
      FLDVRT(JF,IF)=FLDVRT(JF,IF)+ANOMV
C**   FIND SCALAR ANOMALY (DOT PRODUCT OF VECT. ANOM. AND UNIT MAIN FLD)
      SCANOM=(ANOMN*REFNOR+ANOME*REFEST+ANOMV*REFVRT)/REFTOT
      FLDSCA(JF,IF)=FLDSCA(JF,IF)+SCANOM
      IF(ITIME.EQ.O)  WRITE(6,61)
     & CNTLAT,CNTLNG,CNTALT,CRHO,CPHI,CLAMDA,SNLENG,WIDTH,DEPTH,
     & OBSLAT,OBSLNG,OBSALT,OBSRHO,OBSPHI,OBSLAM,OBSX,OBSY,OBSZ,
     & DIPLAT,DIPLNG,DIPALT,DIPRHO,DIPPHI,DIPLAM,DIPX,DIPY,DIPZ,
     & PMAGN,PMAGE,PMAGV,JX,JY,JZ,R2,CONST1,CONST2,
     & ANOMN,ANOME,ANOMV,XANOM,YANOM,ZANOM
      ITIME=1
  100 CONTINUE
   11 CONTINUE
   10 CONTINUE
C**
      RETURN
C**---------------------------------------------------------------------
C**                                                              FORMATS
   60 FORMAT(' ','******  WARNING  ******',/
     &       ' ','   PRISMS ARE TOO BIG FOR THIS ELEVATION',/
     &   ' ','   LARGEST DIPOLE SEPARATION IS ',F6.2,' KM AND OBSER',
     &          'VATION HEIGHT IS ONLY ',F6.2,' KM')
   61 FORMAT(' ','CENTRE',9F14.4,///' ','OBSERV',9F14.4,///' ',
     &       'DIPOLE',9F14.4,///' ','MAG   ',9F14.4,///' ','ANOM  ',
     &       9F14.4,///)
      END
      SUBROUTINE BLKIN(NMEAST,NMNORT,NMDOWN)
C**
C** ##################################################################
C** ##                                                              ##
C** ##                         BLOCK READIN                         ##
C** ##                                                              ##
C** ##        READ IN TYPE CODES FOR PRISMS AND STORE IN LOCBLK     ##
C** ##                                                              ##
C** ##################################################################
C**
      COMMON /PRISMS/ LOCBLK
      COMMON /GRID/ IROWMT,ILVLMT
      DIMENSION LOCBLK(50,50,10)
      DIMENSION IROWMT(50,10),ILVLMT(10)
      DIMENSION ISTORE(50)
      DATA ISTORE/50*0/
C**
C**                 DEFINITION OF VARIABLES
C**
C**          LOCBLK - GRID SPECIFYING LOCATION OF BLOCKS
C**          NMEAST - DIMENSION OF GRID IN EAST - WEST DIRECTION
C**          NMNORT - DIMENSION OF GRID IN NORTH - SOUTH DIRECTION
C**          NMDOWN - DIMENSION OF GRID IN VERTICAL DIRECTION
C**          IROWMT - DETERMINES IF A GIVEN ROW IN THE GRID IS
C**                   EMPTY OR NOT
C**          ILVLMT - DETERMINES IF A GIVEN PLANE IN THE GRID IS
C**                   EMPTY OR NOT
C**
      DO 10 KKK=1,10
      READ(5,50) K
```

```
      IF(K.EQ.999) GO TO 200
C**
  100 READ(5,51) J,(ISTORE(I),I=1,50)
      IF(J.EQ.999) GO TO 150
      DO 11 I=1,NMEAST
   11 LOCBLK(I,J,K)=ISTORE(I)
      ILVLMT(K)=1
      IROWMT(J,K)=1
C**
      GO TO 100
  150 CONTINUE
   10 CONTINUE
C**
  200 CONTINUE
   50 FORMAT(I3)
   51 FORMAT(I3,1X,76I1)
      RETURN
      END
      SUBROUTINE BLKOUT(NMEAST,NMNORT,NMDOWN)
C** #################################################################
C** ##                                                             ##
C** ##                      BLOCK PRINT OUT                        ##
C** ##                                                             ##
C** ##       PRINT OUT TYPE CODES FOR PRISMS FROM LOCBLK           ##
C** ##                                                             ##
C** #################################################################
C**
      COMMON /PRISMS/ LOCBLK
      COMMON /GRID/ IROWMT,ILVLMT
      DIMENSION LOCBLK(50,50,10),IROWMT(50,10)
      DIMENSION ILVLMT(10)
      DIMENSION A(80)
      DIMENSION AN(40),SYMBOL(9)
      DATA AN/'0','1','2','3','4','5','6','7','8','9','A','B','C','D',
     1       'E','F','G','H','I','J','K','L','M','N','O','P','Q','R',
     2       'S','T','U','V','W','X','Y','Z','*','+','#',' '/
      DATA ITIME/0/
      DATA SYMBOL/'1','2','3','4','5','6','7','8','9'/
C**
C**                    DEFINITION OF VARIABLES
C**
C**            LOCBLK - GRID SPECIFYING LOCATION OF BLOCKS
C**            NMEAST - DIMENSION OF GRID IN EAST - WEST DIRECTION
C**            NMNORT - DIMENSION OF GRID IN NORTH - SOUTH DIRECTION
C**            NMDOWN - DIMENSION OF GRID IN VERTICAL DIRECTION
C**            IROWMT - DETERMINES IF A GIVEN ROW IN THE GRID IS
C**                     EMPTY OR NOT
C**            ILVLMT - DETERMINES IF A GIVEN PLANE IN THE GRID IS
C**                     EMPTY OR NOT
C**
C**
      DO 400 K=1,NMDOWN
      IF(ILVLMT(K).EQ.0) GO TO 400
C**
      WRITE(6,10) K
C**
C**  PRINT BORDER
C**
      IMAX=NMEAST
      IF(IMAX.GT.125) IMAX=125
      CALL UBLANK(A,IMAX)
      IN=0
      DO 50 II=1,IMAX
      III=II/10
```

```
      IF(III.GE.100) III=III/10
      IF(III.LT.IN) GO TO 50
      IN=IN+1
      A(II)=AN(IN)
   50 CONTINUE
      WRITE(6,11) (A(II),II=1,IMAX)
C**
      DO 55 II=1,IMAX
      III=II-(II/10)*10+1
   55 A(II)=AN(III)
      WRITE(6,11) (A(II),II=1,IMAX)
      WRITE(6,99)
C**
C**
      DO 300 JJ=1,NMNORT
      J=NMNORT-JJ+1
      CALL UBLANK(A,IMAX)
      IF(IROWMT(J,K).EQ.0) GO TO 250
C**
      DO 200 I=1,IMAX
      IF(LOCBLK(I,J,K).EQ.0) GO TO 200
      II=LOCBLK(I,J,K)
      IF(II.LT.0.OR.II.GT.9) GO TO 500
      A(I)=SYMBOL(II)
  200 CONTINUE
C**
  250 WRITE(6,20) J,(A(II),II=1,IMAX)
  300 CONTINUE
      WRITE(6,99)
      DO 260 II=1,IMAX
      III=II-(II/10)*10+1
  260 A(II)=AN(III)
      WRITE(6,11) (A(II),II=1,IMAX)
      CALL UBLANK(A,IMAX)
C**
      IN=0
      DO 270 II=1,IMAX
      III=II/10
      IF(III.GE.100) III=III/10
      IF(III.LT.IN) GO TO 270
      IN=IN+1
      A(II)=AN(IN)
  270 CONTINUE
      WRITE(6,11) (A(II),II=1,IMAX)
  400 CONTINUE
      ITIME=1
      RETURN
  500 CONTINUE
      WRITE(6,30) I,J,K,II
      CALL TRMIN8
C**
   10 FORMAT('1'///,' ',30X,'DEPTH LEVEL - ',I4/)
   11 FORMAT(' ',4X,125A1)
   20 FORMAT(' ',I3,1X,125A1)
   30 FORMAT(' ','** ERROR IN BLKOUT - LOCBLK(',3I3,') =',I3)
   99 FORMAT(' ')
      RETURN
      END
      SUBROUTINE UBLANK(A,NUM)
C**
C** ####################################################################
C** ##                         SUBROUTINE  UBLANK                     ##
C** ##                                                                ##
C** ##           INSERTS BLANKS IN ARRAY A FROM 1 TO NUM              ##
```

```
C** ##                                                                   ##
C** #######################################################################
C**
C**
      DIMENSION A(80)
      DATA BLANK/' '/
      DO 100 I=1,NUM
  100 A(I)=BLANK
      RETURN
      END
      SUBROUTINE PRTOUT(F,NFEAST,NFNORT,TITLE,IOUT,FDELTE,FDELTN)
C**
C** #######################################################################
C** ##                        SUBROUTINE PRTOUT                          ##
C** ##                                                                   ##
C** ##                                                                   ##
C** #######################################################################
C**
C**
      DIMENSION TITLE(20)
      DIMENSION F(35,35)
C**
      IPRT=(IOUT+1)/10
      IFLAG=IOUT-IPRT*10
      IF(IFLAG.EQ.9) RETURN
      IF(IPRT.EQ.1) WRITE(6,12) (JJ,JJ=1,21)
      IF(IFLAG.EQ.1) WRITE(8,11) TITLE
      IF(IFLAG.EQ.1) WRITE(8,15) NFEAST,NFNORT,FDELTE,FDELTN
      IF(IFLAG.EQ.2) WRITE(9,11) TITLE
      IF(IFLAG.EQ.2) WRITE(9,15) NFEAST,NFNORT,FDELTE,FDELTN
      DO 100 J=1,NFNORT
      IF(IFLAG.EQ.1) WRITE(8,4) (F(J,I),I=1,NFEAST)
      IF(IFLAG.EQ.2) WRITE(9,4) (F(J,I),I=1,NFEAST)
      IF(IPRT.EQ.1) WRITE(6,10) J,(F(J,I),I=1,NFEAST)
  100 CONTINUE
C**
    4 FORMAT(8E10.3)
   10 FORMAT(' ',I2,2X,21F6.2,250(/' ',4X,21F6.2))
   11 FORMAT(20A4)
   12 FORMAT('1',///' ',4X,21(2X,I2,2X)/)
   15 FORMAT(4X,2I3,2F7.3)
      RETURN
      END
      SUBROUTINE VECTRA(RHO,PHI,ELAMDA,VECTN,VECTE,VECTV,VECTX,VECTY,
     &                     VECTZ,IROT)
C**  ######################################################################
C**  ##                                                                  ##
C**  ##             TRANSFORMS VECTOR COMPONETS BETWEEN TOPOCENTRIC      ##
C**  ##      (N,E,V) CO-ORD SYSTEM AND FIXED EARTH (X,Y,Z) CO-ORD        ##
C**  ##      SYSTEM. RHO, PHI, LAMBDA ARE THE GEOCENTRIC CO-ORDS         ##
C**  ##      OF THE VECTOR.  IROT GIVES DIRECTION OF TRANSFORMATION      ##
C**  ##      IROT = -1     XYZ ==> NEV    ;  IROT = +1     NEV ==> XYZ   ##
C**  ##      PHI = GEOCENTRIC CO-LATITUDE  ELAMDA = EAST LONGITUDE       ##
C**  ######################################################################
C**
      DATA CON/.0174533/
C**
C**
      SINP=SIN(PHI*CON)
      COSP=COS(PHI*CON)
      SINL=SIN(ELAMDA*CON)
      COSL=COS(ELAMDA*CON)
C**
C**
```

```
      IF(IROT) 100,300,200
  100 CONTINUE
      VECTN = -VECTX*COSL*COSP - VECTY*SINL*COSP + VECTZ*COSP
      VECTE = -VECTX*SINL + VECTY*COSL
      VECTV = -VECTX*COSL*SINP - VECTY*SINL*SINP - VECTZ*COSP
      RETURN
C**
  200 CONTINUE
      VECTX = -VECTN*COSP*COSL - VECTE*SINL - VECTV*SINP*COSL
      VECTY = -VECTN*COSP*SINL + VECTE*COSL - VECTV*SINP*SINL
      VECTZ = VECTN*SINP - VECTV*COSP
      RETURN
C**
  300 CONTINUE
      WRITE(6,10)
   10 FORMAT(' ','#####  ERROR IN VECTRA   #####       IROT=0')
      CALL TRMIN8
      RETURN
      END
      SUBROUTINE DETCEN(BLAT,ELONG,HEIGHT,RHO,PHI,ELAMDA)
C**
C** ##################################################################
C** ##                                                              ##
C** ##            CONVERTS GEODETIC CO-ORDINATES (LATITUDE,         ##
C** ##            EAST LONG,HEIGHT) TO GEOCENTRIC CO-ORDS           ##
C** ##            (RADIAL DISTANCE, CO-LATITUDE, EAST LONGITUDE)    ##
C** ##                                                              ##
C** ##        RHO = RADIAL DISTANCE                                 ##
C** ##        PHI = GEOCENTRIC CO-LATITUDE                          ##
C** ##        ELAMDA = EAST LONGITUDE                               ##
C** ##################################################################
C**
      DATA CON/.0174533/
      DATA A2/40680925./
      DATA B2/40408585./
C**
      ALT=HEIGHT
C**
      ONE=(90.0-BLAT)*CON
      SLAT=COS(ONE)
      CLAT = SIN(ONE)
      ONE = A2*CLAT*CLAT
      TWO = B2*SLAT*SLAT
      THREE = ONE + TWO
      FOUR = SQRT(THREE)
      R = SQRT(ALT*(ALT + 2.0*FOUR) + (A2*ONE + B2*TWO)/THREE)
      CD = (ALT + FOUR)/R
      SD = (A2 -B2)/FOUR*SLAT*CLAT/R
      ONE = SLAT
      SLAT= SLAT*CD - CLAT*SD
      CLAT = CLAT*CD + ONE*SD
C**
      RHO=R
      PHI=ARCOS(SLAT)/CON
      ELAMDA=ELONG
C**
      RETURN
      END
      SUBROUTINE CENFIX(RHO,PHI,ELAMDA,X,Y,Z,IROT)
C** ##################################################################
C** ##                     SUBROUTINE CENFIX                        ##
C** ##     CONVERTS GEOCENTRIC CO-ORDS RADIAL DISTANCE (RHO),       ##
C** ##   GEOCENTRIC CO-LATITUDE (PHI), AND EAST LONG. (ELAMDA)      ##
C** ##   TO EARTH-FIXED CO-ORDINATES X, Y, AND Z.  THE X-AXIS       ##
```

```
C** ##   PIERCES THE EARTH'S SURFACE AT THE INTERSECTION OF          ##
C** ##   GREENWICH MERIDIAN AND THE EQUATOR, WHILE THE Z-AXIS        ##
C** ##   IS COINCIDENT WITH THE NORTH ROTATIONAL AXIS.               ##
C** ##                                                               ##
C** ##    THE SIGN OF IROT GIVES THE DESIRED TRANSFORMATION          ##
C** ##     IROT = -1  ====>   XYZ --> RHO,PHI,LAMBDA                 ##
C** ##            +1  ====>   RHO,PHI,LAMBDA --> XYZ                 ##
C** ##                                                               ##
C** #################################################################
C**
      DATA CON/.0174533/
C**
      IF(IROT) 100,300,200
  100 CONTINUE
      RHO=SQRT(X*X+Y*Y+Z*Z)
      ELAMDA=(ATAN(Y/X))/CON
      PHI=(ARCOS(Z/RHO))/CON
      RETURN
C**
  200 CONTINUE
      COSP = COS(PHI*CON)
      SINP = SIN(PHI*CON)
      COSL = COS(ELAMDA*CON)
      SINL = SIN(ELAMDA*CON)
C**
      X = RHO*COSL*SINP
      Y = RHO*SINL*SINP
      Z = RHO*COSP
      RETURN
C**
  300 CONTINUE
      WRITE(6,10)
   10 FORMAT(' ','#######  ERROR IN CENFIX  #######   IROT=0')
      CALL TRMIN8
      RETURN
      END
      SUBROUTINE IGRF (DATE,ITYPE,ALT,COLAT,ELONG,X,Y,Z,T)
C**
C ######################################################################
C ##                                                                  ##
C ##                                                                  ##
C ## THIS SUBROUTINE COMPUTES VALUES OF X,Y,Z AND T FOR A GIVEN EPOCH ##
C ## AND POSITION FROM THE SPHERICAL HARMONIC COEFFICIENTS OF THE     ##
C ## INTERNATIONAL GEOMAGNETIC REFERENCE FIELD                        ##
C ##                                                                  ##
C ## DATA DATE = REQUIRED EPOCH IN YEARS AND DECIMALS OF A YEAR, A.D. ##
C ##      ITYPE = 1 IF GEODETIC CORRDINATES ARE BEING USED            ##
C ##      ITYPE = 2 IF GEOCENTRIC COORDINATES ARE BEING USED          ##
C ##        ALT = HEIGHT ABOVE MEAN SEA LEVEL IN KM (ITYPE=1)         ##
C ##        ALT = RADIAL DISTANCE FROM CENTRE OF EARTH IN KM (ITYPE=2)##
C ##      COLAT = COLATITUDE IN DEGREES (0.0 TO 180.0)                ##
C ##      ELONG = EAST LONGITUDE IN DEGREES (0.0 TO 360.0)            ##
C ##                                                                  ##
C ## OUTPUT X = NORTH COMPONENT OF MAGNETIC FORCE IN GAMMA            ##
C ##        Y = EAST COMPONENT OF MAGNETIC FORCE IN GAMMA             ##
C ##        Z = VERTICAL COMPONENT OF MAGNETIC FORCE IN GAMMA         ##
C ##                                                                  ##
C ##        T = TOTAL MAGNETIC FORCE IN GAMMA                         ##
C ## N.B. THE COORDINATE SYSTEM FOR X,Y AND Z IS THE SAME AS THAT     ##
C ##      SPECIFIED BY ITYPE                                          ##
C ##                                                                  ##
C ##                                                                  ##
C ## THE S.H. COEFFICIENTS ARE SUPPLIED BY A DATA STATEMENT;          ##
C ##                                                                  ##
```

```
C ## DATA FORMAT: G(N,1) G(N,2) H(N,2) G(N,3) H(N,3)...G(N,M) H(N,M)  ##
C ##                                                                    ##
C ## NGTERM IS THE NUMBER OF G(N,M)'S                                   ##
C ## NGTERM OF 77 ===>  DEGREE AND ORDER 11                             ##
C ## NGTERM OF 104 ===> DEGREE AND ORDER 13                             ##
C ##                                                                    ##
C ##                                                                    ##
C ## ALTERNATIVELY, THE COEFFICIENTS MAY BE SUPPLIED BY STATEMENTS OF ##
C ## THE FORM:      AGH(1) = -30339.      AGH(2) = -2123.      ETC.     ##
C ## OR THE COEFFICIENTS MAY BE READ IN THE MASTER PROGRAM AND MADE    ##
C ## AVAILABLE TO THE SUBROUTINE BY A COMMON STATEMENT                 ##
C ##                                                                    ##
C ######################################################################
C**
      DIMENSION AGH(200),DGH(200),P(150),Q(150),CL(20),SL(20)
C**-------------------------------------------------------------------
C60  POGO(10/68)
C60   DATA NGTERM/77/
C60   DATA RYEAR/1960.0/
C60   DATA AGH/-30465.0,-2163.3,5791.0,
C60  2          -1541.4,2976.3,-1977.2,1607.5,156.6,
C60  3          1325.8,-1983.7,-445.3,1316.9,233.4,842.0,-94.9,
C60  4          959.1,819.6,135.4,486.4,-266.7,-372.4,20.7,256.2,-241.5,
C60  5          -234.3,357.7,16.9,233.9,113.3,-21.0,-128.7,-147.1,-115.1,
C60  5          -45.2,130.3,
C60  6          49.1,54.5,-9.6,4.8,106.4,-249.1,56.8,1.7,-27.2,-3.7,
C60  6          -14.9,-91.6,-4.3,
C60  7          75.9,-52.4,-57.9,8.0,-25.0,10.0,-0.8,-36.7,6.3,-8.3,9.5,
C60  7          6.6,-11.7,-22.7,-37.6,
C60  8          7.4,6.0,10.1,-8.1,-13.0,-9.2,11.5,-0.8,-16.4,9.1,5.5,
C60  8          -11.4,22.3,7.9,-4.9,35.1,-26.2,
C60  9          11.0,6.6,-20.4,1.8,14.4,-12.5,0.6,15.8,-1.5,1.7,1.4,
C60  9          2.6,3.4,8.7,14.8,5.1,2.4,-2.4,-0.9,
C60  &          -2.6,-2.0,1.1,1.0,0.9,-5.5,-0.3,-0.7,7.5,7.5,-2.3,7.8,
C60  &          1.4,1.7,-0.5,-5.3,4.3,1.3,8.0,-2.7,-13.7,
C60  1          2.3,-1.8,-0.8,-2.1,4.4,5.5,-0.1,-1.5,-3.9,2.4,-0.6,
C60  1          -3.5,1.8,-1.3,-3.2,2.5,0.8,-1.2,-5.9,12.7,-1.7,5.0,10.5,
C60  *          57*0.0/
C**
C60   DATA DGH/25.42,9.88,-4.66,
C60  2          -23.9,3.5,-7.07,-2.14,-10.7,
C60  3          -5.59,-11.52,8.48,-4.41,0.68,2.87,-14.89,
C60  4          -0.62,-2.51,3.45,-1.22,-0.39,-2.96,-0.87,0.86,-6.52,
C60  5          2.72,0.48,0.05,3.17,3.00,-2.46,0.32,-0.89,3.11,-3.15,
C60  5          -6.35,
C60  6          -0.61,1.06,-0.26,0.62,-0.48,3.96,2.58,-0.94,-0.80,1.49,
C60  6          0.50,-1.67,0.82,
C60  7          -0.89,-0.21,-0.87,-1.08,-0.46,0.70,-1.02,1.07,0.25,0.96,
C60  7          1.88,1.01,-2.43,5.23,2.32,
C60  8          0.61,-0.12,-0.15,0.87,-0.10,-0.33,-1.22,-0.14,-0.26,
C60  8          -0.85,0.15,0.99,-0.37,0.81,0.29,-4.98,0.91,
C60  9          -0.24,0.30,-0.38,0.04,0.16,0.04,0.67,-0.40,-0.14,-0.28,
C60  9          -0.83,-0.57,1.3,-1.32,-0.33,-0.14,-0.38,0.50,0.99,
C60  &          -0.01,-0.09,0.21,0.12,0.05,0.19,0.54,-0.20,-0.26,-0.02,
C60  &          -0.30,-0.43,-0.03,-0.33,-0.39,1.03,-0.02,0.22,-1.04,.46,
C60  &          0.79,
C60  1          0.03,0.11,0.35,0.05,-0.26,-0.30,-0.17,0.01,0.17,-0.34,
C60  1          0.18,0.48,-0.50,0.52,0.23,-0.19,-0.34,-0.03,0.37,-1.65,
C60  1          0.22,-0.40,-1.55,57*0.0/
C**
C**-------------------------------------------------------------------
      DUMMY=1.
C**-------------------------------------------------------------------
C**
```

```
C65    DATA NGTERM/44/
C65    DATA RYEAR/1965.0/
C65    DATA AGH/-30339.,-2123., 5758.,-1654., 2994.,-2006., 1567.,  130.,
C65   *          1297.,-2036., -403., 1289.,  242.,  843., -176.,  958.,
C65   *           805.,  149.,  492., -280., -392.,    8.,  256., -265.,
C65   *          -223.,  357.,   16.,  246.,  125.,  -26., -123., -161.,
C65   *          -107.,  -51.,   77.,   47.,   60.,  -14.,    4.,  106.,
C65   *          -229.,   68.,    3.,  -32.,   -4.,  -10., -112.,  -13.,
C65   *            71.,  -54.,  -57.,    0.,  -27.,   12.,   -8.,  -25.,
C65   *             9.,   -9.,   23.,   13.,  -19.,   -2.,  -17.,   10.,
C65   *             9.,    3.,   -3.,  -13.,  -12.,    5.,   -4.,  -17.,
C65   *             7.,    4.,   -5.,   22.,   12.,   -3.,    6.,  -16.,
C65   *             120*0.0/
C**
C65    DATA DGH/  15.3,   8.7,  -2.3, -24.4,   0.3, -11.8,  -1.6, -16.7,
C65   *            0.2, -10.8,   4.2,   0.7,   0.7,  -3.8,  -7.7,  -0.7,
C65   *            0.2,  -0.1,  -3.0,   1.6,  -0.1,   2.9,  -2.1,  -4.2,
C65   *            1.9,   1.1,   2.3,   2.9,   1.7,   0.6,  -2.4,   0.0,
C65   *            0.8,   1.3,  -0.3,  -0.1,  -0.3,  -0.9,   1.1,  -0.4,
C65   *            1.9,   2.0,  -0.4,  -1.1,  -0.4,   0.1,  -0.2,   0.9,
C65   *           -0.5,  -0.3,  -1.1,  -0.7,   0.3,  -0.5,   0.4,   0.3,
C65   *            0.2,   0.0,   0.4,  -0.2,   0.2,  -0.6,   0.3,   0.1,
C65   *            0.4,   0.1,   0.6,  -0.2,   0.0,  -0.3,   0.0,  -0.2,
C65   *           -0.1,  -0.3,   0.3,  -0.4,  -0.3,  -0.3,  -0.5,  -0.3,
C65   *             120*0.0/
C**
C**-----------------------------------------------------------------
       DUMMY=2.
C**-----------------------------------------------------------------
C**
C75    DATA NGTERM/90/
C75    DATA RYEAR/1975.0/
C75    DATA AGH/-30055.7,-2017.0,5670.5,
C75   2          -1932.0,3001.3,-2044.4,1619.7,-69.2,
C75   3          1267.1,-2127.2,-343.5,1259.4,263.2,818.0,-208.5,
C75   4          953.8,786.1,196.7,437.8,-257.0,-412.8,20.1,232.3,-287.5,
C75   5          -214.2,357.4,31.4,256.1,150.7,-42.8,-137.4,-166.7,-81.9,
C75   6          41.7,64.2,-19.9,18.3,105.6,-199.4,60.8,3.2,-39.2,10.6,
C75   6          1.8,-108.5,14.6,
C75   7          74.3,-49.7,-73.0,5.4,-27.9,24.8,-5.2,-11.8,8.2,-3.7,13.9,
C75   7          15.0,-21.0,0.3,-9.3,
C75   8          12.4,8.4,6.9,-3.7,-15.4,-11.7,4.8,-8.5,-17.0,5.9,11.0,
C75   8          2.9,15.5,7.1,-9.6,3.1,-19.1,
C75   9          12.5,5.2,-17.2,1.5,17.2,-7.4,4.2,11.9,-0.1,2.3,-4.9,
C75   9          -0.4,9.1,2.9,12.2,1.6,-2.9,-0.8,0.8,
C75   &          -5.5,-2.0,0.2,2.0,0.6,-2.7,-0.5,-4.0,4.3,9.1,-4.0,4.2,
C75   &          2.7,-2.2,-2.0,-0.8,4.3,5.0,0.1,2.1,-4.5,
C75   1          4.4,-3.1,1.0,-2.7,2.4,5.0,-2.1,-0.3,2.4,-1.3,3.2,-1.0,
C75   1          1.7,1.0,-0.7,0.9,-3.0,-2.1,-2.1,0.8,0.2,-0.5,-0.1,
C75   2          -0.7,0.0,1.3,1.6,-1.8,0.4,0.9,-1.5,0.1,-1.2,-1.8,-.4,1.4,
C75   2          -3.6,-1.1,0.6,0.1,0.8,1.9,-0.3,-3.3,1.3,0.6,0.7,1.5,
C75   &          32*0.0/
C**
C75    DATA DGH/24.4,9.9,-10.3,
C75   2          -24.9,1.2,-3.1,3.1,-19.0,
C75   3          -3.7,-10.4,6.7,-3.4,2.1,-3.7,-3.5,
C75   4          0.5,-1.8,4.7,-3.7,1.0,-2.1,0.9,-1.6,-1.4,
C75   5          0.3,-0.3,1.5,1.0,2.0,-1.2,-1.3,-0.4,1.3,0.6,1.0,
C75   6          -0.3,0.1,-0.7,1.7,0.0,2.1,-0.6,-0.1,-1.0,0.9,1.1,0.2,1.5,
C75   7          0.4,.2,-1.5,.6,.0,.9,.5,.9,.2,.0,-0.8,.1,.2,-0.2,.4,
C75   8          .0,.4,-0.2,.1,-0.4,-0.1,.0,-0.5,-0.3,-0.3,.4,.5,-0.2,
C75   8          -0.4,-0.7,-0.2,0.0,
C75   *          120*0.0/
C**
```

```
C**-----------------------------------------------------------------
      DUMMY=3.
C**-----------------------------------------------------------------
C**
C**   MAGSAT MGS481#2  EPOCH 1980.0  MEAN EARTH RADIUS 6371.1992
C**          DEGREE AND ORDER 13 FOR G AND H, 7 FOR TIME DERIVATIVES.
C**
      DATA NGTERM/104/
      DATA RYEAR/1980.0/
      DATA AGH/-29987.2,-1956.9,5604.7,
     2 -1996.2,3027.4,-2129.5,1663.5,-199.6,
     3 1279.8,-2181.0,-334.3,1251.4,271.1,833.0,-252.2,
     4 937.7,782.5,212.2,396.9,-256.7,-419.4,52.4,198.1,-297.8,
     5 -217.2,357.8,45.9,261.1,150.,-74.3,-150.6,-162.,-77.7,-48.1,92.3,
     6 48.5,65.,-14.6,41.9,93.2,-192.,71.,3.5,-43.,13.8,-2.2,-107.6,17.3
     7,72.,-59.2,-82.5,1.6,-27.2,20.9,-5.2,-12.1,15.9,.4,17.9,10.3,-23.,
     7 -1.8,-9.9,
     8 18.5,6.7,7.2,-.2,-17.6,-10.9,3.8,-7.2,-22.2,4.4,9.1,2.5,16.1,6.1,
     8 -13.3,-0.8,-14.8,
     9 5.3,10.4,-20.9,1.4,15.5,-12.1,8.7,9.5,-5.1,-3.6,-6.8,-1.,9.,6.9,
     9 9.7,1.4,-5.7,-5.0,2.2,
     & -3.2,-3.8,1.2,2.4,.4,-5.6,2.9,-1.8,5.8,4.5,-4.3,3.3,-.1,.7,-1.3,
     & 2.3,3.1,3.1,-0.2,-0.5,-6.4,
     1 2.5,-1.3,.9,-1.8,2.,2.4,-1.5,.2,-3.2,-.9,.5,-.4,-.3,1.4,-2.4,1.5,
     1 -0.3,-0.6,-1.5,1.9,-1.9,3.5,1.1,
     2 -1.7,0.,.4,-.2,.6,-.2,2.3,.8,-1.4,.5,.4,-.5,.1,-.2,-.3,.3,.1,-.6,
     2 0.0,-0.2,-1.3,0.8,0.5,-0.0,0.9,
     3 0.,-.4,-.5,.5,.3,-.6,1.2,-.1,-.2,.9,-.5,-.5,-.1,.2,.9,-.9,.3,.2,
     3 1.0,-0.1,0.2,0.3,-0.1,-0.5,-.4,.4,-.9,5*0.0/
C**
      DATA DGH/25.50,12.78,-22.43,
     2          -10.91,0.50,-12.87,11.09,-20.78,
     3          -5.56,-6.58,3.95,-2.87,1.25,-0.46,-9.36,
     4          -0.87,1.80,-0.41,-6.72,-1.73,0.75,5.71,-7.18,-4.05,
     5          0.55,-1.83,1.12,-0.23,1.50,-3.31,-1.93,1.54,3.56,
     5          -2.58,0.63,
     6          1.54,2.22,-1.54,0.55,-2.71,0.56,-0.74,0.90,1.15,
     6          0.29,0.61,-1.34,3.84,
     7          1.08,-2.45,-1.28,0.15,0.94,0.65,0.99,-0.69,-0.25,
     7          -1.66,-0.51,1.40,-0.68,1.46,1.80,
     *          137*0.0/
C**
C**
C**-----------------------------------------------------------------
C**
C**   SET INITIAL VALUES
C**
      T=DATE-RYEAR
      R = ALT
      ONE=COLAT*.0174533
      SLAT=COS(ONE)
      CLAT = SIN(ONE)
      ONE = ELONG*0.0174533
      CL(1)= COS(ONE)
      SL(1)= SIN(ONE)
      X = 0.0
      Y= 0.0
      Z = 0.0
      CD = 1.0
      SD = 0.0
      L = 1
      M = 1
      N =0
      GO TO (1,2),ITYPE
```

```
C**
C**  CONVERSION FROM GEODETIC TO GEOCENTRIC COORDINATES
C**
    1 A2= 40680925.
      B2= 40408585.
      ONE = A2*CLAT*CLAT
      TWO = B2*SLAT*SLAT
      THREE = ONE + TWO
      FOUR = SQRT(THREE)
      R = SQRT(ALT*(ALT + 2.0*FOUR) + (A2*ONE + B2*TWO)/THREE)
      CD = (ALT + FOUR)/R
      SD = (A2 -B2)/FOUR*SLAT*CLAT/R
      ONE = SLAT
      SLAT= SLAT*CD - CLAT*SD
      CLAT = CLAT*CD + ONE*SD
    2 RATIO = 6371.2/R
C**
C**  COMPUTATION OF SCHMIDT QUASI-NORMAL COEFFICIENTS P AND X(=Q)
C**
      P(1) = 2.0*SLAT
      P(2) = 2.0*CLAT
      P(3) = 4.5*SLAT*SLAT - 1.5
      P(4) = 5.1961524*CLAT*SLAT
      Q(1) =-CLAT
      Q(2) = SLAT
      Q(3) = -3.0*CLAT*SLAT
      Q(4) = 1.7320508*(SLAT*SLAT- CLAT*CLAT)
      DO 15 K=1,NGTERM
      IF (N-M) 3,4,4
    3 M = 0
      N = N+1
      RR = RATIO**(N+2)
      FN = N
    4 FM = M
      IF (K-5) 8,5,5
    5 IF (M-N) 7,6,7
    6 ONE = SQRT(1.0 - 0.5/FM)
      J = K-N-1
      P(K) = (1.0+1.0/FM)*ONE*CLAT*P(J)
      Q(K) = ONE*(CLAT*Q(J) + SLAT/FM*P(J))
      SL(M) = SL(M-1)*CL(1) + CL(M-1)*SL(1)
      CL (M) = CL(M-1)*CL(1)-SL(M-1)*SL(1)
      GO TO 8
    7 ONE = SQRT(FN*FN-FM*FM)
      TWO = SQRT((FN-1.0)**2-FM*FM)/ONE
      THREE = (2.0*FN-1.0)/ONE
      I=K-N
      J=K-2*N+1
      P(K) = (FN+1.0)*(THREE*SLAT/FN*P(I) -TWO/(FN-1.0)*P(J))
      Q(K) = THREE*(SLAT*Q(I) - CLAT/FN*P(I)) -TWO*Q(J)
C**
C**  SYNTHESIS OF X, Y AND Z IN GEOCENTRIC COORDINATES
C**
    8 ONE = (AGH(L) + DGH(L)*T)*RR
      IF (M) 10,9,10
    9 X = X + ONE*Q(K)
      Z = Z - ONE*P(K)
      L=L+1
      GO TO 14
   10 TWO = (AGH(L+1) + DGH(L+1)*T)*RR
      THREE = ONE*CL(M) + TWO*SL(M)
      X = X+THREE*Q(K)
      Z = Z - THREE*P(K)
      IF (CLAT) 12,12,11
```

```
   11 Y = Y+(ONE*SL(M) - TWO*CL(M))*FM*P(K)/((FN + 1.0)*CLAT)
      GO TO 13
   12 Y = Y+(ONE*SL(M) - TWO*CL(M))*Q(K)*SLAT
   13 L = L+2
   14 M = M+1
   15 CONTINUE
C**
C**  CONVERSION TO COORDINATE SYSTEM SPECIFIED BY ITYPE
C**
      ONE = X
      X = X*CD + Z*SD
      Z = Z*CD - ONE*SD
      T = SQRT(X*X + Y*Y + Z*Z)
C**
      RETURN
C**
C**  LIBRARY FUNCTIONS USED BY THIS SUBROUTINE ARE SIN,COS,SQRT
C**
C**
C**  SAMPLE RESULTS:
C**  IGRF(1965.0,1,  0.0, 0.0, 30.0, 2541., -240., 56349.,56407.)
C**  IGRF(1965.0,1,  0.0,180.0,295.0, 12923., 9661.,-56900.,59144.)
C**  IGRF(1969.3,1,  0.0, 57.0,195.0, 25092., 5729., 30145.,39638.)
C**  IGRF(1965.0,2,6371.2, 45.0, 10.0, 21848.,-1052., 40417.,45956.)
C**  IGRF(1967.5,2,9000.0, 31.0,359.0,  5750.,-1226., 17853.,18796.)
      END
      SUBROUTINE TRMIN8
C**  ########################################################
C**  ##                 TERMINATE  JOB RUN                 ##
C**  ##    CALLED WHEN PROGRAM USER HAS SUPPLIED INVALID   ##
C**  ##    PARAMETERS                                      ##
C**  ########################################################
C**
      WRITE(6,10)
   10 FORMAT(' ','#####  PROGRAM TERMINATED BY A CALL TO TRMIN8  #####')
      STOP
      END
//GO.FT08F001 DD SYSOUT=A
//GO.SYSIN DD *
```

Appendix B

PROGRAM MAGSAT

Following is program MAGSAT. This program was designed specifically for MAGSAT data and has limited value in other respects. However, it is included here since several of the subroutines may be of use in a variety of applications.

```
/*ROUTE PRINT LOCAL
/*D6250 MSAT06 BIN 451
/*TAPE VPLOT
//TREAD  EXEC ASMGC
//ASM.SYSPRINT DD DUMMY
//ASM.SYSIN DD *
         TITLE 'POGSON''S SECOND VERSION OF TREAD WITH ''TWIND'' ENTRY'
*TAPE READING ROUTINE -- FORTRAN USAGE: CALL TREAD(IREC,&77)
*READS A RECORD INTO ARRAY IREC AT EACH CALL AND RETURNS TO FORTRAN
*STATEMENT LABELED 77 (OR ANY LABEL INDICATED BY THE &) AT END-OF-FILE.
* ARRAY MUST BE LARGE ENOUGH TO HOLD ONE RECORD WHOSE LENGTH IS DEFINED
* IN THE JCL OR DATA SET DCB.
* THIS VERSION HAS BEEN MODIFIED FOR FIXED, UNBLOCKED RECORDS.
* USE 'CALL TWIND' INSTEAD OF 'REWIND 11'
TREAD    CSECT
         USING TREAD,15
         STM     14,2,12(13) SAVE REGISTERS
         ST      13,SAVE+4
         BAL     13,84(15)
         USING   *,13
         DROP    15
SAVE             DS    18F
* GET THE ARRAY AREA ADDRESS AFTER SAVING REGISTERS AND SETTING BASE
         L       2,0(1)
*INSERT CODING HERE TO VARY DCB PARAMETERS THROUGH COMMON AT EXECUTION
SWITCH   BC      0,AROUND    NO BRANCH FIRST TIME THROUGH
         OI      SWITCH+1,X'F0'        NO NEED TO REOPEN
         PRINT   NOGEN
INIT     OPEN    (IN,INPUT)           OPEN TAPE DCB
AROUND   GET     IN,(2)
         L       13,SAVE+4
         LM      14,2,12(13)  RESTORE REGISTERS AND RETURN
         MVI     12(13),X'FF'
         BCR     15,14
*    MACRF=GD IS THE SAME AS GM EXCEPT THAT THE RDW IS NOT MOVED
*          USE "GD" FOR "RECFM=VBS"
*          USE "GM" FOR "RECFM=F" OR "FB"
IN       DCB DDNAME=FT08F001,RECFM=VBS,EODAD=FINISH,MACRF=GD,DSORG=PS, X
               BUFNO=2,EROPT=SKP
FINISH   L       13,SAVE+4
         LM      14,2,12(13)
         LA      15,4(0,0)    SIMULATE 'RETURN 1'
         MVI     12(13),X'FF'     INDICATE RETURN TO USER
         BCR     15,14
TWIND    STM     14,15,12(13)
         USING   TWIND,15
         DROP    13
         L       14,=A(SAVE) WHY NOT REUSE TREAD'S SAVE AREA?
         DROP    15
         USING   SAVE,13
         ST      13,4(0,14)
         LR      13,14
         CLOSE   (IN,REREAD)
         OPEN    (IN,INPUT)
         L       13,SAVE+4
         LM      14,15,12(13)
         MVI     12(13),X'FF'     INDICATE RETURN TO USER
         BCR       15,14      RETURN
         ENTRY   TWIND,TREAD
         END
//STEP1 EXEC FORTHCL,USERLIB='SYS2.VPLOTLIB',SIZE=512K
//FORT.SYSPRINT DD DUMMY
//FORT.SYSIN DD *
```

```
C**
C**.........................................................
C**.                                                       .
C**.                   PROGRAM MAGSAT                      .
C**.                                                       .
C**.        READS AND ANALYSES MAGSAT DATA STORED ON       .
C**.        MAG TAPE                                       .
C**.                                                       .
C**.........................................................
C**
      COMMON/BNDRY/ CSBLNG(182),CSBLAT(182),PB1LNG(5),PB1LAT(5),
     *              PB2LNG(50),PB2LAT(50),PB3LNG(16),PB3LAT(16),
     *              PB4LNG(12),PB4LAT(12),PB5LNG(4),PB5LAT(4),
     *              PB6LNG(7),PB6LAT(7),BAYLNG(254),BAYLAT(254),
     *              SUPLNG(116),SUPLAT(116),RIVLNG(109),RIVLAT(109)
      COMMON/VARBLS/ VAR(100),NWVAR
      COMMON/HEADER/ MPASS,MJD,IPASS,HCONST(18),NRECH,NPOINT,DST(12),
     *   MODELF(3),TZERO,ABAR,FEXT(3),COMM(30),GH(289),GHT(196)
      COMMON/MAGOUT/ AOUT(50,300),NP
      COMMON/PLPARM/ XSTART,XASCAL,YSTART,YASCAL,IPNUM,CSBF,PROVF,
     *               BAYF,RIVF,LAKF
C**
      DIMENSION IBUF(8000),JVAR(300),ITITLE(20),FCOEF(8),C(10),DATIME(7)
      DIMENSION DIFF1(300),DIFF2(300),DIFF3(300),DIFF4(300)
      DIMENSION BNDRY(3000),SUM(300),VECT(300),ICONST(18)
C**
      EQUIVALENCE(VAR(1),JVAR(1))
      EQUIVALENCE(HCONST(1),ICONST(1))
C**
      DOUBLE PRECISION VNAME,NWRITE,KPINDX,NSUM,NFILTR
      DOUBLE PRECISION NAME,NINT,NIDUMP,NODUMP,NSTAT
      DOUBLE PRECISION NPLOT,NEND,NRUN,NULAT,NNPASS,NFIXUP,NCSB
      DOUBLE PRECISION NPOLIT,NHUDSN,NLAKES,NRIVER,NFIT,NSTACK
C**
      LOGICAL IDUMPF,ODUMPF,EXITF,PLOTF,CSBF,PROVF,BAYF,RIVF,LAKF
      LOGICAL UNILAF,FIXUPF,FITF,SUMF,FILTF,WRITEF,KPFLAG,STATF
C**
      DATA NFIT/'POLYFIT '/
      DATA NIDUMP/'INDUMP  '/
      DATA NODUMP/'OUTDUMP '/
      DATA NPLOT/'PLOT    '/
      DATA NFIXUP/'FIXUP   '/
      DATA NULAT/'UNILAT  '/
      DATA NRUN/'RUN     '/
      DATA NEND/'END     '/
      DATA NNPASS/'PASS    '/
      DATA NCSB/'CSBDATA '/
      DATA NPOLIT/'POLDATA '/
      DATA NHUDSN/'BAYDATA '/
      DATA NLAKES/'LAKDATA '/
      DATA NRIVER/'RIVDATA '/
      DATA NSTACK/'STACK   '/
      DATA NSUM/'SUM     '/
      DATA NFILTR/'FILTER  '/
      DATA KPINDX/'KPINDEX '/
      DATA NWRITE/'WRITEOUT'/
      DATA NSTAT/'STATIC  '/
C**
C**
C** CONTROL WORD              PARAMETERS
C** -------------------------------------------------------------
C**
C**  POLYFIT     MDEG - DEGREE OF POLYNOMIAL FIT TO ANOMALY DATA TO
C**                     PERFORM
```

```
C**              IY1 -
C**              IY2 -
C**              IY3 -
C**              IY4 - VARIABLE NUMBERS TO FIT.  X VARIABLE ASSUMED TO
C**                    TO BE LATITUDE UNLESS SPECIFIED IN PLOT
C**
C**  PASS      IPFRST - STARTING PASS NUMBER
C**            IPLAST - STOPPING PASS NUMBER
C**
C**  KPINDEX    KPMIN - MINIMUM KP INDEX TO INCLUDE
C**             KPMAX - MAXIMUM KP INDEX TO INCLUDE
C**
C**  UNILAT      LINC - LATITUDE INCREMENT (MINUTES)
C**
C**  FIXUP     RANGE  - RANGE AGAINST WHICH VECTOR DATA IS TESTED
C**                     TO DETERMINE IF IT IS TO BE REMOVED
C**
C**  PLOT          IX - VARIABLE NUMBER TO BE USED AS X VAR. IN PLOTS
C**
C**  INDUMP    LIHEAD - LEVEL OF HEADER RECORD DUMP
C**            LIDATA - LEVEL OF DATA RECORD DUMP
C**            NISTRT - PASS NUMBER TO START DUMP
C**            NISTOP - PASS NUMBER TO STOP DUMP
C**
C**  OUTDUMP   LOHEAD - LEVEL OF HEADER RECORD DUMP
C**            LODATA - LEVEL OF DATA RECORD DUMP
C**            NOSTRT - PASS NUMBER TO START DUMP
C**            NOSTOP - PASS NUMBER TO STOP DUMP
C**
C**  STATIC             - ALIGN PASSES SUCH THAT CHURCHILL-SUPERIOR
C**                         BOUNDARY IS AT 56 DEG. LATITUDE
C**                     - ARRAY BNDRY FOLLOWS (BNDRY(IPASS)=CSBLAT)
C**
C**  SUM        ISVAR - VARIABLE NUMBER TO BE SUMMED FOR AVG. TRACE
C**            LSTRTD - DEGREES LATITUDE FOR START OF SUM
C**            LSTRTM - MINUTES    "       "     "    "   "
C**            LSTOPD - DEGREES LATITUDE FOR END OF SUM
C**            LSTOPM - MINUTES    "       "    "   "    "
C**
C**  STACK              - FIND AVG. OF PREVIOUSLY SUMMED TRACES
C**
C**  FILTER     IFVAR - VAR. NUMBER TO FILTER PRIOR TO STACK OR POLYFIT
C**                     AND AFTER UNILAT
C**            LAMSML - SMALLEST WAVELENGTH (DEGREES LAT) TO PASS
C**            LAMBIG - LARGEST WAVELENGTH TO PASS
C**
C**  WRITEOUT           - WRITE DIFF ARRAYS TO UNIT 7.  (POLYNOMIAL FITS)
C**
C**  CSBDATA            - DIGITIZED DATA FOR PLOTTING CHURCHILL-SUPERIOR
C**                       BOUNDARY FOLLOWING    (10F7.1)
C**
C**  POLDATA            - DATA FOR PLOTTING POLITICAL BOUNDARIES FOLLOWS
C**
C**  BAYDATA            - DATA FOR PLOTTING HUDSON BAY FOLLOWS
C**
C**  LAKDATA            - DATA FOR PLOTTING THE GREAT LAKES FOLLOWS
C**
C**  RIVDATA            - DATA FOR PLOTTING ST LAWRENCE AND GASPE FOLLOWS
C**
C**
C**DEFINE DEFAULT VALUES FOR INPUT DATA
C**
      IX=1
      IPFRST=1
```

```
      IPLAST=9999
      IPNUM=0
      LIHEAD=0
      LIDATA=0
      LOHEAD=0
      LODATA=0
      ICALL=0
      UNILAF=.FALSE.
      IDUMPF=.FALSE.
      ODUMPF=.FALSE.
      PLOTF=.FALSE.
      FIXUPF=.FALSE.
      CSBF=.FALSE.
      PROVF=.FALSE.
      BAYF=.FALSE.
      RIVF=.FALSE.
      LAKF=.FALSE.
      FITF=.FALSE.
      STACKF=.FALSE.
      SUMF=.FALSE.
      FILTF=.FALSE.
      WRITEF=.FALSE.
      KPFLAG=.FALSE.
      STATF=.FALSE.
      DO 100 I=1,300
  100 SUM(I)=0.0
      DO 101 I=1,3000
  101 BNDRY(I)=0.0
C**
      CALL $DATE(DATIME)
      WRITE(4,10) DATIME
      WRITE(4,12)
      WRITE(4,14)
C**
C**
C**
C**-----------------------------------------------------------------
C**                                                       READ IN
C**READ IN TITLE
C**
      READ(5,23) ITITLE
C**
C**READ IN INPUT INFORMATION
C**
  200 READ(5,20) NAME,I1,I2,I3,I4,I5,I6
      WRITE(4,16) NAME,I1,I2,I3,I4,I5,I6
C**
      IF(NAME.EQ.NEND) GO TO 9000
      IF(NAME.EQ.NRUN) GO TO 3000
      IF(NAME.EQ.NSTACK) GO TO 8000
C**
      IF(NAME.EQ.NFIXUP) GO TO 205
      IF(NAME.EQ.NULAT) GO TO 210
      IF(NAME.EQ.NFIT) GO TO 215
      IF(NAME.EQ.NNPASS) GO TO 220
      IF(NAME.EQ.NCSB) GO TO 225
      IF(NAME.EQ.NIDUMP) GO TO 230
      IF(NAME.EQ.NODUMP) GO TO 235
      IF(NAME.EQ.NPLOT) GO TO 240
      IF(NAME.EQ.NPOLIT) GO TO 245
      IF(NAME.EQ.NHUDSN) GO TO 250
      IF(NAME.EQ.NLAKES) GO TO 255
      IF(NAME.EQ.NRIVER) GO TO 260
      IF(NAME.EQ.NSUM) GO TO 265
```

```
      IF(NAME.EQ.NFILTR) GO TO 270
      IF(NAME.EQ.KPINDX) GO TO 275
      IF(NAME.EQ.NWRITE) GO TO 280
      IF(NAME.EQ.NSTAT) GO TO 285
C**
C**        ERRONEOUS INPUT
      WRITE(6,91) NAME
      GO TO 9000
C**
C**
  205 FIXUPF=.TRUE.
      RANGE=FLOAT(I1)
      GO TO 200
C**
  210 UNILAF=.TRUE.
      LINC=I1
      GO TO 200
C**
  215 FITF=.TRUE.
      MDEG=I1
      IY1=I2
      IY2=I3
      IY3=I4
      IY4=I5
      GO TO 200
C**
  220 IPFRST=I1
      IPLAST=I2
      IDONE=0
      GO TO 200
C**
  225 READ(5,92) (CSBLNG(I),I=1,180)
      READ(5,92) (CSBLAT(I),I=1,180)
      CSBF=.TRUE.
      GO TO 200
C**
  230 LIHEAD=I1
      LIDATA=I2
      NISTRT=I3
      NISTOP=I4
      GO TO 200
C**
  235 LOHEAD=I1
      LODATA=I2
      NOSTRT=I3
      NOSTOP=I4
      GO TO 200
C**
  240 PLOTF=.TRUE.
      IX=I1
      CALL PLOTS(IBUF,1)
      CALL FACTOR(0.5)
      CALL PLOT(0.0,-11.0,-3)
      CALL PLOT(0.0,1.5,-3)
      GO TO 200
C**
  245 READ(5,92) (PB1LNG(I),I=1,3)
      READ(5,92) (PB1LAT(I),I=1,3)
      READ(5,92) (PB2LNG(I),I=1,48)
      READ(5,92) (PB2LAT(I),I=1,48)
      READ(5,92) (PB3LNG(I),I=1,14)
      READ(5,92) (PB3LAT(I),I=1,14)
      READ(5,92) (PB4LNG(I),I=1,10)
      READ(5,92) (PB4LAT(I),I=1,10)
```

```
      READ(5,92) (PB5LNG(I),I=1,2)
      READ(5,92) (PB5LAT(I),I=1,2)
      READ(5,92) (PB6LNG(I),I=1,5)
      READ(5,92) (PB6LAT(I),I=1,5)
      PROVF=.TRUE.
      GO TO 200
C**
  250 READ(5,92) (BAYLNG(I),I=1,252)
      READ(5,92) (BAYLAT(I),I=1,252)
      BAYF=.TRUE.
      GO TO 200
C**
  255 READ(5,92) (SUPLNG(I),I=1,114)
      READ(5,92) (SUPLAT(I),I=1,114)
      LAKF=.TRUE.
      GO TO 200
C**
  260 READ(5,92) (RIVLNG(I),I=1,107)
      READ(5,92) (RIVLAT(I),I=1,107)
      RIVF=.TRUE.
      GO TO 200
C**
  265 SUMF=.TRUE.
      ISVAR=I1
      SSTART=FLOAT(I2) + FLOAT(I3)/60.
      SUMEND=FLOAT(I4) + FLOAT(I5)/60.
      NUMVEC=0
      GO TO 200
C**
  270 FILTF=.TRUE.
      IFVAR=I1
      LAMSML=I2
      LAMBIG=I3
      GO TO 200
C**
  275 KPFLAG=.TRUE.
      KPMIN=I1
      KPMAX=I2
      GO TO 200
C**
  280 WRITEF=.TRUE.
      GO TO 200
C**
  285 STATF=.TRUE.
  286 READ(5,21) II,BNDRY(II)
      IF(II.NE.9999) GO TO 286
      GO TO 200
C**
C**---------------------------------------------------------------
C**                                                      PRINT
C**                                                 RUN PARAMETERS
 3000 CONTINUE
C**
      WRITE(6,10) DATIME
      WRITE(6,12)
C**
C**PRINT INPUT INFORMATION
C**
      WRITE(6,24) ITITLE
      WRITE(6,30)
      WRITE(6,32) IPFRST,IPLAST
      WRITE(6,35)
      IF(FIXUPF) WRITE(6,37) RANGE
      IF(UNILAF) WRITE(6,31) LINC
```

```
      IF(FITF) WRITE(6,38) MDEG
      IF(FILTF) WRITE(6,41) LAMSML,LAMBIG
      IF(STATF) WRITE(6,42)
      IF(SUMF) WRITE(6,39) SSTART,SUMEND
C**
C**-------------------------------------------------------------------
C**                                                        INITIALIZE
C**
C**INITIALIZE SUBROUTINES AND VARIABLES
C**
      NLINE=0
      EXITF=.FALSE.
      DO 400 I=1,300
      DIFF1(I)=0.0
      DIFF2(I)=0.0
      DIFF3(I)=0.0
  400 DIFF4(I)=0.0
C**
C**
C**-------------------------------------------------------------------
C**                                                        START PASS
      WRITE(6,50)
  500 CONTINUE
C**
C**READ PASS HEADER FROM INPUT TAPE
C**
      IF(IDONE.EQ.1) GO TO 200
      CALL HTAPE(EXITF)
      IF(EXITF) GO TO 9000
      IF(IPASS.LT.IPFRST) GO TO 500
      IF(IPASS.EQ.IPLAST) IDONE=1
      IF(IPASS.GT.IPLAST) GO TO 200
      IF(.NOT.KPFLAG) GO TO 501
      KPA=ICONST(11)
      KPD=ICONST(12)
      WRITE(6,40) IPASS,KPA,KPD
      IF(KPA.LT.KPMIN.OR.KPA.GT.KPMAX) GO TO 500
      IF(KPD.LT.KPMIN.OR.KPD.GT.KPMAX) GO TO 500
  501 CONTINUE
C**
C**
C**PRINT CONTENTS OF HEADER RECORD
C**
      IDUMPH=LIHEAD
      IF(IDUMPH.LT.LOHEAD)IDUMPH=LOHEAD
      IF(IDUMPH.LE.0) GO TO 504
      IF(MPASS.GE.NISTRT.AND.MPASS.LE.NISTOP) CALL PRTHED(IDUMPH,NLINE)
  504 CONTINUE
C**
C**
C**READ IN ONE COMPLETE PASS, STORE IN 2D ARRAY 'AOUT'
C**
      IFLAG=0
      IP=0
  510 IP=IP+1
      CALL TREAD(AOUT(1,IP),&9999)
      IF(AOUT(1,IP).EQ.888888.0) GO TO 515
      GO TO 510
  515 CONTINUE
      NP=IP-1
C**
C**FIXUP DATA IF REQUESTED
      IF(FIXUPF) CALL FIXUP(30,RANGE)
C**
```

```
C**INTERPOLATE DATA TO UNIFORM INTERVAL IN LATITUDE
C**
      IF(UNILAF) CALL UNILAT(IX,LINC)
C**
      NWVAR=30
C**
C**
      DO 599 IP=1,NP
      DO 516 IVAR=1,30
  516 VAR(IVAR)=AOUT(IVAR,IP)
C**
C**INPUT DUMP
C**
      IF(MPASS.LT.NISTRT.OR.MPASS.GT.NISTOP) GO TO 522
      IF(LIDATA.GT.O) CALL PRIDAT(LIDATA,NLINE,IP,NP)
  522 CONTINUE
C**
C**ADD VARIABLES TO EACH POINT
C**
      CALL ADDVAR
C**
C**PUT NEW VARIABLES IN AOUT
      DO 530 IVAR=30,44
  530 AOUT(IVAR,IP)=VAR(IVAR)
C**
C**--------------------------------------
C**OUTPUT DUMP
C**
      IF(MPASS.LT.NOSTRT.OR.MPASS.GT.NOSTOP) GO TO 590
      IF(LODATA.GT.O) CALL PRODAT(LODATA,NLINE,IP,NP)
  590 CONTINUE
C**
  599 CONTINUE
C**-------------------------------------------------------------------
C**                                                     END OF PASS
C** CALCULATE AND SUBTRACT POLYNOMIAL FIT IF REQUESTED
C**
      IF(.NOT.FITF) GO TO 610
      IF(IY1.GT.O) CALL POLY(IX,IY1,MDEG,DIFF1)
      IF(IY2.GT.O) CALL POLY(IX,IY2,MDEG,DIFF2)
      IF(IY3.GT.O) CALL POLY(IX,IY3,MDEG,DIFF3)
      IF(IY4.GT.O) CALL POLY(IX,IY4,MDEG,DIFF4)
  610 CONTINUE
C**
      IF(.NOT.WRITEF) GO TO 620
      WRITE(7,70) IPASS,NP,(ITITLE(I),I=1,15)
      WRITE(7,71) (AOUT(IX,I),AOUT(2,I),DIFF1(I),DIFF2(I),DIFF3(I),
     &             DIFF4(I),I=1,NP)
  620 CONTINUE
C**
      DO 625 I=1,NP
      AOUT(45,I)=DIFF1(I)
      AOUT(46,I)=DIFF2(I)
      AOUT(47,I)=DIFF3(I)
      AOUT(48,I)=DIFF4(I)
  625 CONTINUE
C**
C**  FILTER IF REQUESTED
      IF(.NOT.FILTF) GO TO 604
      IF(ICALL.GT.O) GO TO 601
      ICALL=1
      FREQLO=1./FLOAT(LAMBIG)
      FREQHI=1./FLOAT(LAMSML)
      DIGI=FLOAT(LINC)/60.
```

```
      CALL BNDPAS(FREQLO,FREQHI,DIGI,FCOEF,FGAIN)
  601 CONTINUE
      DO 602 I=1,NP
  602 VECT(I)=AOUT(IFVAR,I)
      CALL FILTER(VECT,NP,FCOEF,FGAIN)
      DO 603 I=1,NP
  603 AOUT(IFVAR,I)=VECT(I)
  604 CONTINUE
C**
C**  APPLY STATIC CORRECTIONS IF REQUESTED
      IF(.NOT.STATF) GO TO 615
      CSBNDR=BNDRY(IPASS)
      IF(CSBNDR.EQ.O.) GO TO 615
      DIGI=FLOAT(LINC)/60.
      DO 611 I=1,NP
  611 VECT(I)=AOUT(1,I)
      CALL STATIC(VECT,NP,CSBNDR,DIGI)
      DO 612 I=1,NP
  612 AOUT(1,I)=VECT(I)
  615 CONTINUE
C**
C**  SUM FOR STACKED TRACE IF REQUESTED
      IF(.NOT.SUMF) GO TO 606
      DO 605 I=1,NP
  605 VECT(I)=AOUT(ISVAR,I)
      VSTART=AOUT(IX,1)
      VEND=AOUT(IX,NP)
      DIGI=FLOAT(LINC)/60.
      CALL STACK(VECT,VSTART,VEND,SUM,SSTART,SUMEND,DIGI,NUMVEC,LENGS)
  606 CONTINUE
C**
C**
      IF(.NOT.PLOTF) GO TO 500
C     CALL PLOTTR(4,1,45,ITITLE)
C     CALL PLOTTR(6,1,41,ITITLE)
C     CALL PLOTTR(6,1,42,ITITLE)
C     CALL PLOTTR(6,1,43,ITITLE)
C     CALL PLOTTR(6,1,44,ITITLE)
C     CALL PLOTTR(1,1,1,ITITLE)
C     CALL PLOTTR(5,2,1,ITITLE)
      CALL PLOTTR(7,IX,44,ITITLE)
C**
C**
      GO TO 500
C**
C**  CALCULATE AND PLOT STACKED TRACE
 8000 CONTINUE
      READ(5,23) ITITLE
      DO 801 I=1,LENGS
      AOUT(49,I)=SSTART + (I-1)*DIGI
  801 AOUT(50,I)=SUM(I)/FLOAT(NUMVEC)
      NP=LENGS
      WRITE(7,72) ITITLE
      WRITE(7,73) (AOUT(49,I),AOUT(50,I),I=1,NP)
      CALL PLOTTR(1,1,1,ITITLE)
      CALL PLOTTR(4,49,50,ITITLE)
      GO TO 200
 9999 WRITE(6,90)
 9000 CONTINUE
      CALL PLOT(12.0,0.0,999)
   10 FORMAT(///' ',45X,'DEPT. OF EARTH SCIENCES, UNIV. OF MANITOBA',
     1             5X,7A4//)
   12 FORMAT(' ',56X,'*** PROGRAM MAGPLOT ***'//)
   14 FORMAT(///' ',56X,'INPUT DATA CARDS'///
```

```
     1       ' ',27X,'CONTROL WORD',1X,'----------------- PARAMETERS ---
     2-----------------------'/)
  23 FORMAT(20A4)
  24 FORMAT(//' ',20X,'TITLE:- ',20A4)
  16 FORMAT(' ',32X,A8,6I6)
  20 FORMAT(A8,6I6)
  21 FORMAT(I4,F4.1)
  30 FORMAT(' '  //,' ',56X,'RUN PARAMETERS'///)
  31 FORMAT(' ',10X,'LATITUDE INTERVAL',14X,I5,' MINUTES')
  32 FORMAT(//' ',10X,'PASSES',I5,' TO',I5)
  35 FORMAT(' ',10X,'------------------------ PROCESSING OPTIONS ------
     1--------------'//)
  37 FORMAT(' ',10X,'FIXUP RANGE',18X,F7.2,' NANOTESLA')
  38 FORMAT(' ',10X,'POLYNOMIAL FIT OF DEGREE',5X,I4,3X,'SUBTRACTED')
  39 FORMAT(' ',10X,'PROFILES STACKED BETWEEN',F7.2,' AND',F7.2,
     &          ' DEGREES LATITUDE')
  40 FORMAT(' ',5X,'PASS',I5,' ;',5X,'AKP =',I3,5X,'DKP =',I3)
  41 FORMAT(' ',10X,'BUTTERWORTH BANDPASSED FILTERED:  PASSBAND',
     &          I4,' TO',I4,' DEGREES LATITUDE')
  42 FORMAT(' ',10X,'STATIC CORRECTIONS APPLIED')
  70 FORMAT(2I4,4X,15A4)
  71 FORMAT(6F7.2)
  72 FORMAT(20A4)
  73 FORMAT(2F7.2)
  50 FORMAT('1')
  90 FORMAT(' ',20X,'** EOF ENCOUNTERED WHILE READING DATA RECORD **')
  91 FORMAT(' ',20X,'*** NAME ',A8,' NOT RECOGNIZED ***')
  92 FORMAT(10F7.1)
     STOP
     END
     SUBROUTINE HTAPE(EXITF)
C**
C**............................................................
C**.                                                          .
C**.                     SUBROUTINE HTAPE                     .
C**.                                                          .
C**.         READS PASS HEADER RECORDS FROM INPUT TAPE        .
C**.                                                          .
C**............................................................
C**
     COMMON/HEADER/ MPASS,MJD,IPASS,HCONST(18),NRECH,NPOINT,DST(12),
    *   MODELF(3),TZERO,ABAR,FEXT(3),COMM(30),GH(289),GHT(196)
     LOGICAL EXITF
     DOUBLE PRECISION TIME
C**
     DIMENSION A(30)
     DIMENSION IA(30)
     EQUIVALENCE(IA(1),A(1))
C**
C**
C**
 100 CALL TREAD(A,&2000)
     IF(A(1).NE.999999.0) GO TO 100
C**
C**-----------------------------------------------------------------
C**                                                      RECORD   1
     MPASS=IA(2)
     MJD=IA(3)
     IPASS=IA(4)
     DO 110 I=1,18
 110 HCONST(I)=A(I+4)
     NRECH=IA(23)
     NPOINT=IA(24)
C**
```

```
C**-----------------------------------------------------------------
C**                                                    RECORD  2
      CALL TREAD(A,&2000)
      DO 200 I=1,12
  200 DST(I)=A(I)
      MODELF(1)=IA(13)
      MODELF(2)=IA(14)
      MODELF(3)=IA(15)
      TZERO=A(16)
      ABAR=A(17)
      FEXT(1)=A(18)
      FEXT(2)=A(19)
      FEXT(3)=A(20)
C**
C**-----------------------------------------------------------------
C**                                                    RECORD  3
      CALL TREAD(A,&2000)
      DO 300 I=1,30
  300 COMM(I)=A(I)
C**
C**-----------------------------------------------------------------
C**                                               RECORDS 4 TO 12
      II=0
      DO 400 I=1,9
      CALL TREAD(A,&2000)
      DO 410 J=1,30
      II=II+1
      GH(II)=A(J)
  410 CONTINUE
  400 CONTINUE
C**
C**-----------------------------------------------------------------
C**                                                   RECORD 13
      CALL TREAD(A,&2000)
      DO 420 I=1,19
      II=II+1
      GH(II)=A(I)
  420 CONTINUE
C**
C**-----------------------------------------------------------------
C**                                             RECORDS 14 TO 19
      II=0
      DO 500 I=1,6
      CALL TREAD(A,&2000)
      DO 510 J=1,30
      II=II+1
      GHT(II)=A(J)
  510 CONTINUE
  500 CONTINUE
C**
C**-----------------------------------------------------------------
C**                                                   RECORD 20
      CALL TREAD(A,&2000)
      DO 520 I=1,16
      II=II+1
      GHT(II)=A(I)
  520 CONTINUE
C**
C**-----------------------------------------------------------------
C**                                          DONE READING HEADER
      RETURN
C**
C**
 2000 CONTINUE
```

```
      EXITF=.TRUE.
      WRITE(6,99) IPASS
      RETURN
C**
 9999 CONTINUE
C**
C**COME HERE IF END OF PASS ENCOUNTERED
C**
      WRITE(6,10) IPASS
      EXITF=.TRUE.
C**
   10 FORMAT(///' ',10X,'***** END OF PASS ENCOUNTERED WHILE READING ',
     & 'HEADER RECORD FOR PASS ',I4)
   99 FORMAT(///' ',10X,'END OF INPUT TAPE ENCOUNTERED WHILE LOOKING ',
     & 'FOR HEADER RECORD AFTER PASS ',I4)
      RETURN
      END
      SUBROUTINE PRTHED(LEVEL,NLINE)
C**
C**.............................................................
C**.                                                           .
C**.                  SUBROUTINE PRTHED                        .
C**.                                                           .
C**.         PRINTS SOME OR ALL OF THE HEADER RECORD           .
C**.                                                           .
C**.............................................................
C**
      COMMON/HEADER/ MPASS,MJD,IPASS,HCONST(18),NRECH,NPOINT,DST(12),
     *   MODELF(3),TZERO,ABAR,FEXT(3),COMM(30),GH(289),GHT(196)
C**
      DIMENSION ASC(2),DSC(2),MSEC(2),ALTM(2),ALONG(2),KP(2),GSM(6)
C**
      EQUIVALENCE(HCONST(1),ASC(1))
      EQUIVALENCE(HCONST(3),DSC(1))
      EQUIVALENCE(HCONST(5),MSEC(1))
      EQUIVALENCE(HCONST(7),ALTM(1))
      EQUIVALENCE(HCONST(9),ALONG(1))
      EQUIVALENCE(HCONST(11),KP(1))
      EQUIVALENCE(HCONST(13),GSM(1))
C**
      EQUIVALENCE(MODELF(1),NMAX)
      EQUIVALENCE(MODELF(2),NMAXT)
      EQUIVALENCE(MODELF(3),MODEXT)
C**
C**
C**      NLINE - CURRENT OUTPUT PAGE LINE NUMBER
C**      LEVEL - DETERMINES LENGTH OF DUMP
C**
      GO TO (1000,2000,3000,4000,5000),LEVEL
C**
 1000 CONTINUE
C**
C**SHORT PRINTOUT
C**
      IF(NLINE.GT.52)NLINE=0
      IF(NLINE.EQ.0)WRITE(6,100)
      WRITE(6,10) MPASS,MJD,IPASS,ASC,DSC,MSEC,ALTM,ALONG,KP
      NLINE=NLINE+8
      GO TO 9000
C**
 2000 CONTINUE
      IF(NLINE.GT.51)NLINE=0
      IF(NLINE.EQ.0)WRITE(6,100)
      WRITE(6,20) MPASS,MJD,IPASS,ASC,DSC,MSEC,ALTM,ALONG,KP,COMM
```

```
      NLINE=NLINE+9
      GO TO 9000
C**
 3000 CONTINUE
      IF(NLINE.GT.49)NLINE=0
      IF(NLINE.EQ.0)WRITE(6,100)
      WRITE(6,30)MPASS,MJD,IPASS,ASC,DSC,MSEC,ALTM,ALONG,KP,GSM,DST,COMM
      NLINE=NLINE+11
      GO TO 9000
C**
 4000 CONTINUE
      IF(NLINE.GT.47)NLINE=0
      IF(NLINE.EQ.0)WRITE(6,100)
      WRITE(6,40) MPASS,MJD,IPASS,ASC,DSC,MSEC,ALTM,ALONG,KP,GSM,DST,
     1            NMAX,NMAXT,MODEXT,TZERO,ABAR,FEXT,COMM
      NLINE=NLINE+13
      GO TO 9000
C**
 5000 CONTINUE
      IF(NLINE.NE.0)WRITE(6,100)
      WRITE(6,50) MPASS,MJD,IPASS,ASC,DSC,MSEC,ALTM,ALONG,KP,GSM,DST,
     1            NMAX,NMAXT,MODEXT,TZERO,ABAR,FEXT,COMM,GH,GHT
      NLINE=61
C**
 9000 CONTINUE
      IF(NLINE.GT.60) NLINE=0
C**
   10 FORMAT(////' ','MPASS',I4,';  MJ DAY=',I5,';  PASS=',I4,
     *';  ASCE=',F8.2,';  ASCI=',F8.2,';  DSCE=',F8.2,';  DSCI=',F8.2/
     *' ',4X,'AMSEC=',I10,';  DMSEC=',I10,';  ALMST=',F8.2,';  DLMST=',
     *F8.2,';  ALONG=',F8.2,';  DLONG=',F8.2,';  AKP=',I3,';  DKP=',I3/)
   20 FORMAT(////' ','MPASS',I4,';  MJ DAY=',I5,';  PASS=',I4,
     *';  ASCE=',F8.2,';  ASCI=',F8.2,';  DSCE=',F8.2,';  DSCI=',F8.2/
     *' ',4X,'AMSEC=',I10,';  DMSEC=',I10,';  ALMST=',F8.2,';  DLMST=',
     *F8.2,';  ALONG=',F8.2,';  DLONG=',F8.2,';  AKP=',I3,';  DKP=',I3/
     *          ' ',30A4/)
   30 FORMAT(////' ','MPASS',I4,';  MJ DAY=',I5,';  PASS=',I4,
     *';  ASCE=',F8.2,';  ASCI=',F8.2,';  DSCE=',F8.2,';  DSCI=',F8.2/
     *' ',4X,'AMSEC=',I10,';  DMSEC=',I10,';  ALMST=',F8.2,';  DLMST=',
     *F8.2,';  ALONG=',F8.2,';  DLONG=',F8.2,';  AKP=',I3,';  DKP=',I3/
     *          ' ','GSM;  ',6F15.5/
     *          ' ','DST;  ',12F10.5/
     *          ' ',30A4/)
   40 FORMAT(////' ','MPASS',I4,';  MJ DAY=',I5,';  PASS=',I4,
     *';  ASCE=',F8.2,';  ASCI=',F8.2,';  DSCE=',F8.2,';  DSCI=',F8.2/
     *' ',4X,'AMSEC=',I10,';  DMSEC=',I10,';  ALMST=',F8.2,';  DLMST=',
     *F8.2,';  ALONG=',F8.2,';  DLONG=',F8.2,';  AKP=',I3,';  DKP=',I3/
     *          ' ','GSM;  ',6F15.5/
     *          ' ','DST;  ',12F10.5/
     *          ' ','NMAX=',I3,'   NMAXT=',I3,'   MODEXT=',I3,
     *              '   TZERO=',F10.4,'   ABAR=',F10.4/
     *          ' ','EXTERIOR FIELD COEFF.',3F15.5/
     *          ' ',30A4/)
   50 FORMAT(////' ','MPASS',I4,';  MJ DAY=',I5,';  PASS=',I4,
     *';  ASCE=',F8.2,';  ASCI=',F8.2,';  DSCE=',F8.2,';  DSCI=',F8.2/
     *' ',4X,'AMSEC=',I10,';  DMSEC=',I10,';  ALMST=',F8.2,';  DLMST=',
     *F8.2,';  ALONG=',F8.2,';  DLONG=',F8.2,';  AKP=',I3,';  DKP=',I3/
     *        /' ','GSM;  ',6F15.5//
     *          ' ','DST;  ',12F10.5//
     *          ' ','NMAX=',I3,'   NMAXT=',I3,'   MODEXT=',I3,
     *              '   TZERO=',F10.4,'   ABAR=',F10.4//
     *          ' ','EXTERIOR FIELD COEFF.',3F15.5//
     *          ' ',30A4///
     *          ' ','*****  GH  *****'/
```

```
     *        ' ',17(17F7.1/' ')
     *     //' ','*****  GHT *****'/
     *        ' ',14(14F7.1/' '))
  100 FORMAT('1')
      RETURN
      END
      SUBROUTINE PRIDAT(LEVEL,NLINE,IP,NP)
C**
C**.........................................................
C**.                                                        .
C**.                    SUBROUTINE PRIDAT                   .
C**.                                                        .
C**.        PRINTS SOME OR AL OF THE INPUT DATA RECORD      .
C**.                                                        .
C**.........................................................
C**
      COMMON/VARBLS/ VAR(100),NWVAR
C**
      DIMENSION RDAT(10,50)
      DIMENSION IDAT(10,50)
      DIMENSION JVAR(100)
C**
      EQUIVALENCE(RDAT(1,1),IDAT(1,1))
      EQUIVALENCE(VAR(1),JVAR(1))
C**
      DOUBLE PRECISION VNAME(50)
C**
      DATA VNAME(1)/'LAT'/
      DATA VNAME(2)/'LONG'/
      DATA VNAME(3)/'RADIUS'/
      DATA VNAME(4)/'MLT'/
      DATA VNAME(5)/'INV LAT'/
      DATA VNAME(6)/'DIP LAT'/
      DATA VNAME(7)/'SC FIELD'/
      DATA VNAME(8)/'VE FIELD'/
      DATA VNAME(9)/'X COMP'/
      DATA VNAME(10)/'Y COMP'/
      DATA VNAME(11)/'Z COMP'/
      DATA VNAME(12)/'AV FIELD'/
      DATA VNAME(13)/'AVG X'/
      DATA VNAME(14)/'AVG Y'/
      DATA VNAME(15)/'AVG Z'/
      DATA VNAME(16)/'V FLD SD'/
      DATA VNAME(17)/'X COM SD'/
      DATA VNAME(18)/'Y COM SD'/
      DATA VNAME(19)/'Z COM SD'/
      DATA VNAME(20)/'MODL FLD'/
      DATA VNAME(21)/'MODEL X'/
      DATA VNAME(22)/'MODEL Y'/
      DATA VNAME(23)/'MODEL Z'/
      DATA VNAME(24)/'ATT QUAL'/
      DATA VNAME(25)/'MJ DAY'/
      DATA VNAME(26)/'UT MSEC'/
      DATA VNAME(27)/'UT HOUR'/
      DATA VNAME(28)/'GLAT'/
      DATA VNAME(29)/'ALT'/
C**
      GO TO (1000,2000,3000),LEVEL
C**
 1000 CONTINUE
      IF(IP.GT.1)RETURN
      IF(NLINE.GT.56)NLINE=0
      IF(NLINE.EQ.0) WRITE(6,500)
      WRITE(6,10)
```

```
      WRITE(6,11) IP,(VAR(I),I=1,15)
      NLINE=NLINE+4
      RETURN
C**
 2000 CONTINUE
      IF(IP.GT.1) RETURN
      IF(NLINE.GT.52) NLINE=0
      IF(NLINE.EQ.0) WRITE(6,500)
      WRITE(6,10)
      WRITE(6,11) IP,(VAR(I),I=1,15)
      WRITE(6,20)
      WRITE(6,21) (VAR(I),I=16,24),JVAR(25),JVAR(26),(VAR(J),J=27,29)
      NLINE=NLINE+8
      RETURN
C**
 3000 CONTINUE
      IF(IP.EQ.1) IPP=0
      IPP=IPP+1
      DO 300 J=1,29
  300 RDAT(IPP,J)=VAR(J)
      IF(IP.LT.NP.AND.IPP.NE.10) RETURN
      IF(NLINE.GT.37)NLINE=0
      IF(NLINE.EQ.0) WRITE(6,500)
      WRITE(6,30)
      DO 310 J=1,29
      IF(J.NE.25.AND.J.NE.26)WRITE(6,31) J,VNAME(J),(RDAT(I,J),I=1,IPP)
      IF(J.EQ.25.OR.J.EQ.26) WRITE(6,32) J,VNAME(J),(IDAT(I,J),
     *I=1,IPP)
  310 CONTINUE
      IPP=0
      NLINE=NLINE+23
C**
C**
   10 FORMAT(/' ','POINT  LAT    LONG   RADIUS    MLT   I LAT D LAT SCL FLD'
     *,'   VCT FLD    X COMP    Y COMP    Z COMP   AVG FLD    AVG X    AVG Y   '
     *,' AVG Z')
   11 FORMAT(' ',I4,1X,F6.2,F7.2,F8.2,3F6.2,9F9.2)
   20 FORMAT(/' ',5X,' V SD   X SD   Y SD   Z SD MODEL FLD MODEL X  MODEL',
     *' Y  MODEL Z  ATT QUAL MJ DAY DAY MSEC  HOUR   COLAT RAD DIST')
   21 FORMAT(' ',5X,4F6.2,4F9.2,F10.7,I6,I10,F7.3,2F8.2//)
   30 FORMAT(' ','---------------------------------------------------------
     1---------------------------------------------------------------------
     *---------'/' ','INPUT DATA',8X,'1',10X,'2',10X,'3',10X,'4',10X,
     *'5',10X,'6',10X,'7',10X,'8',10X,'9',10X,'10'/)
   31 FORMAT(' ',I2,2X,A8,10F11.4)
   32 FORMAT(' ',I2,2X,A8,10I11)
  500 FORMAT('1')
      RETURN
      END
      SUBROUTINE PRODAT(LEVEL,NLINE,IP,NP)
C**
C**..........................................................
C**.                                                        .
C**.                    SUBROUTINE PRODAT                   .
C**.                                                        .
C**.       PRINTS SOME OR AL OF THE OUTPUT DATA RECORD      .
C**.                                                        .
C**..........................................................
C**
      COMMON/VARBLS/ VAR(100),NWVAR
C**
      DIMENSION RDAT(10,50)
      DIMENSION IDAT(10,50)
      DIMENSION JVAR(100)
```

```
C**
      EQUIVALENCE(RDAT(1,1),IDAT(1,1))
      EQUIVALENCE(VAR(1),JVAR(1))
C**
      DOUBLE PRECISION VNAME(50)
C**
      DATA VNAME(25)/'MJ DAY'/
      DATA VNAME(26)/'UT MSEC'/
      DATA VNAME(27)/'UT HOUR'/
      DATA VNAME(28)/'GLAT'/
      DATA VNAME(29)/'ALT'/
      DATA VNAME(30)/'KP'/
      DATA VNAME(31)/'X IMF'/
      DATA VNAME(32)/'Y IMF'/
      DATA VNAME(33)/'Z IMF'/
      DATA VNAME(34)/'DST'/
      DATA VNAME(35)/'MPASS'/
      DATA VNAME(36)/'IPASS'/
      DATA VNAME(37)/'TOT ANOM'/
      DATA VNAME(38)/'X ANOMLY'/
      DATA VNAME(39)/'Y ANOMLY'/
      DATA VNAME(40)/'Z ANOMLY'/
      DATA VNAME(41)/'AVG ANOM'/
      DATA VNAME(42)/'AVX ANOM'/
      DATA VNAME(43)/'AVY ANOM'/
      DATA VNAME(44)/'AVZ ANOM'/
C**
      GO TO (1000,2000,3000),LEVEL
C**
 1000 CONTINUE
      IF(IP.GT.1)RETURN
      IF(NLINE.GT.56)NLINE=0
      IF(NLINE.EQ.0) WRITE(6,500)
      WRITE(6,10)
      WRITE(6,11)IP,JVAR(25),JVAR(26),(VAR(I),I=27,34),JVAR(35),JVAR(36)
      NLINE=NLINE+4
      RETURN
C**
 2000 CONTINUE
      IF(IP.GT.1) RETURN
      IF(NLINE.GT.52) NLINE=0
      IF(NLINE.EQ.0) WRITE(6,500)
      WRITE(6,10)
      WRITE(6,11)IP,JVAR(25),JVAR(26),(VAR(I),I=27,34),JVAR(35),JVAR(36)
      WRITE(6,20)
      WRITE(6,21) (VAR(I),I=37,44)
      NLINE=NLINE+8
      RETURN
C**
 3000 CONTINUE
      IF(IP.EQ.1) IPP=0
      IPP=IPP+1
      DO 300 J=25,44
  300 RDAT(IPP,J)=VAR(J)
      IF(IP.LT.NP.AND.IPP.NE.10) RETURN
      IF(NLINE.GT.37)NLINE=0
      IF(NLINE.EQ.0) WRITE(6,500)
      WRITE(6,30)
      DO 310 J=25,44
      IF(J.NE.25.AND.J.NE.26.AND.J.NE.35.AND.J.NE.36)WRITE(6,31)J,
     *  VNAME(J),(RDAT(I,J),I=1,IPP)
      IF(J.EQ.25.OR.J.EQ.26.OR.J.EQ.35.OR.J.EQ.36) WRITE(6,32)J,
     *  VNAME(J),(IDAT(I,J),I=1,IPP)
  310 CONTINUE
```

```
      IPP=0
      NLINE=NLINE+23
C**
C**
   10 FORMAT(/' ','POINT    MJ DAY  DAY MSEC     HOUR      COLAT  RAD',
     *             ' DIST      KP   INTERPL X INTERPL Y INTERPL Z      ',
     *             'DST      MPASS     IPASS')
   11 FORMAT(' ',I4,1X,2I10,F10.3,7F10.2,2I10)
   20 FORMAT(/' ',' TOTAL-MODEL   X-MODEL   Y-MODEL   Z-MODEL AVG-',
     *             'MODEL AVX-MODEL AVY-MODEL AVZ-MODEL')
   21 FORMAT(' ',5X,8F10.2//)
   30 FORMAT(' ','-------------------------------------------------------
     1-------------------------------------------------------------
     *---------'/' ','OUTPUT DATA',7X,'1',10X,'2',10X,'3',10X,'4',10X,
     *'5',10X,'6',10X,'7',10X,'8',10X,'9',10X,'10'/)
   31 FORMAT(' ',I2,2X,A8,10F11.4)
   32 FORMAT(' ',I2,2X,A8,10I11)
  500 FORMAT('1')
      RETURN
      END
      SUBROUTINE FIXUP(NWVAR,RANGE)
C**
C**..........................................................
C**.                          FIXUP DATA                     .
C**.                                                          .
C**.          REPLACE ERRONEOUS SCALAR DATA                   .
C**.          DELETE POINTS LACKING AVG. VECTOR DATA          .
C**.                                                          .
C**..........................................................
C**
      COMMON/MAGOUT/ AOUT(50,300),NP
C**
      INEW=0
      DO 400 IP=1,NP
C**
C**RANGE TEST
C**
      TEST=ABS(AOUT(12,IP)-AOUT(20,IP))
      IF(TEST.GT.RANGE) AOUT(12,IP)=99999.
C**
C**REPLACE MISSING SCALAR DATA WITH AVG. VECTOR DATA
C**
      IF(AOUT(7,IP).EQ.99999.) AOUT(7,IP)=AOUT(12,IP)
C**
C**REMOVE POINT IF NO AVERAGE VECTOR DATA
C**
      IF(AOUT(12,IP).EQ.99999.0) GO TO 400
C**
      INEW=INEW+1
      DO 350 IVAR=1,NWVAR
  350 AOUT(IVAR,INEW)=AOUT(IVAR,IP)
C**
  400 CONTINUE
C**
      NP=INEW
C**
      RETURN
      END
      SUBROUTINE UNILAT(IX,LINC)
C**
C**..........................................................
C**.                       SUBROUTINE UNILAT                  .
C**.                   UNIFORM LATITUDE SPACING               .
C**.                                                          .
```

```
C**.          COMPUTES THE DATA VALUES FOR EACH VARIABLE         .
C**.          IN ONE COMPLETE PASS FOR A UNIFORM LATITUDE        .
C**.          SPACING.                                           .
C**.          A MODIFIED CUBIC SPLINE PROCEEDURE IS USED         .
C**.                                                             .
C**...............................................................
C**
      COMMON/MAGOUT/ AOUT(50,300),NP
      DIMENSION X(300),Y(300),U(300),V(300)
      DIMENSION IAOUT(50,300)
      EQUIVALENCE(AOUT(1,1),IAOUT(1,1))
C**
C**               DEFINITIONS OF VARIABLES
C**          IX - VARIABLE NUMBER OF "LATITUDE" TO USE  1,5, OR 6
C**        LINC - LATITUDE INCREMENT (MINUTES)
C**
C**
      XMAX=AOUT(IX,1)
      XMIN=XMAX
      BEGLAT=AOUT(IX,1)
      ENDLAT=AOUT(IX,NP)
C**
C**
      DO 100 IP=1,NP
      I=IP
      IF(ENDLAT.LT.BEGLAT) I=NP-IP+1
      X(I)=AOUT(IX,IP)
      IF(X(I).LT.XMIN) XMIN=X(I)
      IF(X(I).GT.XMAX) XMAX=X(I)
  100 CONTINUE
C**
      ALINC=FLOAT(LINC)/60.
      IXLOW=XMIN/ALINC
      XLOW=(IXLOW+1)*ALINC
      IXUP=XMAX/ALINC
      XUP=IXUP*ALINC
      NCHS=0
      DO 200 IP=1,300
      XX=XLOW+(IP-1)*ALINC
      IF(XX.GT.XMAX) GO TO 250
      NCHS=NCHS+1
      U(NCHS)=XX
      AOUT(IX,NCHS)=XX
  200 CONTINUE
C**
  250 CONTINUE
      IF(NCHS.EQ.0) RETURN
C**
      DO 400 IVAR=1,30
      IF(IVAR.EQ.24.OR.IVAR.EQ.25.OR.IVAR.EQ.IX) GO TO 400
C**
      DO 300 IP=1,NP
      I=IP
      IF(ENDLAT.LT.BEGLAT) I=NP-IP+1
      Y(I)=AOUT(IVAR,IP)
      IF(IVAR.EQ.26) Y(I)=FLOAT(IAOUT(IVAR,IP))/10.
  300 CONTINUE
C**
      CALL INTERP(X,Y,NP,U,V,NCHS)
C**
      DO 350 IP=1,NCHS
      AOUT(IVAR,IP)=V(IP)
      IF(IVAR.EQ.26) IAOUT(IVAR,IP)=V(IP)*10.
  350 CONTINUE
```

```
C**
  400 CONTINUE
C**
      NP=NCHS
C**
      RETURN
      END
      SUBROUTINE ADDVAR
C**
C**.............................................................
C**.                                                           .
C**.                     SUBROUTINE ADDVAR                     .
C**.                                                           .
C**.         COMPUTE AND ADD SOME ADDITIONAL VARIABLES         .
C**.         TO EACH POINT                                     .
C**.                                                           .
C**.............................................................
C**
      COMMON/VARBLS/ VAR(100),NWVAR
      COMMON/HEADER/ MPASS,MJD,IPASS,HCONST(18),NRECH,NPOINT,DST(12),
     *   MODELF(3),TZERO,ABAR,FEXT(3),COMM(30),GH(289),GHT(196)
C**
      DIMENSION JVAR(100)
      DIMENSION ASC(2),DSC(2),MSEC(2),ALTM(2),ALONG(2),KP(2),GSM(6)
C**
      DOUBLE PRECISION VNAME
      EQUIVALENCE(VAR(1),JVAR(1))
      EQUIVALENCE(HCONST(1),ASC(1))
      EQUIVALENCE(HCONST(3),DSC(1))
      EQUIVALENCE(HCONST(5),MSEC(1))
      EQUIVALENCE(HCONST(7),ALTM(1))
      EQUIVALENCE(HCONST(9),ALONG(1))
      EQUIVALENCE(HCONST(11),KP(1))
      EQUIVALENCE(HCONST(13),GSM(1))
      DOUBLE PRECISION TIMEA,TIMED,TIMEC,FRAC
C**
C**NOTE:- TIMES 'MSEC(1)' OR 'MSEC(2)' MAY BE UNDEFINED AND SET
C** TO -99999
C**
      TIMEA=DFLOAT(MSEC(1))
      TIMED=DFLOAT(MSEC(2))
      TIMEC=DFLOAT(JVAR(26))
      FRAC=(TIMEC-TIMEA)/(TIMED-TIMEA)
C**
C**
C**KP INDEX
C**
      AKP=FLOAT(KP(1))
      DKP=FLOAT(KP(2))
      IF(AKP.LT.0.OR.AKP.GT.40.0) AKP=DKP
      IF(DKP.LT.0.OR.DKP.GT.40.0) DKP=AKP
      CKP=AKP+(DKP-AKP)*FRAC
      KPC=CKP+0.5
      VAR(30)=FLOAT(KPC)
C**
C**INTERPLANETARY MAGNETIC FIELD
C**
      AGSMX=GSM(1)
      DGSMX=GSM(2)
      AGSMY=GSM(3)
      DGSMY=GSM(4)
      AGSMZ=GSM(5)
      DGSMZ=GSM(6)
      IF(AGSMX.EQ.99999.) AGSMX=DGSMX
```

```
      IF(DGSMX.EQ.99999.) DGSMX=AGSMX
      IF(AGSMY.EQ.99999.) AGSMY=DGSMY
      IF(DGSMY.EQ.99999.) DGSMY=AGSMY
      IF(AGSMZ.EQ.99999.) AGSMZ=DGSMZ
      IF(DGSMZ.EQ.99999.) DGSMZ=AGSMZ
      VAR(31)=AGSMX+(DGSMX-AGSMX)*FRAC
      VAR(32)=AGSMY+(DGSMY-AGSMY)*FRAC
      VAR(33)=AGSMZ+(DGSMZ-AGSMZ)*FRAC
C**
C**DST
C**
C**NOTE:- INTERPOLATING DST USING CALCULATED VALUE AT NODES
C**THIS MAY NOT BE CORRECT PROCEEDURE
C**
      ADST=DST(11)
      DDST=DST(12)
      IF(ADST.EQ.99999.) ADST=DDST
      IF(DDST.EQ.99999.) DDST=ADST
      VAR(34)=ADST+(DDST-ADST)*FRAC
C**
      JVAR(35)=MPASS
      JVAR(36)=IPASS
      VAR(37)=VAR(8)-VAR(20)
      VAR(38)=VAR(9)-VAR(21)
      VAR(39)=VAR(10)-VAR(22)
      VAR(40)=VAR(11)-VAR(23)
      VAR(41)=VAR(12)-VAR(20)
      VAR(42)=VAR(13)-VAR(21)
      VAR(43)=VAR(14)-VAR(22)
      VAR(44)=VAR(15)-VAR(23)
      IF(VAR(8).EQ.99999..OR.VAR(20).EQ.99999.) VAR(37)=99999.
      IF(VAR(9).EQ.99999..OR.VAR(21).EQ.99999.) VAR(38)=99999.
      IF(VAR(10).EQ.99999..OR.VAR(22).EQ.99999.) VAR(39)=99999.
      IF(VAR(11).EQ.99999..OR.VAR(23).EQ.99999.) VAR(40)=99999.
      IF(VAR(12).EQ.99999..OR.VAR(20).EQ.99999.) VAR(41)=99999.
      IF(VAR(13).EQ.99999..OR.VAR(21).EQ.99999.) VAR(42)=99999.
      IF(VAR(14).EQ.99999..OR.VAR(22).EQ.99999.) VAR(43)=99999.
      IF(VAR(15).EQ.99999..OR.VAR(23).EQ.99999.) VAR(44)=99999.
C**
      NWVAR=44
C**
      RETURN
      END
      SUBROUTINE INTERP(X,Y,L,U,V,N)
C**
C**.....................................................................
C**.                          SUBROUTINE INTERP                         .
C**.                     SMOOTH INTERPOLATION                           .
C**.                                                                    .
C**.          INTERPOLATES THE VALUE OF THE FUNCTION 'Y'               .
C**.          (DEFINED AT LOCATIONS 'X', DIMENSION 'L')                .
C**.          FOR THE LOCATIONS STORED IN 'U',DIMENSION 'N'            .
C**.          THE OUTPUT IS STORED IN 'V'                              .
C**.                                                                    .
C**.   REF:-  AKIMA H, COMM OF ACM, VOL 15 1972, P914                  .
C**.                                                                    .
C**.....................................................................
C**
C**THE INPUT PARAMETERS ARE
C**          X - ARRAY OF DIMENSION L STORING THE X VALUES
C**              OF INPUT DATA POINTS (IN ASCENDING ORDER)
C**          Y - ARRAY OF DIMENSION L STORING THE Y VALUES
C**              (ORDINATES) OF INPUT DATA POINTS
C**          L - NUMBER OF INPUT DATA POINTS
```

```
C**              (MUST BE 2 OR GREATER)
C**           U ARRAY OF DIMENSION N STORING THE X VALUES
C**              (ABSCISSAS) OF DESIRED POINTS
C**           N - NUMBER OF POINTS AT WHICH INTERPOLATION OF
C**              THE Y VALUE IS DESIRED
C**              (MUST BE 1 OR GREATER)
C**
C**THE OUTPUT PARAMETER IS
C**
C**           V - ARRAY OF DIMENSION N WHERE THE INTERPOLAYED
C**              Y VALUES (ORDINATES) ARE TO BE DISPLAYED
C**
      DIMENSION X(300),Y(300),U(300),V(300)
      LOGICAL INTEG
      REAL M1,M2,M3,M4,M5,M24,M35
      DATA IU/6/
C**
      V(1)=0.0
      INTEG=.FALSE.
      IF(N.LT.1) INTEG=.TRUE.
      LPI=L+1
C**CHECKS
C**
      IF(INTEG) N=L-1
      IF(L-2) 90,600,20
   20 CONTINUE
C**
C**MAIN DO LOOP
C**
      I=1
      DO 900 K=1,N
      IF(INTEG) GO TO 15
      UK=U(K)
C**
C**ROUTINE TO LOCATE THE DESIRED POINT
C**
      IF(UK.LT.X(1).OR.UK.GT.X(L)) GO TO 800
C**
      IF(UK-X(I)) 70,700,22
   22 I=I+1
      IF(X(I-1)-X(I)) 11,95,96
   11 CONTINUE
      IF(UK-X(I)) 23,700,22
C**
   15 I=K+1
   23 CONTINUE
C**
C**
C**ROUTINES TO PICK UP NECESSARY X AND Y VALUES AND TO
C**ESTIMATE THEM IF NECESSARY
C**
   40 J=I
      A3=X(J)-X(J-1)
      Y3=Y(J-1)
      M3=(Y(J)-Y(J-1))/A3
      IF(J.EQ.2) GO TO 41
      M2=(Y(J-1)-Y(J-2))/(X(J-1)-X(J-2))
      IF(J.EQ.L) GO TO 42
C**
   41 M4=(Y(J+1)-Y(J))/(X(J+1)-X(J))
      IF(J.EQ.2) M2=M3+M3-M4
      GO TO 45
   42 M4=M3+M3-M2
   45 IF(J.LE.3) GO TO 46
```

```
      M1=(Y(J-2)-Y(J-3))/(X(J-2)-X(J-3))
      GO TO 47
   46 M1=M2+M2-M3
   47 IF(J.GE.(L-1)) GO TO 48
      M5=(Y(J+2)-Y(J+1))/(X(J+2)-X(J+1))
      GO TO 50
   48 M5=M4+M4-M3
C**
C**NUMERICAL DIFFERENTIATION
C**
   50 CONTINUE
      IF(J.EQ.2) GO TO 101
      M24=(Y(J)-Y(J-2))/(X(J)-X(J-2))
      GO TO 102
  101 M24=.5*(M2+M3)
  102 IF(M1.GT.M24.AND.M4.LT.M24) GO TO 103
      IF(M1.LT.M24.AND.M4.GT.M24) GO TO 103
      T3=M24
      GO TO 52
C**
  103 W2=SQRT(ABS((M3-M1)*(M4-M3)))
      W3=SQRT(ABS((M2-M1)*(M4-M2)))
      SW=W2+W3
      IF(SW.NE.0.0) GO TO 51
      W2=0.5
      W3=0.5
      SW=1.0
   51 T3=(W2*M2+W3*M3)/SW
C**
   52 CONTINUE
      IF(J.EQ.L) GO TO 111
      M35=(Y(J+1)-Y(J-1))/(X(J+1)-X(J-1))
      GO TO 112
  111 M35=.5*(M3+M4)
  112 IF(M2.GT.M35.AND.M5.LT.M35) GO TO 113
      IF(M2.LT.M35.AND.M5.GT.M35) GO TO 113
      T4=M35
      GO TO 60
  113 W3=SQRT(ABS((M4-M2)*(M5-M4)))
      W4=SQRT(ABS((M3-M2)*(M5-M3)))
      SW=W3+W4
      IF(SW.NE.0.0) GO TO 53
      W3=0.5
      W4=0.5
      SW=1.0
   53 T4=(W3*M3+W4*M4)/SW
C**
C**DETERMINE THE COEFFICIENTS
C**
   60 Q2=(2.0*(M3-T3)+M3-T4)/A3
      Q3=(-M3-M3+T3+T4)/(A3*A3)
C**
C**COMPUTATION OF THE POLYNOMIAL
C**
      IF(INTEG) GO TO 400
   70 DX=UK-X(J-1)
      V(K)=Y3+DX*(T3+DX*(Q2+DX*Q3))
      GO TO 900
C**
  400 CONTINUE
C**COMPUTE INTEGRAL
C**
      DX=X(K+1)-X(K)
      V(1)=V(1)+DX*(Y3+DX*T3/2.+DX*DX*Q2/3.+DX*DX*DX*Q3/4.)
```

```
      GO TO 900
C**
  700 V(K)=Y(I)
      GO TO 900
C**
  800 V(K)=Y(1)
      IF(UK.GT.Y(K)) V(K)=Y(L)
  900 CONTINUE
      RETURN
C**
  600 CONTINUE
C**
C**LINEAR INTERPOLATION
C**
      M1=(Y(2)-Y(1))/(X(2)-X(1))
      DO 610 K=1,N
  610 V(K)=Y(1)+(U(K)-X(1))*M1
      RETURN
C**
C**ERROR EXIT
C**
   90 WRITE(IU,2090)
      GO TO 99
   91 WRITE(IU,2091)
      GO TO 99
   95 WRITE(IU,2095)
      GO TO 97
   96 WRITE(IU,2096)
   97 WRITE(IU,2097) I,X(I)
   99 WRITE(IU,2099) LO,NO
      RETURN
C**
C**FORMAT STATEMENTS
C**
 2090 FORMAT(' ',22H  ***    L = 1 OR LESS./)
 2091 FORMAT(' ',22H  ***    N = 0 OR LESS./)
 2095 FORMAT(' ',27H  ***    IDENTICAL X VALUES./)
 2096 FORMAT(' ',33H  ***    X VALUES OUT OF SEQUENCE./)
 2097 FORMAT(' ',6H   I =,I7,10X,6HX(I) =,E12.3)
 2099 FORMAT(' ',6H   L =,I7,10X,3HN =,I7,/
     1       ' ',36H ERROR DETECTED IN ROUTINE    INTRPL)
      END
      SUBROUTINE PLOTTR(LEVEL,IX,IY,ITITLE)
C**.............................................................
C**.                                                           .
C**.                    SUBROUTINE PLOTTR                      .
C**.                                                           .
C**.      LEVEL                 PURPOSE OF CALL                .
C**.                                                           .
C**.        1          - MOVES PEN TO NEXT PLOTTING POSITION   .
C**.        2          - BOUNDARY AND LONG-LAT OF SATELLITE    .
C**.                      ARE PLOTTED ON SAME GRAPH            .
C**.        3          - LONG-LAT OF SATELLITE IS PLOTTED      .
C**.        4          - ANOMALY VS LAT IS PLOTTED             .
C**.        5          - MULTIPLE PLOTS OF LAT-LONG ARE PLOTTED .
C**.                      AS WELL AS CHURCHILL-SUPERIOR BOUNDARY .
C**.        6          - SCALAR, NORTH, EAST, AND VERTICAL ANOM .
C**.                      ARE PLOTTED ON SAME GRAPH WITH FOUR CALLS .
C**.        7          - SUCCESSIVE PLOTS ARE SUPERPOSED ON SAME .
C**.                      PLOT WITH A SINGLE CALL              .
C**.............................................................
C**
      COMMON/BNDRY/ CSBLNG(182),CSBLAT(182),PB1LNG(5),PB1LAT(5),
     *              PB2LNG(50),PB2LAT(50),PB3LNG(16),PB3LAT(16),
```

```
     *              PB4LNG(12),PB4LAT(12),PB5LNG(4),PB5LAT(4),
     *              PB6LNG(7),PB6LAT(7),BAYLNG(254),BAYLAT(254),
     *              SUPLNG(116),SUPLAT(116),RIVLNG(109),RIVLAT(109)
      COMMON/MAGOUT/ AOUT(50,300),NP
      COMMON/PLPARM/ XSTART,XASCAL,YSTART,YASCAL,IPNUM,CSBF,PROVF,
     *               BAYF,RIVF,LAKF
C**
      DIMENSION IAOUT(50,300),XP(300),FP(300),TESTX(4),TESTY(4)
      DIMENSION ITITLE(20)
C**
      EQUIVALENCE(AOUT(1,1),IAOUT(1,1))
C**
      LOGICAL CSBF,PROVF,BAYF,RIVF,LAKF
C**
C**
      DO 10 IPNT=1,NP
      XP(IPNT)=AOUT(IX,IPNT)
   10 FP(IPNT)=AOUT(IY,IPNT)
C**
      NPNT=NP
      PASS=FLOAT(IAOUT(36,1))
C**
      GO TO (1000,2000,3000,4000,5000,6000,7000),LEVEL
      WRITE(6,100) LEVEL
  100 FORMAT(' ','*** ERROR IN PLOTTR ***    LEVEL=',I5)
      RETURN
C**
 1000 CONTINUE
      CALL PLOT(11.,0.,-3)
      RETURN
C**
 2000 CONTINUE
C**PRINT PLOT TITLE
      CALL SYMBOL(0.,-.8,.14,ITITLE,0.,80)
      CALL SYMBOL(0.,-1.1,.14,'PASS',0.,4)
      CALL NUMBER(.7,-1.1,.14,PASS,0.,-1)
C**
C**OPTIMIZE SCALES
  200 CONTINUE
      XSTART=-140.0
      XASCAL=10.0
      YSTART=40.0
      YASCAL=5.0
C**
C**PRINT AXES
      CALL AXISI(0.,0.,'LATITUDE (DEG)',14,8.,90.,YSTART,YASCAL)
      CALL AXISI(9.,0.,' ',-1,8.,90.,YSTART,YASCAL)
      CALL AXISI(0.,0.,'LONGITUDE (DEG)',-15,9.,0.,XSTART,XASCAL)
      CALL AXISI(0.,8.,' ',1,9.,0.,XSTART,XASCAL)
C**
C**PLOT THE DATA
      IF(.NOT.CSBF) GO TO 20
      CSBLNG(181)=XSTART
      CSBLNG(182)=XASCAL
      CSBLAT(181)=YSTART
      CSBLAT(182)=YASCAL
      CALL NEWPEN(4)
      CALL LINE(CSBLNG,CSBLAT,180,1,0,0)
      CALL NEWPEN(1)
C**
   20 IF(.NOT.PROVF) GO TO 21
      PB1LNG(4)=XSTART
      PB1LNG(5)=XASCAL
      PB1LAT(4)=YSTART
```

```
      PB1LAT(5)=YASCAL
      PB2LNG(49)=XSTART
      PB2LNG(50)=XASCAL
      PB2LAT(49)=YSTART
      PB2LAT(50)=YASCAL
      PB3LNG(15)=XSTART
      PB3LNG(16)=XASCAL
      PB3LAT(15)=YSTART
      PB3LAT(16)=YASCAL
      PB4LNG(11)=XSTART
      PB4LNG(12)=XASCAL
      PB4LAT(11)=YSTART
      PB4LAT(12)=YASCAL
      PB5LNG(3)=XSTART
      PB5LNG(4)=XASCAL
      PB5LAT(3)=YSTART
      PB5LAT(4)=YASCAL
      PB6LNG(6)=XSTART
      PB6LNG(7)=XASCAL
      PB6LAT(6)=YSTART
      PB6LAT(7)=YASCAL
      CALL DASHLN(PB1LNG,PB1LAT,3,1,15)
      CALL DASHLN(PB2LNG,PB2LAT,48,1,15)
      CALL DASHLN(PB3LNG,PB3LAT,14,1,15)
      CALL DASHLN(PB4LNG,PB4LAT,10,1,15)
      CALL DASHLN(PB5LNG,PB5LAT,2,1,15)
      CALL DASHLN(PB6LNG,PB6LAT,5,1,15)
C**
   21 IF(.NOT.BAYF) GO TO 22
      BAYLNG(253)=XSTART
      BAYLNG(254)=XASCAL
      BAYLAT(253)=YSTART
      BAYLAT(254)=YASCAL
      CALL LINE(BAYLNG,BAYLAT,252,1,0,0)
C**
   22 IF(.NOT.LAKF) GO TO 23
      SUPLNG(115)=XSTART
      SUPLNG(116)=XASCAL
      SUPLAT(115)=YSTART
      SUPLAT(116)=YASCAL
      CALL LINE(SUPLNG,SUPLAT,114,1,0,0)
C**
   23 IF(.NOT.RIVF) GO TO 24
      RIVLNG(108)=XSTART
      RIVLNG(109)=XASCAL
      RIVLAT(108)=YSTART
      RIVLAT(109)=YASCAL
      CALL LINE(RIVLNG,RIVLAT,107,1,0,0)
C**
   24 XP(NPNT+1)=XSTART
      XP(NPNT+2)=XASCAL
      FP(NPNT+1)=YSTART
      FP(NPNT+2)=YASCAL
C&&&&&CALL NEWPEN(2)
      CALL LINE(XP,FP,NPNT,1,0,0)
C&&&&&CALL NEWPEN(1)
      RETURN
C**
 3000 CONTINUE
C**PRINT PLOT TITLE
      CALL SYMBOL(0.,-.8,.14,ITITLE,0.,80)
      CALL SYMBOL(0.,-1.1,.14,'PASS',0.,4)
      CALL NUMBER(.7,-1.1,.14,PASS,0.,-1)
C**
```

```
C**OPTIMIZE SCALES
      CALL SCALE(XP,8.,NPNT,1)
      XSTART=XP(NPNT+1)
      XASCAL=XP(NPNT+2)
      CALL SCALE(FP,8.,NPNT,1)
      YSTART=FP(NPNT+1)
      YASCAL=FP(NPNT+2)
C**
C**PRINT AXES
      CALL AXIS(O.,O.,'LATITUDE (DEG)',14,8.,90.,YSTART,YASCAL)
      CALL AXIS(8.,O.,' ',-1,8.,90.,YSTART,YASCAL)
      CALL AXIS(O.,O.,'LONGITUDE (DEG)',-15,8.,O.,XSTART,XASCAL)
      CALL AXIS(O.,8.,' ',1,8.,O.,XSTART,XASCAL)
C**
C**PLOT THE DATA
      CALL LINE(XP,FP,NPNT,1,O,O)
      RETURN
C**
 4000 CONTINUE
C**PRINT PLOT TITLE
      CALL SYMBOL(O.,-.8,.14,ITITLE,O.,80)
C---> CALL SYMBOL(O.,-1.1,.14,'PASS',O.,4)
C---> CALL NUMBER(.7,-1.1,.14,PASS,O.,-1)
C**
C**OPTIMIZE SCALES
C**   CALL SCALE(XP,8.,NPNT,1)
      XSTART=40.O
      XASCAL=5.O
C**   CALL SCALE(FP,8.,NPNT,1)
      YSTART=-20.O
      YASCAL=5.O
C**
C**PRINT AXES
      CALL AXIS(O.,O.,'MAGNETIC ANOMALY FIELD   (NT)',29,8.,90.,
     *          YSTART,YASCAL)
      CALL AXIS(O.,4.,'LATITUDE (DEG)',-14,8.,O.,XSTART,XASCAL)
C**
C**PLOT THE DATA
      XP(NPNT+1)=XSTART
      XP(NPNT+2)=XASCAL
      FP(NPNT+1)=YSTART
      FP(NPNT+2)=YASCAL
      CALL LINE(XP,FP,NPNT,1,O,O)
      RETURN
C**
 5000 CONTINUE
      IPNUM=IPNUM+1
      IF(IPNUM.EQ.1) GO TO 200
      INTEQ=IPNUM-2
      IF(INTEQ.GT.14) INTEQ=INTEQ+50
C**
C**PLOT THE DATA
      XP(NPNT+1)=XSTART
      XP(NPNT+2)=XASCAL
      FP(NPNT+1)=YSTART
      FP(NPNT+2)=YASCAL
C&&&&&CALL NEWPEN(2)
      CALL LINE(XP,FP,NPNT,1,40,INTEQ)
C&&&&&CALL NEWPEN(1)
      IF(IPNUM.LT.25) RETURN
      IPNUM=O
      GO TO 1000
C**
C**
```

```
 6000 CONTINUE
      IPNUM=IPNUM+1
      GO TO (60,61,62,63),IPNUM
      WRITE(6,666) IPNUM
  666 FORMAT(' ','#### ERROR IN PLOTTR ####   IPNUM =',I4)
      RETURN
   60 INTEQ=11
C**    PRINT PLOT TITLE
      CALL SYMBOL(O.,-.8,.14,ITITLE,O.,80)
      CALL SYMBOL(O.,-1.1,.14,'PASS',O.,4)
      CALL NUMBER(.7,-1.1,.14,PASS,O.,-1)
C**    SET SCALES
      XSTART=40.O
      XASCAL=5.O
      YSTART=-40.O
      YASCAL=10.O
C**PRINT AXES
      CALL AXIS(O:,O.,'MAGNETIC ANOMALY FIELD   (NT)',29,8.,90.,
     *          YSTART,YASCAL)
      CALL AXIS(O.,4.,'LATITUDE (DEG)',-14,8.,O.,XSTART,XASCAL)
C**
      GO TO 64
   61 INTEQ=4
      GO TO 64
   62 INTEQ=9
      GO TO 64
   63 INTEQ=8
      IPNUM=O
C**PLOT THE DATA
   64 XP(NPNT+1)=XSTART
      XP(NPNT+2)=XASCAL
      FP(NPNT+1)=YSTART
      FP(NPNT+2)=YASCAL
      CALL LINE(XP,FP,NPNT,1,+5,INTEQ)
      RETURN
 7000 CONTINUE
      IPNUM=IPNUM+1
      IF(IPNUM.GT.1) GO TO 700
C**PRINT PLOT TITLE
      CALL SYMBOL(O.,-1.,.14,ITITLE,O.,80)
C**
C**OPTIMIZE SCALES
C**   CALL SCALE(XP,8.,NPNT,1)
      XSTART=40.O
      XASCAL=5.O
C**   CALL SCALE(FP,8.,NPNT,1)
      YSTART=-20.O
      YASCAL=5.O
C**
C**PRINT AXES
      CALL AXIS(O.,O.,'MAGNETIC ANOMALY FIELD   (NT)',29,8.,90.,
     *          YSTART,YASCAL)
      CALL AXIS(O.,4.,'LATITUDE (DEG)',-14,8.,O.,XSTART,XASCAL)
C**
  700 CONTINUE
C**PLOT THE DATA
      XP(NPNT+1)=XSTART
      XP(NPNT+2)=XASCAL
      FP(NPNT+1)=YSTART
      FP(NPNT+2)=YASCAL
      CALL LINE(XP,FP,NPNT,1,O,O)
      IF(IPNUM.LT.50) RETURN
      IPNUM=O
      GO TO 1000
```

```
      END
      SUBROUTINE FITTER(IX,IY,MDEG,C,BETA)
C*********************************************************************
C***                       SUBROUTINE FITTER                         *
C***                                                                 *
C***    S/R FITTER FITS A POLYNOMIAL TO A SET OF DATA.  THE S/R      *
C***  REQUIRES N PAIRS OF X AND Y VALUES AND RETURNS THE COEFFICIENTS *
C***  OF THE NORMAL EQUATIONS FOR THE LEAST SQUARES METHOD.          *
C***                                                                 *
C***     REF: C.F. GERALD, 1978.  "APPLIED NUMERICAL ANALYSIS"       *
C***           2ND EDITION, ADDISON-WESLEY, PP.505-507.              *
C***                                                                 *
C*********************************************************************
C**
C**
C**                       PARAMETERS
C**   IX,IY    - VARIABLE NUMBERS IN ARRAY AOUT TO BE USED AS
C**              X AND Y ARRAYS
C**   X(300)   - X VALUES
C**   Y(300)   - Y VALUES
C**   N        - NUMBER OF DATA PAIRS
C**   MDEG     - DEGREE OF POLYNOMIAL TO COMPUTE - MAX = 9
C**   A(10,11)- AUGMENTED MATRIX OF THE COEFFICIENTS OF THE NORMAL
C**              EQUATIONS
C**   C(10)    - ARRAY OF COEFFICIENTS OF LEAST SQUARES POLYNOMIALS
C**
      COMMON/MAGOUT/ AOUT(50,300),NP
C**
      DIMENSION X(300),Y(300),XN(300),C(10),A(10,11)
C**
      DO 111 I=1,NP
      X(I)=AOUT(IX,I)
      Y(I)=AOUT(IY,I)
  111 CONTINUE
C**
C**CHECK MDEG TO ENSURE IT IS .LE. N-1
      IF(MDEG.LE.(NP-1)) GO TO 5
      MDEG=NP-1
      WRITE(6,200) MDEG
  200 FORMAT('1','DEGREE OF POLYNOMIAL CANNOT EXCEED NPNT-1.'/
     *       ' ','REQUESTED DEGREE TOO LARGE, REDUCED TO',I5)
    5 N=NP
C**
      MDEGP1=MDEG+1
      MDEGP2=MDEG+2
C**PUT "1'S" INTO A NEW ARRAY.  THIS WILL HOLD THE POWERS OF X
      DO 10 I=1,N
   10 XN(I)=1.0
C**COMPUTE 1ST COL. AND N+1ST COL. OF A.  I MOVES DOWN ROWS, J SUMS OVER
C**THE N VALUES
      DO 30 I=1,MDEGP1
      A(I,1)=0.0
      A(I,MDEGP2)=0.0
      DO 20 J=1,N
      A(I,1)=A(I,1)+XN(J)
      A(I,MDEGP2)=A(I,MDEGP2)+Y(J)*XN(J)
   20 XN(J)=XN(J)*X(J)
   30 CONTINUE
C**COMPUTE THE LAST ROW OF A.  I MOVES ACROSS COL.'S, J SUMS OVER N
      DO 50 I=2,MDEGP1
      A(MDEGP1,I)=0.0
      DO 40 J=1,N
      A(MDEGP1,I)=A(MDEGP1,I)+XN(J)
   40 XN(J)=XN(J)*X(J)
```

```
   50 CONTINUE
C**NOW FILL IN THE REST OF THE A MATRIX.  I MOVES DOWN ROWS, J ACROSS
C**COLUMNS
      DO 70 J=2,MDEGP1
      DO 60 I=1,MDEG
   60 A(I,J)=A(I+1,J-1)
   70 CONTINUE
C**CALL A SUBROUTINE TO SOLVE THE SYSTEM OF EQUATIONS.  GET THE LU
C**DECOMPOSITION OF A.
      CALL LUDCMP(A,MDEGP1,10)
C**RESET THE R.H.S. INTO C
      DO 90 J=1,MDEGP1
   90 C(J)=A(J,MDEGP2)
      CALL SOLN(A,C,MDEGP1,10)
C**WRITE COEFF. OF LEAST SQUARES FIT
      WRITE(6,202) MDEG,(C(J),J=1,MDEGP1)
  202 FORMAT('1','FOR DEGREE OF',I3,' COEFFICIENTS ARE',/
     *        ' ',11(5X,E12.5,/' '))
C**COMPUTE AND PRINT THE VALUE OF BETA = (SUM OF(DEV**2))/(N-M-1)
      BETA=0.0
      DO 94 IPNT=1,N
      SUM=0.0
      DO 93 ICOEF=2,MDEGP1
      JCOEF=MDEGP1-ICOEF+2
      SUM=(SUM+C(JCOEF))*X(IPNT)
   93 CONTINUE
      SUM=SUM+C(MDEGP1)
      BETA=BETA+(Y(IPNT)-SUM)**2
   94 CONTINUE
      BETA=BETA/(N-MDEGP1)
      WRITE(6,203) BETA
  203 FORMAT(' ',9X,'BETA = ',E12.5)
      RETURN
      END
      SUBROUTINE LUDCMP(A,N,NDIM)
C******************************************************************
C***                   SUBROUTINE LUDCMP                          *
C***                                                              *
C***    THIS S/R FORMS THE LU EQUIVALENT OF THE SQUARE MATRIX A.  *
C***  THE LU, IN COMPACT FORM, IS RETURNED IN THE A MATRIX SPACE. *
C***  THE UPPER TRIANGULAR MATRIX U HAS 1'S ON ITS DIAGONAL -      *
C***  THESE VALUES ARE NOT INCLUDED IN THE RESULT                 *
C***                                                              *
C***     CALLED BY FITTER                                         *
C******************************************************************
C**
      DIMENSION A(NDIM,NDIM)
C**
      DO 35 I=1,N
      DO 30 J=2,N
      SUM=0.0
      IF(J.GT.I) GO TO 15
      JM1=J-1
      DO 10 K=1,JM1
   10 SUM=SUM+A(I,K)*A(K,J)
      A(I,J)=A(I,J)-SUM
      GO TO 30
   15 IM1=I-1
      IF(IM1.EQ.0) GO TO 25
      DO 20 K=1,IM1
   20 SUM=SUM+A(I,K)*A(K,J)
C**TEST FOR SMALL VALUE ON DIAGONAL
   25 IF(ABS(A(I,I)).LT.1.E-10) GO TO 99
      A(I,J)=(A(I,J)-SUM)/A(I,I)
```

```
   30 CONTINUE
   35 CONTINUE
      RETURN
   99 WRITE(6,100) I
  100 FORMAT(' ','REDUCTION NOT COMPLETED BECAUSE SMALL VALUE FOUND',
     *            ' FOR DIVISOR IN ROW AND COLUMN',I3)
      RETURN
      END
      SUBROUTINE SOLN(A,B,N,NDIM)
C*******************************************************************
C***                    SUBROUTINE SOLN                            *
C***                                                               *
C***     THIS S/R FINDS THE SOLUTION TO A SET OF N LINEAR          *
C***  EQUATIONS THAT CORRESPOND TO THE R.H.S. VECTOR B.  THE A     *
C***  MATRIX IS THE LU DECOMPOSITION EQUIVALENT TO THE COEFF.      *
C***  MATRIX OF THE ORIGINAL EQUATIONS, AS REDUCED BY S/R LUDCMP.*
C***  THE SOLUTION VECTOR IS RETURNED IN B.                        *
C***                                                               *
C***      CALLED BY FITTER                                         *
C********************************************************************
C**
      DIMENSION A(NDIM,NDIM),B(NDIM)
C**
C**DO THE REDUCTION STEP
      B(1)=B(1)/A(1,1)
      DO 20 I=2,N
      IM1=I-1
      SUM=0.0
      DO 10 K=1,IM1
   10 SUM=SUM+A(I,K)*B(K)
   20 B(I)=(B(I)-SUM)/A(I,I)
C**NOW READY FOR BACK SUBSTITUTION.  ELEMENTS OF U ON DIAG. ARE ALL 1'S.
      DO 40 J=2,N
      NMJP2=N-J+2
      NMJP1=N-J+1
      SUM=0.0
      DO 30 K=NMJP2,N
   30 SUM=SUM+A(NMJP1,K)*B(K)
   40 B(NMJP1)=B(NMJP1)-SUM
      RETURN
      END
      SUBROUTINE POLY(IXVAR,IYVAR,MDEG,DIFF)
C** *****************************************************************
C** *                       SUBROUTINE POLY                          *
C** *                                                               *
C** *    FITS A POLYNOMIAL OF DEGREE MDEG TO A SET OF DATA,         *
C** *    CALCULATES THE POLYNOMIAL, AND SUBTRACTS THE FIT FROM      *
C** *    THE INPUT DATA, STORING THE DIFFERENCE IN THE ARRAY DIFF   *
C** *****************************************************************
C**
      COMMON/MAGOUT/ AOUT(50,300),NP
C**
      DIMENSION DIFF(300),FIT(300),COEF(10)
C**
      DO 5 I=1,10
    5 COEF(I)=0.0
      CALL FITTER(IXVAR,IYVAR,MDEG,COEF,BETA)
      DO 10 I=1,NP
      FIT(I)=COEF(1) + COEF(2)*AOUT(IXVAR,I) + COEF(3)*AOUT(IXVAR,I)**2.
   10 DIFF(I)=AOUT(IYVAR,I)-FIT(I)
C**
      RETURN
      END
      SUBROUTINE STACK(VECT,VSTART,VEND,SUM,SSTART,SUMEND,DIGI,NUMVEC,
```

```
     &                    LENGS)
C**
C**  ################################################################
C**  ##                    SUBROUTINE STACK                        ##
C**  ##  INPUT A VECTOR (ANOMALY FIELD) OF UNIFORM DIGITIZATION     ##
C**  ##  INTERVAL DIGI WITH LATITUDE ENDPOINTS OF VSTART AND VEND.  ##
C**  ##  ALSO INPUT THE DESIRED LATITUDE ENDPOINTS FOR THE SUMMED   ##
C**  ##  VECTORS.                                                   ##
C**  ##  S/R STACK RETURNS THE SUM, ITS LENGTH, AND THE NUMBER OF   ##
C**  ##  VECTORS SUMMED.                                            ##
C**  ################################################################
C**
      DIMENSION VECT(300),SUM(300)
C**
      NUMVEC=NUMVEC+1
      LENGS=IFIX((SUMEND-SSTART)/DIGI)+1
      ISHIFT=IFIX((SSTART-VSTART)/DIGI)
      IPAD=IFIX((SUMEND-VEND)/DIGI)
C**
      IF(IPAD.LT.0) IPAD=0
      ILENG=LENGS-IPAD
      IF(ISHIFT.LT.0) GO TO 10
C**
      DO 100 I=1,ILENG
  100 SUM(I)=SUM(I)+VECT(I+ISHIFT)
C**
      IF(IPAD.EQ.0) GO TO 11
      DO 101 I=1,IPAD
  101 SUM(I+ILENG)=SUM(I+ILENG)+VECT(ILENG+ISHIFT)
C**
   11 RETURN
C**
   10 CONTINUE
      JPAD=-ISHIFT
      DO 102 I=1,JPAD
  102 SUM(I)=SUM(I)+VECT(1)
C**
      INEXT=JPAD+1
      DO 103 I=INEXT,ILENG
  103 SUM(I)=SUM(I)+VECT(I-JPAD)
C**
      IF(IPAD.EQ.0) GO TO 12
      DO 104 I=1,IPAD
  104 SUM(I+ILENG)=SUM(I+ILENG)+VECT(ILENG+ISHIFT)
   12 RETURN
      END
      SUBROUTINE BNDPAS(F1,F2,DT,D,G)
C
C
C                     THIS SUBROUTINE DESIGNS A RECURSIVE BUTTERWORTH
C               BANDPASS FILTER.
C                     THIS SUBROUTINE WAS WRITTEN BY DAVE GANLEY
C               AND IS LISTED IN 'TIME SEQUENCE ANALYSIS IN GEOPHYSICS'
C               BY E.R. KANASEWICH
C
C
      COMPLEX P(4),S(8),Z1,Z2
      REAL D(8),W1,W2,TDT,HWID,WW,G,B,C,A,TWOPI
C
      TDT=2.0/DT
      TWOPI=6.2831853
      FDT=4.0/DT
      P(1)=CMPLX(-.3826834,.9238795)
      P(2)=CMPLX(-.3826834,-.9238795)
```

```
      P(3)=CMPLX(-.9238795,.3826834)
      P(4)=CMPLX(-.9238795,-.3826834)
      W1=TWOPI*F1
      W2=TWOPI*F2
      W1=TDT*TAN(W1/TDT)
      W2=TDT*TAN(W2/TDT)
      HWID=(W2-W1)/2.0
      WW=W1*W2
      DO 19 I=1,4
      Z1=P(I)*HWID
      Z2=CSQRT(Z1*Z1-WW)
      S(I)=Z1+Z2
   19 S(I+4)=Z1-Z2
      G=(.5/HWID)**4.0
      DO 29 I=1,7,2
      B=-2.0*REAL(S(I))
      Z1=S(I)*S(I+1)
      C=REAL(Z1)
      A=TDT+B+C/TDT
      G=G*A
      D(I)=(C*DT-FDT)/A
   29 D(I+1)=(A-2.0*B)/A
      G=G*G
      WRITE(6,1) F1,F2,DT
    1 FORMAT('1',20X,'BUTTERWORTH BANDPASS FILTER',//' ',10X,
     &       'PASSBAND;',2F10.3,/' ',10X,'DIGITIZATION;',F10.3,//)
      WRITE(6,3)
    3 FORMAT(' ',10X,'FILTER IS  (1 - Z**2)**4 / B1*B2*B3*B4',/)
      WRITE(6,4) D
    4 FORMAT(' ',4(10X,'B(I) = 1 +',F10.3,'*Z +',F10.3,'*Z**2'/' '))
      WRITE(6,5) G
    5 FORMAT(' ',10X,'FILTER GAIN IS',F15.3)
      RETURN
      END
      SUBROUTINE FILTER(X,N,D,G)
C
C
C                THIS SUBROUTINE DOES THE ACTUAL FILTERING OF THE
C                DATA WITH THE BANDPASS FILTER CREATED BY BNDPAS
C
C         D- FILTER COEFFICIENTS
C         X- DATA VECTOR
C         G- FILTER GAIN
C
C
C                         APPLY FILTER IN FORWARD DIRECTION
C
      REAL X(300),XC(3),XD(3),XE(3),D(8)
      XM2=X(1)
      XM1=X(2)
      XM=X(3)
      XC(1)=X(1)
      XC(2)=XM1-D(1)*XC(1)
      XC(3)=XM-XM2-D(1)*XC(2)-D(2)*XC(1)
      XD(1)=XC(1)
      XD(2)=XC(2)-D(3)*XD(1)
      XD(3)=XC(3)-XC(1)-D(3)*XD(2)-D(4)*XD(1)
      XE(1)=XD(1)
      XE(2)=XD(2)-D(5)*XE(1)
      XE(3)=XD(3)-XD(1)-D(5)*XE(2)-D(6)*XE(1)
      X(1)=XE(1)
      X(2)=XE(2)-D(7)*X(1)
      X(3)=XE(3)-XE(1)-D(7)*X(2)-D(8)*X(1)
      DO 39 I=4,N
```

```
      XM2=XM1
      XM1=XM
      XM=X(I)
      K=I-((I-1)/3)*3
      GO TO (34,35,36),K
   34 M=1
      M1=3
      M2=2
      GO TO 37
   35 M=2
      M1=1
      M2=3
      GO TO 37
   36 M=3
      M1=2
      M2=1
   37 CONTINUE
      XC(M)=XM-XM2-D(1)*XC(M1)-D(2)*XC(M2)
      XD(M)=XC(M)-XC(M2)-D(3)*XD(M1)-D(4)*XD(M2)
      XE(M)=XD(M)-XD(M2)-D(5)*XE(M1)-D(6)*XE(M2)
   39 X(I)=XE(M)-XE(M2)-D(7)*X(I-1)-D(8)*X(I-2)
C
C                 FILTER IN REVERSE DIRECTION
C
      XM2=X(N)
      XM1=X(N-1)
      XM=X(N-2)
      XC(1)=XM2
      XC(2)=XM1-D(1)*XC(1)
      XC(3)=XM-XM2-D(1)*XC(2)-D(2)*XC(1)
      XD(1)=XC(1)
      XD(2)=XC(2)-D(3)*XD(1)
      XD(3)=XC(3)-XC(1)-D(3)*XD(2)-D(4)*XD(1)
      XE(1)=XD(1)
      XE(2)=XD(2)-D(5)*XE(1)
      XE(3)=XD(3)-XD(1)-D(5)*XE(2)-D(6)*XE(1)
      X(N)=XE(1)
      X(N-1)=XE(2)-D(7)*X(1)
      X(N-2)=XE(3)-XE(1)-D(7)*X(2)-D(8)*X(1)
      DO 49 I=4,N
      XM2=XM1
      XM1=XM
      J=N-I+1
      XM=X(J)
      K=I-((I-1)/3)*3
      GO TO (44,45,46),K
   44 M=1
      M1=3
      M2=2
      GO TO 47
   45 M=2
      M1=1
      M2=3
      GO TO 47
   46 M=3
      M1=2
      M2=1
   47 XC(M)=XM-XM2-D(1)*XC(M1)-D(2)*XC(M2)
      XD(M)=XC(M)-XC(M2)-D(3)*XD(M1)-D(4)*XD(M2)
      XE(M)=XD(M)-XD(M2)-D(5)*XE(M1)-D(6)*XE(M2)
   49 X(J)=XE(M)-XE(M2)-D(7)*X(J+1)-D(8)*X(J+2)
      DO 59 I=1,N
   59 X(I)=X(I)/G
      RETURN
```

```
      END
      SUBROUTINE STATIC(VECT,NP,CSBNDR,DIGI)
C**   ################################################################
C**   ##                  SUBROUTINE STATIC                         ##
C**   ##   LATITUDE DATA SUPPLIED THROUGH VECT IS ALTERED SUCH THAT  ##
C**   ##   THE LATITUDE OF BOUNDARY CROSSING (CSBNDR) IS SET AT 56.0 ##
C**   ##   DEGREES LATITUDE.                                         ##
C**   ################################################################
C**
      DIMENSION VECT(300)
      IF(DIGI.EQ.0) DIGI=.3
      SHIFT = IFIX((CSBNDR-56.0)/DIGI) * DIGI
      DO 100 I=1,NP
  100 VECT(I) = VECT(I) - SHIFT
      RETURN
      END
```

Appendix C

MGS481#2 SPHERICAL HARMONIC MODEL

Following is the spherical harmonic model supplied as GH and GHT on the INV-B MAGSAT data tapes. This model was subtracted from the raw data to obtain the anomaly data, and was used with program SPEPS to model the induction field producing the synthetic anomalies. The epoch for this model is 1980.0, and the mean Earth radius is 6371.1992 kilometres. Time derivatives are given for the first 7 degrees. Units are nanotesla.

n	m	g_n^m	h_n^m	$\dot{g}_n^m$	$\dot{h}_n^m$
1	0	-29987.1992	0.0	25.5006	0.0
	1	-1956.8501	5604.6992	12.7797	-22.4291
2	0	-1996.1599	0.0	-10.9121	0.0
	1	3027.3999	-2129.4900	0.4997	-12.8701
	2	1663.4700	-199.5940	11.0924	-20.7837
3	0	1279.8401	0.0	-5.5591	0.0
	1	-2181.0100	-334.3181	-6.5758	3.9476
	2	1251.3899	271.1260	-2.8656	1.2512
	3	832.9939	-252.2270	-0.4574	-9.3632
4	0	937.7241	0.0	-0.8666	0.0
	1	782.4900	212.1590	1.7974	-0.4077
	2	396.8811	-256.7009	-6.7219	-1.7278
	3	-419.4490	52.3576	0.7498	5.7137
	4	198.1100	-297.8259	-7.1757	-4.0504
5	0	-217.1930	0.0	0.5506	0.0
	1	357.8259	45.8589	-1.8311	1.1179
	2	261.0791	150.0330	-0.2326	1.5023
	3	-74.3122	-150.6050	-3.3072	-1.9304
	4	-161.9970	-77.7046	1.5411	3.5556
	5	-48.0779	92.3465	-2.5848	0.6250
6	0	48.4670	0.0	1.5391	0.0
	1	65.0140	-14.6005	2.2172	-1.5358
	2	41.8842	93.2305	0.5549	-2.7061
	3	-191.9640	70.9701	0.5589	-0.7413
	4	3.4732	-43.0250	0.8978	1.1510
	5	13.8394	-2.1551	0.2948	0.6146
	6	-107.5630	17.2746	-1.3382	3.8416
7	0	72.0457	0.0	1.0795	0.0
	1	-59.1687	-82.5246	-2.4521	-1.2790
	2	1.6301	-27.1809	0.1498	0.9416
	3	20.9040	-5.1868	0.6488	0.9903
	4	-12.1437	15.9127	-0.6911	-0.2454
	5	0.4333	17.9332	-1.6620	-0.5056
	6	10.2831	-23.0047	1.3996	-0.6845
	7	-1.8357	-9.9483	1.4643	1.7987

n	m	g_n^m	h_n^m
8	0	18.4998	0.0
	1	6.7175	7.2322
	2	-0.2359	-17.5606
	3	-10.8967	3.7609
	4	-7.2094	-22.2458
	5	4.3976	9.1350
	6	2.5015	16.1418
	7	6.0789	-13.3017
	8	-0.8228	-14.8067
9	0	5.3647	0.0
	1	10.4460	-20.9417
	2	1.4050	15.4728
	3	-12.1238	8.6556
	4	9.4872	-5.0625
	5	-3.5681	-6.8346
	6	-1.0295	8.9911
	7	6.8808	9.6780
	8	1.4149	-5.6725
	9	-5.0474	2.1845
10	0	-3.1655	0.0
	1	-3.7985	1.2410
	2	2.4283	0.3517
	3	-5.6169	2.8965
	4	-1.8245	5.8108
	5	4.4932	-4.2533
	6	3.3183	-0.1433
	7	0.6620	-1.3152
	8	2.2744	3.1207
	9	3.0744	-0.2220
	10	-0.5127	-6.4101
11	0	2.5306	0.0
	1	-1.3179	0.8516
	2	-1.7512	1.9518
	3	2.4466	-1.5451
	4	0.1943	-3.2202
	5	-0.8793	0.4874
	6	-0.3620	-0.3112
	7	1.3695	-2.3564
	8	1.5004	-0.2571
	9	-0.6277	-1.4790
	10	1.8995	-1.8808
	11	3.5150	1.1033

n	m	g_n^m	h_n^m
12	0	-1.6658	0.0
	1	0.0256	0.4031
	2	-0.1926	0.6179
	3	-0.1506	2.2822
	4	0.8084	-1.3900
	5	0.5401	0.3849
	6	-0.4846	0.1485
	7	-0.2130	-0.2573
	8	0.3159	0.1197
	9	-0.5973	-0.0053
	10	-0.1681	-1.3414
	11	0.8132	0.5022
	12	-0.0091	0.9256
13	0	0.0411	0.0
	1	-0.4080	-0.4635
	2	0.5084	0.2589
	3	-0.5793	1.2100
	4	-0.1343	-0.2075
	5	0.8523	-0.5053
	6	-0.5145	-0.0883
	7	0.1587	0.8596
	8	-0.8705	0.2600
	9	0.1739	0.9787
	10	-0.0871	0.2080
	11	0.3253	-0.1189
	12	-0.4895	-0.3603
	13	0.4457	-0.9202

Appendix D

CO-ORDINATE SYSTEMS AND CONVERSIONS

Several co-ordinate systems were used in the modelling program SPEPS (Appendix A). Following is a brief overview of the co-ordinate and vector transformations used.

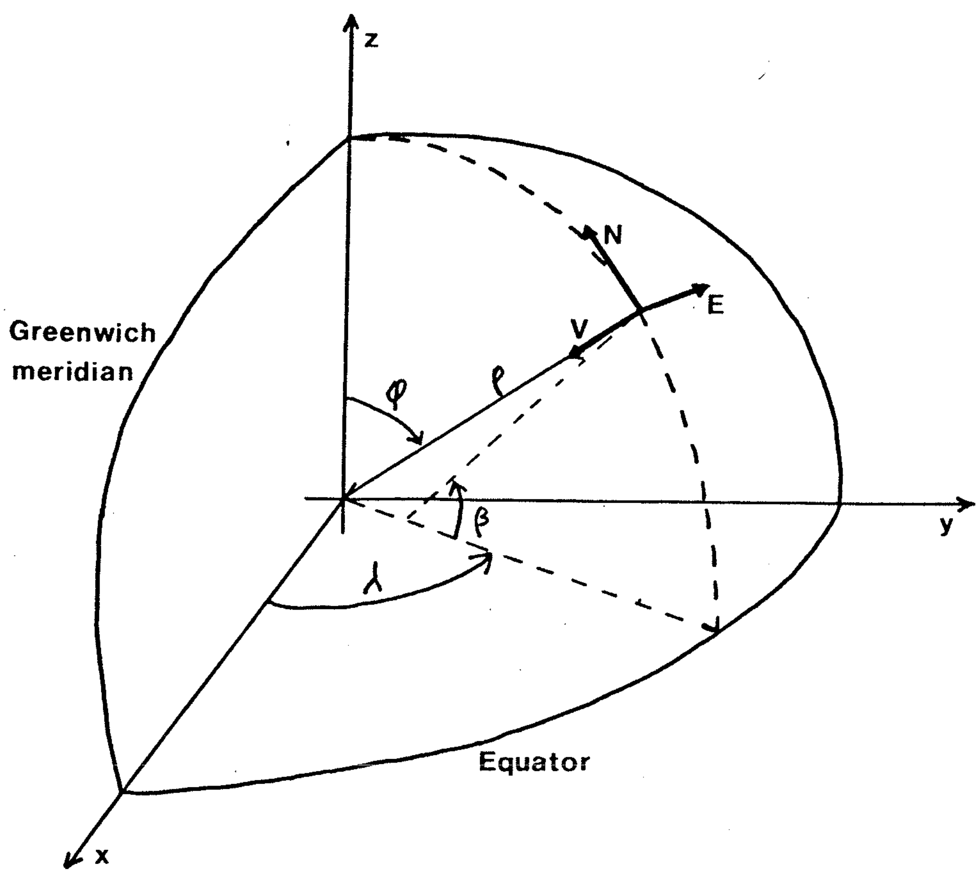

Figure D-1: Co-ordinate Systems of an Elliptic Earth

Figure D-1 illustrates the co-ordinate systems under consideration. The Fixed Earth system is a cartesian system having its origin at the Earth's centre. The x-axis pierces the Earth's surface at the intersection of the equator and the Greenwich meridian. The z-axis is coincident with the north rotational axis, and the y-axix forms the orthogonal third axis.

The Geodetic system is the traditional "map" system. This system consists of the geographic latitude β measured from the equator, east longitude λ measured from the Greenwich meridian, and altitude above the ellipsoid.

The Geocentric system is a spherical system with its origin at the Earth's centre. Geocentric colatitude ϕ is measured from the north rotational axis, east longitude λ is measured from the Greenwich meridian, and the radial distance ρ is measured from the Earth's centre.

In addition to the co-ordinate systems mentioned, the Topocentric system is often used in defining vector quantities. This is a local cartesian system with its origin at the observer's location and its axes aligned with North, East, and Vertical (positive down). The vertical component is directed toward the Earth's centre, and is not in general perpendicular to the ellipsoid. The Topocentric system, then, is the vector equivalent of the Geocentric co-ordinate system. Co-ordinate and Vector transformations between these systems were calculated according to the following formulae.

Co-ordinate transformations:

GEODETIC (altitude, east longitude, north latitude) (h, λ, β)

to GEOCENTRIC (radial distance, colatitude, east longitude) (ρ, φ, λ)

$$\rho = \sqrt{h\ (h+2A) + \frac{a^4 \cos^2\beta + b^4 \sin^2\beta}{A^2}}$$

$$\varphi = \cos^{-1}\left\{\frac{\sin\beta}{\rho}\left[h + A - \frac{(a^2 - b^2)\ \cos^2\beta}{A}\right]\right\}$$

$$\lambda = \lambda$$

where

$A = \sqrt{a^2 \cos^2\beta + b^2 \sin^2\beta}$

a = semi-major axis of earth ellipsoid

b = semi-minor axis of earth ellipsoid

EARTH FIXED (x,y,z) to GEOCENTRIC (radius, colatitude, east long.) (ρ, φ, λ)

$$\rho = \sqrt{x^2 + y^2 + z^2}$$

$$\varphi = \cos^{-1}\left\{\frac{z}{\sqrt{x^2 + y^2 + z^2}}\right\}$$

$$\lambda = \tan^{-1}\left\{\frac{y}{x}\right\}$$

GEOCENTRIC (ρ, φ, λ) to EARTH FIXED (x,y,z)

$$X = \rho \cos\lambda\ \sin\varphi$$

$$Y = \rho \sin\lambda\ \sin\varphi$$

$$Z = \rho \cos\varphi$$

Vector transformations:

TOPOCENTRIC $(\vec{N},\vec{E},\vec{V})$ to EARTH FIXED $(\vec{X},\vec{Y},\vec{Z})$

$$|\vec{X}| = - |\vec{N}| \cos\varphi \cos\lambda - |\vec{E}| \sin\lambda - |\vec{V}| \sin\varphi \cos\lambda$$

$$|\vec{Y}| = - |\vec{N}| \cos\varphi \sin\lambda + |\vec{E}| \cos\lambda - |\vec{V}| \sin\varphi \sin\lambda$$

$$|\vec{Z}| = |\vec{N}| \sin\varphi - |\vec{V}| \cos\varphi$$

EARTH FIXED $(\vec{X},\vec{Y},\vec{Z})$ to TOPOCENTRIC $(\vec{N},\vec{E},\vec{V})$

$$|\vec{N}| = - |\vec{X}| \cos\lambda \cos\varphi - |\vec{Y}| \sin\lambda \cos\varphi + |\vec{Z}| \sin\varphi$$

$$|\vec{E}| = - |\vec{X}| \sin\lambda + |\vec{Y}| \cos\lambda$$

$$|\vec{V}| = - |\vec{X}| \cos\lambda \sin\varphi - |\vec{Y}| \sin\lambda \sin\varphi - |\vec{Z}| \cos\varphi$$